AD-A107 598 UNIVERSITY OF SOUTHERN CALIFORNIA LOS ANGELES ELECTR--ETC F/G 20/12
THE EFFECT OF SOLUTE-VACANCY PAIRS ON THE PHYSICAL PROPERTIES O--ETC(U)
MAY 81 W G SPITZER, J M WHELAN, S M COPLEY AFOSR-76-2990

UNCLASSIFIED AFOSR-TR-81-0746 NL

1 OF 2
AD A
107598

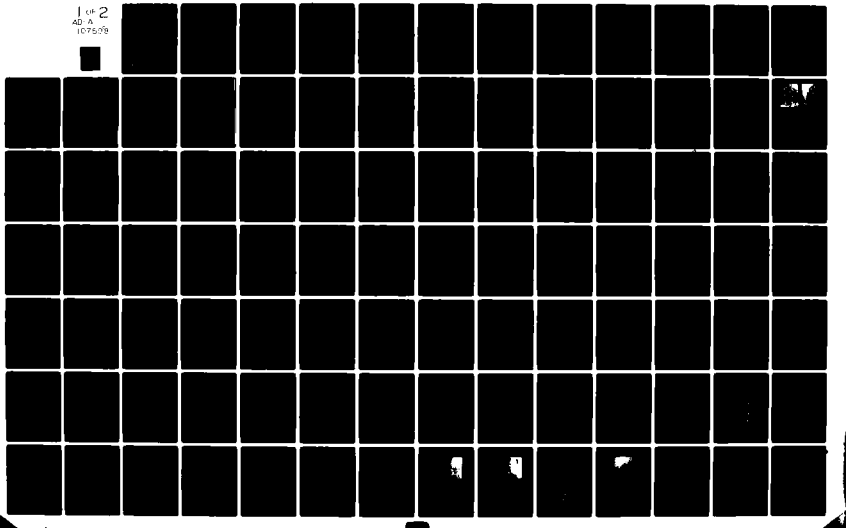

LEVEL

12

AFOSR

THE EFFECT OF SOLUTE-VACANCY PAIRS ON THE PHYSICAL PROPERTIES OF Si DOPED GaAs AND OTHER COMPOUND SEMICONDUCTOR SYSTEMS

Grant AFOSR-76-2990

FINAL REPORT

Period Covered: June 1, 1976 to May 31, 1981

by

W.G. Spitzer, J.M. Whelan, and S.M. Copley
Department of Materials Science
Electronic Sciences Division
University of Southern California
Los Angeles, California 90007

This research was supported by the Air Force Office of Scientific Research (AFSC) under Grant AFOSR-76-2990.

Approved for public release: distribution unlimited.

UNCLASSIFIED

SECURITY CLASSIFICATION OF THIS PAGE (When Data Entered)

REPORT DOCUMENTATION PAGE		READ INSTRUCTIONS BEFORE COMPLETING FORM
1. REPORT NUMBER AFOSR-TR- 81-0746	2. GOVT ACCESSION NO.	3. RECIPIENT'S CATALOG NUMBER
4. TITLE (and Subtitle) THE EFFECT OF SOLUTE-VACANCY PAIRS ON THE PHYSICAL PROPERTIES OF SI-DOPED GaAs AND OTHER COMPOUND SEMICONDUCTOR SYSTEMS		5. TYPE OF REPORT & PERIOD COVERED FINAL REPORT June 1, 1976-May 31, 1981
		6. PERFORMING ORG. REPORT NUMBER
7. AUTHOR(s) W. G. Spitzer, J. M. Whelan and S. M. Copley		8. CONTRACT OR GRANT NUMBER(s) AFOSR-76-2990
9. PERFORMING ORGANIZATION NAME AND ADDRESS Electronic Sciences Laboratory University of Southern California Los Angeles, California 90007		10. PROGRAM ELEMENT, PROJECT, TASK AREA & WORK UNIT NUMBERS 61102F 2306/B2
11. CONTROLLING OFFICE NAME AND ADDRESS Air Force Office of Scientific Research (AFSC) Bolling Air Force Base, Bldg. 410 Washington, D. C. 20332		12. REPORT DATE 1984 81
		13. NUMBER OF PAGES 109
14. MONITORING AGENCY NAME & ADDRESS(if different from Controlling Office)		15. SECURITY CLASS. (of this report) UNCLASSIFIED
		15a. DECLASSIFICATION/DOWNGRADING SCHEDULE

16. DISTRIBUTION STATEMENT (of this Report)

Approved for public release; distribution unlimited.

17. DISTRIBUTION STATEMENT (of the abstract entered in Block 20, if different from Report)

18. SUPPLEMENTARY NOTES

19. KEY WORDS (Continue on reverse side if necessary and identify by block number)

Semiconductors, Defects, Optical Properties, Mechanical Properties, Microstructure.

20. ABSTRACT (Continue on reverse side if necessary and identify by block number)

This is a report of a detailed and quantitative study of the influence of changes in specific defect concentrations on the microstructure and the electrical, optical and mechanical properties of Si-doped GaAs. Evidence for the GaAs:Si system demonstrates that quantitative correlations between Si-related defect concentrations and a diverse set of physical properties are observed. The measured changes in properties are large and have been employed to construct appropriate defect models. GaAs is a material of interest to the

DD FORM 1 JAN 73 1473 EDITION OF 1 NOV 65 IS OBSOLETE

UNCLASSIFIED

SECURITY CLASSIFICATION OF THIS PAGE (When Data Entered)

electronics community as it is used in a number of devices. The role of defects in affecting transport properties is of fundamental importance. The goal of this research is to obtain a more complete understanding of the defect structure of Si-doped GaAs through a quantitative correlation of various physical properties and concentrations of Si-related defects and also to track the effect of defect species such as solute vacancy pairs on several different physical properties. This final report summarizes the work of a 5 year study.

ABSTRACT

This is a final report of a detailed and quantitative study of the influence of changes in specific defect concentrations on the microstructure and the electrical, optical and mechanical properties of Si-doped GaAs. Preliminary evidence for the GaAs:Si system has indicated that qualitative correlations between Si-related defect concentrations and a diverse set of physical properties are observed. The measured changes in properties are large and can be employed to construct appropriate defect models. GaAs is a material of interest to the electronics community as it is used in a number of devices. The role of defects in affecting transport properties is of fundamental importance. The goal of this research is to obtain a more complete understanding of the defect structure of Si-doped GaAs through a quantitative correlation of various physical properties and concentrations of Si-related defects and also to track the effect of defect species such as solute vacancy pairs on several different physical properties. The final report summarizes the work of a five year study. It also includes a description of the work of Professor J. M. Whelan and Mr. John Graham to determine total Si concentrations which is necessary to determine the absorption cross sections of all of the Si-related defects.

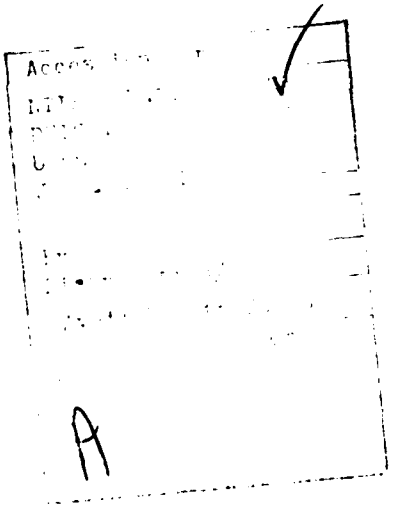

TABLE OF CONTENTS

I. INTRODUCTION

The compound semiconductor GaAs is of great technological interest because of its considerable application in electronic, optical, and opto-electronic devices. In many of its applications the defect structure and properties are of major importance and this importance has stimulated basic studies of the defect structure of doped GaAs and its influence on physical properties. Our interest in this topic led to the original proposal which was to initiate a detailed and quantitative study of the influence of changes in specific defect concentrations on a diverse set of physical properties for a number of doped crystal systems. One system, GaAs:Si, was selected for the major effort and we have now completed this study. As will be discussed most of the original objectives have been achieved. One major task, that of developing an inexpensive and accurate method for measurement of the total Si concentration, still remains incomplete and we anticipate completion by the end of this summer (1981).

In the original proposal it was indicated that preliminary evidence for the GaAs:Si system shows that qualitative or semi-quantitative correlations between Si-related defect concentrations and a number of physical properties are indeed observed. The changes in properties produced by annealing can be large and these changes are useful in helping to construct appropriate defect models. Electrical, optical, mechanical and microstructural characteristics are all part of the system of physical properties which were measured. To our knowledge, this study is the first one in which the changes in quantities such as carrier density, infrared absorption, vacancy loop size and density and yield stress caused by changes in thermodynamic conditions are correlated and all explained on the basis of a common defect model.

There have been a number of earlier studies, primarily at the University of Southern California, which demonstrated that aging produces dramatic effects on the properties of heavily Si-doped GaAs. The aging effect is observed for specimens in which the Si concentration is less than the high temperature solid solubility limit. The effects included changes in the free carrier concentration, defect-induced localized vibration mode absorption, photoluminescence, TEM measured microstructure, and critical resolved shear stress. The results of these earlier investigations suggested that the annealing-induced changes in these various properties are inter-related. Indeed, in the present study, a qualitative correlation has been found between changes in these properties and changes in the concentration of Si-vacancy defects such as $(Si_{Ga}V_{Ga})$ pairs, where V_M indicates a vacant M site. The difficulty with detailed comparisons of the previous measurements is that they were performed using material from different ingots or different sections of an ingot, and therefore, the Si concentrations were different. The primary goal of this research was to determine whether a quantitative correlation exists between physical properties and the concentrations of lattice defects such as $(Si_{Ga}V_{Ga})$ pairs in heavily Si-doped GaAs. This primary goal was achieved in that the correlations were found and the details are given in the body of this report.

II. RESEARCH OBJECTIVES AND RESULTS

A. ABSTRACT

The purpose of this study is to measure and correlate the annealing-induced changes in the carrier density, the microstructure and the yield stress for different Si concentrations in GaAs. The measurement which permits the correlation of these properties is the infrared absorption of the localized vibrational modes (LVM). As described in the following text the LVM measurements allow one to track the annealing-induced changes in specific defect concentrations if one can determine the absorption cross sections associated with the different defect bands. This determination was done by comparing the integrated absorption of four different defect bands with the measured carrier densities for a large number of samples of different Si concentrations (see Section II-B). The absorption cross sections were then used to measure the site transfer of Si from Ga to As sites as a result of Li saturation diffusions at elevated temperatures (see Section II-B). The infrared, electrical, microstructural and mechanical measurements as well as the analysis have been completed. In brief the principal results are:

(1) Detailed analysis of a large number of GaAs:Si having different [Si] enabled us to measure the absorption cross sections of the infrared bands attributable to 4 different Si defects including Si_{Ga} donors and Si_{As} acceptors.

(2) When GaAs:Si is saturated with Li by diffusion at 950°C, Si transfer from Ga to As sites is observed and the degree of site transfer is a function of [Si].

(3) Heavily-doped GaAs:Si have Si-rich faulted loops produced by Li diffusion at 750°C and this excess Si transfers to As sites if Li is diffused at 950°C.

(4) By using the LVM measurements we are able to determine the changes in $[Si_{Ga}]$, $[Si_{As}]$, $[Si_{Ga}\text{-}Si_{As}]$ and two unknown but Si-related defect concentrations as a result of annealing at 400°C, 500°C, 700°C, 800°C, 900°C and 1000°C ([ ] = concentration, M_A = M atom on A site). Detailed isothermal anneal curves for each defect were obtained for the first three temperatures for three different total Si concentrations.

(5) After annealing at 400°C the decrease in carrier density (n_c) the absence of observable microstructure, the increase in yield stress can all be quantitatively explained on the basis of the decrease in observed $[Si_{Ga}]$ from the LVM measurements. No other Si defect concentration changes thus making a $Si_{Ga} = V_{Ga} \rightarrow Si_{Ga} - V_{Ga}$ pair formation an attractive mechanism. The possible $Si_{Ga} - V_{As}$ pair defects would have point group C_{3v} which is too high a symmetry to explain the yield stress results.

(6) For samples annealed at temperatures above 400°C the changes in n_e require the presence of a new and as yet unidentified acceptor. The concentration of this acceptor increases with increasing [Si] and the temperature dependence indicates this acceptor concentration is essentially zero at 400°C and 1000°C and peaks near 700°C.

(7) Microstructural measurements indicate that the new acceptor is not related to the presence of dislocation loops. Extrinsic loops are observed for anneal temperatures near 700°C and are essentially gone at 1000°C. The loops are found to be Si-rich.

(8) At the higher anneal temperatures the changes in yield stress still qualitatively correlates with the changes in $[Si_{Ga}]$ which can be attributed to Si_{Ga}-V_{Ga} pair formation and not with the changes in other measured Si defect concentrations. This indicates the yield stress annealing effect is still controlled by the $[Si_{Ga}$-$V_{Ga}]$. To our knowledge this is the first system for which this type of data has been available.

(9) With very long anneal times, e.g. ∿1200h or more, changes in nearest neighbor pair concentrations $[Si_{Ga}$-$Si_{As}]$ are observed but only for a very limited temperature range - approximately 500-600°C. Above and below these temperatures the pair concentration is constant in time.

In this next section we have given detailed accounts of the research work. Where the work has been published we have included a copy of the paper as the account of that portion of the study. In this way the final report is a complete account of all of the research done under this grant.

1. Infrared absorption bands induced by Si-related defects in GaAs: Absorption cross sections

R.T. Chen, V. Rana,[a] and W.G. Spitzer
Departments of Physics and Materials Science, University of Southern California, Los Angeles, California 90007

(Received 29 June 1979; accepted for publication 30 October 1979)

Silicon is an amphoteric impurity in GaAs and is present in different defect configurations. This work reports measurements of the infrared absorption cross sections for some of the localized vibrational mode bands related to the Si defects. Heavily doped melt-grown samples are used to measure the free-carrier density n_c and the integrated absorption of all bands attributed to electrically active defects. The resulting data are analyzed by using a least-squares-fitting procedure employing two different models. A set of absorption cross sections is given for each model. These results differ from others reported recently. Using the two sets of cross sections to interpret the absorption spectra of *p*-type liquid-phase epitaxial samples seems to reaffirm a previously reported interpretation in which an additional Si-related acceptor defect of unknown nature is present.

PACS numbers: 63.20.Pw, 81.40.Tv, 78.50.Ge

I. INTRODUCTION

The localized vibrational modes, hereafter called LVM, of Si-doped GaAs and the associated infrared absorption have been subjects of a number of studies.[1-15] Silicon is known to be an amphoteric impurity in GaAs, and materials grown from a near-stoichiometric melt are always *n* type. Absorption bands have been observed and attributed to several defects involving Si,[1] and the absorption cross sections for two of the more numerous and electrically important defect species have been reported.[4] The various absorption bands have been used to study a number of properties of GaAs : Si including the annealing-induced changes in the carrier density of heavily Si-doped material,[6-8] the Fermi level effect on the Si-site distribution,[9] the behavior of Si when it is introduced by ion implantation,[10] the pairing of Si with other impurities,[1,11,15] the *p*-type behavior of some liquid-phase epitaxially grown GaAs doped with Si,[4,12,13] lattice strain effects resulting from fast neutron irradiation,[5] and the segregation coefficient of Si in GaAs.[3,14]

The present work is an investigation of the absorption cross sections for the absorption bands induced by Si-related defects in Si-doped GaAs. In the course of some studies of low-temperature annealing effects it became obvious that the absorption obtained here for a large number of samples were not in reasonable agreement with predictions based on the most recent and presumably most accurate values reported[4] for the cross sections. Because of this difficulty and because the cross sections are needed in a number of the studies mentioned earlier, it is important to establish reliable values.

II. BACKGROUND

Because of the amphoteric nature of Si impurities in GaAs, there has been considerable interest in the use of measurements of the LVM frequencies obtained from the infrared absorption for the identification of defect species. Optical measurements[1,3,4] have been used with electrical data and expected defect symmetry properties to identify the Si defects responsible for the observed absorption bands. The $^{28}Si_{Ga}$ defect, ^{28}Si substitutional on a Ga site, is a donor and is responsible for a band at a frequency of 384 cm^{-1}, $^{28}Si_{As}$ is an acceptor and accounts for a band at 399 cm^{-1}, and $^{28}Si_{Ga}$–$^{28}Si_{As}$ are nearest-neighbor pairs which are presumably electrically neutral, account for bands at 464, 393, and 367 cm^{-1}. All frequencies are the liquid-nitrogen-temperature values. There has also been the suggestion that a band near 369 cm^{-1} seen only in electron irradiated Si-doped samples is related to $^{28}Si_{Ga}$–V_{Ga}, where V is a vacancy, or to some other "Si-containing" complex.[2] All of the bands show close to the expected isotope shift[2] when ^{28}Si is replaced by ^{30}Si. The Si_{Ga}–Si_{As} bands at 464 and 393 cm^{-1} show mixed band frequencies for samples containing both ^{28}Si and ^{30}Si, i.e., bands $^{28}Si_{Ga}$–$^{30}Si_{As}$ and $^{30}Si_{Ga}$–$^{28}Si_{As}$ defects. The lack of such a mixed isotope band for the ^{28}Si band at 367 cm^{-1} has led to some question as to the correctness of its identification as Si_{Ga}–Si_{As} pair band.

In order to make the infrared measurements which gave the above frequency assignments it was necessary first to essentially eliminate the free-carrier absorption which effectively obscures the LVM absorption. The electrical compensation has been accomplished by saturation diffusion of Li or Cu at an elevated temperature, i.e., $700 \lesssim T_D \lesssim 1000$ °C, or by penetrating particle irradiation, i.e., 1–2-MeV electrons or neutrons. In a few cases partial compensation was achieved[3,15] by counterdoping during crystal growth. A major difficulty with all of the above procedures is that the compensation process may alter the distribution of Si among the various defects and even create Si-related defects which were not present in significant concentration in the precompensated state. Ample evidence exists for such changes with some of the compensation procedures. Saturation diffusion of Li or Cu results in the formation[1] of Si_{Ga}–Li_{Ga} or Si_{Ga}–Cu_{Ga} second-neighbor pairs. For each of these defects, one

[a]Present address: Bell Telephone Labs, Murray Hill, N.J. 07974.

 0021-8979/80/031532-07$01.10

observes a new set of LVM bands. Moreover, it is known[16] that Li diffusion at $T_D \geq 900$ °C can cause site transfer of substitutional Si from Ga to As sublattice sites. Also if GaAs has a concentration of Si in excess of [Si]$\simeq 2\times10^{18}$ cm^{-3}, thermal aging at temperatures greater than $T\simeq 400$ °C can cause changes in the free-carrier concentration[6,7] which have been shown to be related to changes in Si-defect concentrations. Thus Li and Cu diffusions are done at temperatures and for times for which major aging effects have also been observed. The compensation by electron irradiation is frequently done with the sample maintained near liquid-nitrogen temperature during the irradiation to prevent thermal annealing. After irradiation, the sample is allowed to warm to room temperature. There is the concern that mobile native defects introduced by the irradiation might pair with some of the Si defects and thus alter the original concentrations. In one study[4] the irradiation was continued to fluences of five times that necessary to render the samples transparent at frequencies where there is little lattice or LVM absorption. No significant changes were observed in the absorption at the LVM frequencies. However, it is possible that the charge states of the native defects and the Si-defect complexes and hence the pairing process may be Fermi level dependent. Nevertheless, from the evidence available, the e^--irradiation method of compensation appears to be the least disturbing to the precompensation distribution of Si defects, and it has been used to compensate all the samples in this study as well as in most previous studies.

In order to determine the concentration of each of the defects which induces LVM bands one must know the absorption per center for each of the bands; i.e., $\int_{\text{band}} \alpha_{\text{LVM}}\, d\nu$ /[defect], where α is the LVM absorption coefficient, ν is the frequency, and [ ] indicates concentration. To obtain the absorption per center a comparison is made between the measured free-carrier density n_e prior to compensation and the absorption bands observed after compensation. This comparison is made by using

$$n_e = a(\alpha_p \Delta)_{384} - b(\alpha_p \Delta)_{399}, \tag{1}$$

where n_e is the carrier density, α_p the peak LVM absorption less background, Δ the band width at half-maximum, and a and b densities of centers per unit absorption with $\int \alpha_{\text{LVM}}\, d\nu$ replaced by $(\alpha_p \Delta)$. Comparisons of a large number of samples of different n_e and [Si] should lead to values of the constants a and b satisfying this relation. The a and b values obtained depend upon the validity of several assumptions: (1) the absorption of a LVM band is proportional to the density of centers; (2) the [Si_{Ga}–Si_{As}] does not contribute to the free-carrier density; (3) the compensation technique does not alter the [Si_{Ga}] and [Si_{As}] values; and (4) there is no other defect which has donor or acceptor character and is of concentration significant to [Si_{Ga}] or [Si_{As}]. It is also important that the values of [Si_{Ga}] and [Si_{As}] in the samples studied be both large for at least some cases in order that values of both a and b obtained be meaningful.

The most recent and complete measurements of a and b are those reported by Laithwaite and Newman,[4] hereafter L-N, who measured 14 samples of Bridgman-grown GaAs : Si having n_e values ranging from 5×10^{17} to 6.1×10^{18} cm^{-3} and 10 LPE-grown Si-doped GaAs layers. The samples were all compensated by e^- irradiation and generally very good agreement was obtained between the measured carrier density and that deduced from Eq. (1). The values for a and b used to get this agreement were $a = 5.29\times10^{16}$ cm^{-1} and $b = 6.82\times10^{16}$ cm^{-1}. However, our attempts to use these values for the measurements to be discussed in Sec. III were unsuccessful. Factors as large as between 3 and 5 were noted between the electrically measured n_e values and those obtained from Eq. (1).

Inspection of the L-N data[4] reveals that for all of the Bridgman-grown samples the $(\alpha_p \Delta)_{399}/(\alpha_p \Delta)_{384} \lesssim 0.15$. The n_e values obtained from Eq. (1) by using the L-N a and b values frequently differ from the electrically measured values by as much as 10%. Thus, b is subject to considerable uncertainty. The value of b comes primarily from the application of Eq. (1) to the LPE samples. However, there is considerable question[13] as to the validity of assumption (4) for such samples. While some of the differences between the L-N results, and those to be given here may be attributed to differences between samples, experimental techniques, and instrumental resolution, the quantitative differences are such that it appears unlikely that these are the primary sources of the difficulty. For these reasons Sec. III contains some detail concerning instrumental tests of the accuracy and reproducibility of the absorption measurements which would not usually be presented.

III. EXPERIMENTAL METHOD

The samples used here were taken from a series of horizontal Bridgman-grown ingots. Three additional samples were kindly supplied by Newman. In some cases the ingots were polycrystalline but with very large single-crystal sections having typical dimensions of centimeters. The samples were always taken from these single-crystal regions. A total of 21 samples were used for the a and b determinations. The total [Si] ranged from $\sim1\times10^{18}$ to $\sim1\times10^{20}$ cm^{-3} as estimated from the dopant added during growth and the known segregation coefficient[14] of Si in GaAs and also from spectrochemical analyses. In a few cases the [Si] was also measured by using an electron probe microanalyzer. Most samples used for the a and b determinations were annealed for 1 h at 1200 °C and quenched to room temperature prior to making any measurements or proceeding with electrical compensation of the samples by e^- irradiation. The annealing treatment establishes a common thermodynamic background for all samples and avoids some of the known and previously mentioned lower-temperature annealing effects for both n_e and the Si-defect concentrations. These annealing effects are generally present because of the cool-down cycles employed in the growth procedure. Generally the high-temperatue-quench procedure has almost no effect on the n_e for material with [Si] $\lesssim 1\times10^{18}$ cm^{-3} and substantially increases n_e for samples with [Si] $\gtrsim 1\times10^{19}$ cm^{-3}. The resulting free-electron densities ranged from $n_e \sim 1\times10^{18}$ to 1×10^{19} cm^{-3}. After the high-temperature-quench treatment sufficient material, ~0.1 mm, was removed from the surfaces that infrared reflectivity measurements of the free-car-

rier plasma frequency indicated that further removal of material did not change the carrier density, i.e., we were measuring the bulk carrier density.

Transmission electron microscopy measurements of the high-T annealed + quench samples showed no stacking faults, no precipitates, and almost no dislocation loops. The samples appeared free of microstructure except for an occasional dislocation loop. Samples which had not been given the treatment, i.e., in the as-grown condition, were frequently found to have extrinsic stacking faults, particularly those samples with the larger [Si].[17]

Prior to electrical compensation the free-carrier density of each sample was measured by determining the frequency of the plasma minimum in the infrared reflectivity. The values from this method have been compared with Hall measurement results and very good agreement was obtained.[8] After the n_e measurements all samples were e^- irradiated with 1.4-MeV electrons until they were infrared transparent. The fluences ranged from approximately $5\times10^{18}e^-/cm^2$ to $2\times10^{19}e^-/cm^2$ depending upon the initial n_e value. In all cases dose rates of approximately $5\times10^{14}e^-/cm^2$ sec were used. The samples were maintained at a temperature below $\sim$140 °K during the irradiation with the temperature being monitored by a thermocouple mounted along side the samples. Transmission electron microscopy measurements of samples after e^- irradiation showed no microstructural change as a result of the irradiation, i.e., essentially free of any structure.

Because of the differences between the absorption results to be given here and those reported in the earlier measurements of L-N,[4] the procedures used here are described in some detail. After electrical compensation the infrared absorption coefficient at liquid-nitrogen temperature was measured for all samples. The measurements were made by using a single-beam grating infrared spectrometer employing interference filters to isolate the first order spectrum. The sample Dewar was mounted at a focal point in the exit beam after the monochromator section. The transmission was measured by using the sample in–sample out method with the sample covering one of a pair of matched aperatures. A radiation thermocouple with a commerical 13-Hz phase-sensitive amplifier system was used for the detection. The spectral range covered was $350 < \nu < 500\ cm^{-1}$ which is known to cover the frequencies of all the absorption bands of interest in this study. The samples measured were generally about 0.3–0.8 mm thick and had a small thickness wedge of $\sim$0.2° eliminate transmission interference fringes. The minimum transmission which is at the absorption peak of the strongest band ranged from $\sim$2 to $\sim$10%. The absorption coefficient was calculated from $T = I_{sample}/I_0 = (1-R)^2 \times \exp(-\alpha x)/[1-R^2\exp(-2\alpha x)]$, where R is the reflectivity.

A series of instrumental tests were performed in order to ensure the spectrometer was operating properly. The tests were to ensure that a low scattered light level existed throughout the measured spectral range, that the second- and higher-order beams were properly filtered out, and that the detection system was indeed linear in its response to the input signal. Briefly, some of the tests were as follows:

(1) Room-temperature transmission measurements of $\sim$1-cm-thick crystals of NaCl and KCl were made. Comparisons of the measured absorption with values reported in the literature[18] for $\nu \lesssim 600\ cm^{-1}$ were very good. The transmission of both crystals for $300 \lesssim \nu \lesssim 450\ cm^{-1}$ was less than 1% as expected.

(2) A measurement was made of the room-temperature transmission of a high-purity GaAs sample in the spectral range of the two-phonon absorption ($600 \gtrsim \nu \gtrsim 340\ cm^{-1}$). The measured absorption coefficient was within $<20\%$ of the literature[19] values at all frequencies and within 10% for almost all frequencies. Similar measurements for Ge gave similar results.[20]

(3) Measurements of the Si_{Ga} absorption band were done for a variety of spectral slits widths (0.62 to 1.1 cm^{-1}) with qualitatively the expected results in the measured linewidth being obtained.

(4) Most of the samples were remeasured after an interval of several months with good reproducibility observed in $(\alpha_p \Delta)$ for all bands, generally within 10%.

(5) A sample was remeasured with the I_0 beam (sample out) aperature covered with a high-purity GaAs sample of the same thickness. Both samples were at liquid-nitrogen temperature. The calculated absorption coefficients of the Si bands of the Si-doped sample were essentially identical to those calculated when the sample out position was an open aperature. This test eliminated a possible error due to the temperature dependence of the detector sensitivity.

(6) A different blazed grating was used in our mono-

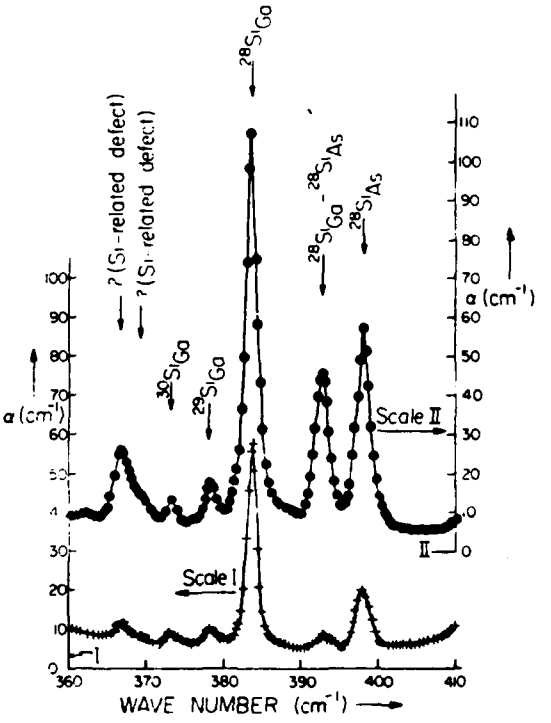

FIG. 1. Localized vibrational mode absorption spectrum of GaAs : Si(1200 °C/1h anneal compensated by electron irradiation at 77 °K). — ● designates WA-Si-2-5, $[Si] \simeq 7.0\times10^{18}\ cm^{-3}$; — + designates KM-16-3, $[Si] \simeq 2.4\times10^{19}\ cm^{-3}$.

chromator and also room-temperature transmission measurements were made of a few samples by using another commerical infrared system with the results in both cases being again very satisfactory.

(7) Several samples were measured with each sample having two thicknesses which differed by a factor of 2. The resulting absorption coefficient spectra for a given material was in good agreement for the two thicknesses, i.e., within 15% at all frequencies and almost always within 10%.

IV. RESULTS AND DISCUSSION

A. Analysis I: Si_{Ga} and Si_{As} only electrically active defects

The absorption of the e^- irradiated samples is illustrated in Fig. 1 for two samples of different [Si]. The results of similar measurements for all samples are summarized in Tables I and II. In a few cases the [Si] is known from electron microprobe measurements and is included in Table II. The peak absorption coefficient less background and half-width for each of the principal bands are given for all measured samples. As mentioned previously the samples were measured twice with several months between measurements, and in all cases the $\alpha_p\Delta$ for each band agreed within 15% for the two measurements. The mean half-widths are 1.5, 2.2, and 2.2 cm^{-1} for the Si_{Ga} (384 cm^{-1}), Si_{As} (399 cm^{-1}), and Si_{Ga}–Si_{As} (393 cm^{-1}) bands, respectively. The instrumental resolution during all of these measurements was ~0.75 cm^{-1}. The measured half-widths for the Si_{Ga} and Si_{As} bands are quite close to the L-N values[4] of 1.4 and 2.0 cm^{-1}. Figure 2 shows a plot of $(\alpha_p\Delta)_{384}/n_e$ versus $(\alpha_p\Delta)_{399}/n_e$, where n_e is the measured carrier density. All of the samples of Tables I and II except the last three samples are included in this plot. These three samples are excluded because of the large uncertainty of the carrier density of the Litronic LiD sample, i.e., $n_e = (1\text{–}2)\times10^{18}$ cm^{-3}, and the significant amounts of other acceptors, particularly Mg, found by the spectrochemical analyses for the two KM-26 samples. The straight line in Fig. 2 is a least-squares fit which yields values for a^1 and b^1 of

$$a^1 = 10.1\times10^{16}\ cm^{-1},$$

$$b^1 = 9.3\times10^{16}\ cm^{-1},$$

which gives $n_e' = 10.1\times10^{16}(\alpha_p\Delta)_{384} - 9.3\times10^{16}(\alpha_p\Delta)_{399}$. In calculating n_e' in this way it is assumed that Si_{Ga} and Si_{As} are the only electrically active defects and that they are entirely responsible for the preirradiation value for n_e. These calculated n_e' values are also given in Table II. In almost all cases the optical value is within 25% of the measured electrical value of n_e. The relative chi, $\chi = [\Sigma_{j=1}^{N}[n_e'(j) - n_e(\text{measured})]^2/N - n - 1]^{1/2}$, value for $N = 18$ samples and $n = 2$ parameters is 1.37×10^{18} cm^{-3}. The values of a and b given here differ significantly from those given by L-N.[4]

We have conducted some measurements in collaboration with Newman in order to help establish the correct absolute values for a and b. In a recent communication, New-

TABLE I. Integrated absorption strength of the LVM bands and free-carrier density for the Bridgeman melt-grown GaAs : Si samples.

Ingot	Sample	n_e(elect. meas.) ($\times10^{18}$ cm^{-3})	Si_{Ga} band (ν_p = 384 cm^{-1}) α_p cm^{-1}	Δ cm^{-1}	$\alpha_p\Delta$ cm^{-2}	Si_{As} band (ν_p = 399 cm^{-1}) α_p cm^{-1}	Δ cm^{-1}	$\alpha_p\Delta$ cm^{-2}	ν_p = 367 cm^{-1} band α_p cm^{-1}	Δ cm^{-1}	$\alpha_p\Delta$ cm^{-2}	ν_p = 369 cm^{-1} band α_p cm^{-1}	Δ cm^{-1}	$\alpha_p\Delta$ cm^{-2}	Si_{Ga}–Si_{As} band (ν_p = 393 cm^{-1}) α_p cm^{-1}	Δ cm^{-1}	$\alpha_p\Delta$ cm^{-2}
KM-16	1[a]	5.42	59.8	1.45	86.7	11.1	2.40	26.6			~ 2.0			0	2.6	2.30	6.0
	2[a]	5.54	65.2	1.30	84.8	13.8	2.00	27.6			~2.0			~ 1.0	3.4	2.05	7.0
	3[a]	5.42	52.7	1.50	79.1	14.5	2.15	31.2	4.0	1.60	6.4			~ 1.0	3.5	2.40	8.4
	4[a]	6.05	58.7	1.55	91.0	18.0	2.00	36.0	3.2	2.00	6.4			~ 1.0	4.3	2.00	8.6
	5[a]	7.20	63.6	1.52	96.7	22.0	2.00	44.0	5.1	1.95	10.0			~ 2.0	6.2	2.30	14.3
	6[a]	7.24	63.5	1.50	95.3	23.0	2.00	46.0	5.6	2.00	11.2			~ 2.0	7.6	2.20	16.7
WA-Si-2	1[a]	7.55	73.8	1.50	110.7	24.3	2.00	48.6	4.6	2.00	9.2			~ 1.5	8.5	1.90	16.2
	2[a]	7.80	81.2	1.60	129.9	26.6	2.15	57.2	4.5	1.90	8.6			~ 1.2	12.9	2.20	28.4
	3[a]	8.00	73.3	1.60	117.3	28.0	2.05	57.4	8.2	2.00	16.4	3.2	2.35	7.0	9.8	2.20	21.6
	4[a]	9.90	126.8	1.40	177.5	49.1	2.15	105.6	16.2	2.80	45.4	10.6	2.55	27.0	32.9	2.10	69.1
	5[a]	9.90	101.4	1.70	172.4	51.4	2.10	107.9	17.6	2.30	40.5	5.2	2.50	13.0	39.8	2.30	91.5
KM-15	1[a]	8.65	124.6	1.40	174.4	30.4	2.40	73.0	5.4	1.50	8.1	1.4	2.00	2.8	21.2	2.20	46.6
WA-99	1[b]	8.90	100.0	1.60	160.0	32.0	2.45	78.4	8.9	2.64	23.5	7.1	2.75	19.7	20.0	2.05	41.0
	2[b]	9.40	110.0	1.55	170.5	37.0	2.25	83.3	9.7	2.12	20.6	6.9	2.67	18.4	20.0	1.95	39.0
KS	1[b]	8.20	154.0	1.45	227.7	62.0	2.30	142.6	16.0	1.80	28.8	6.5	2.40	15.6	45.7	2.55	116.5
	2[c]	5.10	96.5	1.45	139.9	34.5	2.50	86.3	20.8	2.00	41.6	16.0	2.70	43.2	57.0	2.00	114.0
GA529	1[c]	2.50	26.0	1.40	35.8	2.7	2.00	5.4			0			0	1.0	2.00	2.0
GA503	1[c]	1.15	11.8	1.40	15.7	0.8	2.00	1.6			0			0			0
Litronic LiD	1[c,d]	1–2	10.2	1.40	14.3	0.8	2.00	1.6			0			0			0
KM-26	1[c,d]	1.07	16.0	1.30	20.8	1.4	2.60	3.6			0			0			0
	2[c,d]	1.00	15.0	1.35	20.3	1.5	2.20	3.3			0			0			0
			Average	1.47			2.18			2.04			2.49			2.16	

[a]Samples annealed at 1200 °C/1 h + quenched to room temperature.
[b]Samples annealed at 1100 °C/15 min + quenched to room temperature.
[c]Samples are as-grown.
[d]Samples excluded from least-squares-fitting procedure (see text).

Table II. Comparison of electrically measured n_e value and calculated optical n_e values for the samples listed in Table I.

Ingot	Sample	n_e(elect. meas.) ($\times 10^{18}$ cm^{-3})	n_e^{I} ($\times 10^{18}$ cm^{-3})	n_e^{II} ($\times 10^{18}$ cm^{-3})	$n_e^{\mathrm{L\text{-}N}}$ ($\times 10^{18}$ cm^{-3})	[Si](EPMA) ($\times 10^{19}$ cm^{-3})
KM-16	1[a]	5.42	6.26	5.79	3.60	2.7
	2[a]	5.54	5.97	5.28	3.38	2.4
	3[a]	5.42	5.07	5.37	2.70	2.4
	4[a]	6.05	5.82	5.94	3.07	2.6
	5[a]	7.20	5.65	6.22	2.74	3.1
	6[a]	7.24	5.33	6.13	2.47	3.1
WA-Si-2	1[a]	7.55	6.64	6.92	3.30	4.7
	2[a]	7.80	7.77	7.65	3.86	
	3[a]	8.00	6.49	7.24	2.98	
	4[a]	9.90	8.08	10.67	2.85	5.2
	5[a]	9.90	7.35	11.28	2.29	
KM-15	1[a]	8.65	10.78	9.66	5.53	
WA-99	1[b]	8.90	8.84	8.20	4.06	
	2[b]	9.40	9.44	8.14	4.34	
KS	1[b]	8.20	9.70	8.94	3.02	
	2[b]	5.10	6.08	5.33	1.98	
GA529	1[c]	2.50	3.10	2.89	1.99	three samples
GA503	1[c]	1.15	1.43	1.37	0.94	supplied by
Litronic LiD	1[c,d]	1–2	1.29	1.23	0.85	Dr. Newman
KM-26	1[a,d]	1.07	1.76	1.62	1.12	
	2[a,d]	1.00	1.74	1.61	1.11	

[a]Samples are annealed at 1200 °C/1 h + quenched to room temperature.
[b]Samples are annealed at 1100 °C/15 min + quenched to room temperature.
[c]Samples are as-grown.
[d]Samples excluded from least-squares-fitting procedure (see text).

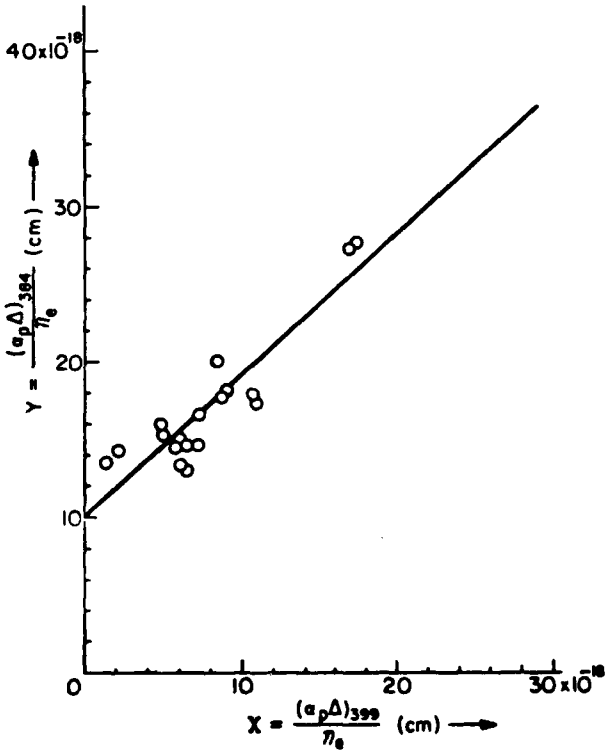

FIG. 2. $(\alpha_p\Delta)_{384}/n_e$ versus $(\alpha_p\Delta)_{399}/n_e$ for all the samples of Tables I and II. The line is a least-squares fit which yields values of $a^1 = 10.1\times10^{16}$ cm^{-1} and $b^1 = 9.3\times10^{16}$ cm^{-1} for $n_e^{\mathrm{I}} = a^1(\alpha_p\Delta)_{384} - b^1(\alpha_p\Delta)_{399}$ of model I (see text).

man indicated that a spectrometer inaccuracy produced α values approximately 30% too large for all of their measurements. This error should not influence the Δ values so the L-N[4] values for a and b should be raised from 5.29×10^{16} and 6.82×10^{16} cm^{-1} to 6.88×10^{16} and 8.87×10^{16} cm^{-1}, respectively. The values of $n_e^{\mathrm{L\text{-}N}}$ given in Table II are calculated by using these corrected L-N a and b values and our measured $(\alpha_p\Delta)$ in Eq. (1). Although the corrected a and b values are closer to our a^1 and b^1 values, the differences between the values of $n_e^{\mathrm{L\text{-}N}}$ in Table II and the n_e values from measurements are still as large as factor of 2–4. Clearly the 30% correction of the L-N measurements reduces but does not resolve the discrepancies discussed above. It should be pointed out that the present a^1 and b^1 values were derived entirely from crystals grown from a near-stoichiometric melt at the GaAs solidification temperature. No samples grown at low temperature from a Ga melt, i.e., LPE material, were used in the analysis. This latter restriction is important as some studies[6–8,12,13] have indicated that the defect chemistry of LPE and melt-grown samples may be quite different.

B. Analysis II: Two-donor and two-acceptor model

Although the principal LVM bands found in GaAs : Si samples have been each assigned to specified Si-related defects, i.e., Si_{Ga} (384 cm^{-1}), Si_{As} (399 cm^{-1}), and Si_{Ga}–Si_{As} (464 cm^{-1}, 393 cm^{-1}), the status of the 367- and 369-cm^{-1} bands is uncertain. As described previously, the 369-cm^{-1} band is found only in electron-irradiated samples of Si-doped GaAs. It has been suggested that this band is related

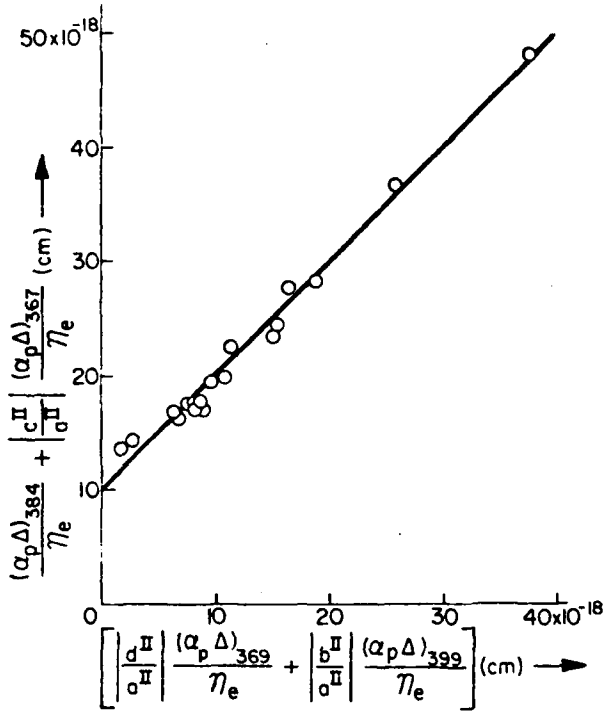

FIG. 3. $|(\alpha_p\Delta)_{384}/n_e + |c^{II}/a^{II}|[(\alpha_p\Delta)_{367}/n_e]|$ versus $\{|b^{II}/a^{II}| \times [(\alpha_p\Delta)_{399}/n_e] + |d^{II}/a^{II}|[(\alpha_p\Delta)_{369}/n_e]\}$ for all the samples of Tables I and II. The line is a least-squares fit which yields values of $a^{II} = +10.0\times10^{16}$ cm^{-1}, $b^{II} = -12.7\times10^{16}$ cm^{-1}, $c^{II} = +25.3\times10^{16}$ cm^{-1}, $d^{II} = -19.0\times10^{16}$ cm^{-1} for $n_e^{II} = a^{II}(\alpha_p\Delta)_{384} + b^{II}(\alpha_p\Delta)_{399} + c^{II}(\alpha_p\Delta)_{367} + d^{II}(\alpha_p\Delta)_{369}$ of model II (see text).

to $Si_{Ga}-V_{Ga}$ or some other "Si-containing" complex. The 367-cm^{-1} band was originally identified as one of the Si_{Ga}-Si_{As} pair bands. There is now question as to the origin of this band for two reasons. The first was mentioned earlier and is the lack of a mixed isotope band as was observed for each of the other two pair bands. The second is that it has been shown[21] that the $(\alpha_p\Delta)_{367}$ band strength can decrease upon prolonged irradiations but the other pair bands do not. The ratio of $(\alpha_p\Delta)_{367}$ to $(\alpha_p\Delta)_{393}$ for the samples in Tables I and II shows a large variation, i.e., from 0.2 to 0.8. Thus it appears that the 367-cm^{-1} band is not one of the Si_{Ga}–Si_{As} pair bands.

The $(\alpha_p\Delta)_{367}$ and $(\alpha_p\Delta)_{369}$ band strengths shown in Table I can become very large for the heavily doped samples. We considered the effect of these two bands with the previous 384-cm^{-1} (Si_{Ga}) and 399-cm^{-1} (Si_{As}) bands by using all four bands in the least-squares-fitting process. One can assume: $n_e^{II} = a^{II}(\alpha_p\Delta)_{384} + b^{II}(\alpha_p\Delta)_{399} + c^{II}(\alpha_p\Delta)_{367} + d^{II}(\alpha_p\Delta)_{369}$ in a four-dimensional least-squares fit without assuming any charge status for these four bands. The values for a^{II}, b^{II}, c^{II}, and d^{II} can be determined by applyng the four-dimensional least-squares-fitting procedure and formula[22] to all of the $(\alpha_p\Delta)$ values in Table I. Figure 3 shows a plot of $\{(\alpha_p\Delta)_{384}/n_e + |c^{II}/a^{II}|[(\alpha_p\Delta)_{367}/n_e]\}$ versus $\{|b^{II}/a^{II}|[(\alpha_p\Delta)_{399}/n_e + |d^{II}/a^{II}|[(\alpha_p\Delta)_{369}/n_e]\}$ for all of the samples of Tables I and II where $|\ |$ is the absolute value. The line is the result of a least-squares fit which yields values of

$$a^{II} = +10.0\times10^{16}\ \text{cm}^{-1},$$
$$b^{II} = -12.7\times10^{16}\ \text{cm}^{-1},$$
$$c^{II} = +25.3\times10^{16}\ \text{cm}^{-1},$$
$$d^{II} = -19.0\times10^{16}\ \text{cm}^{-1},$$

which gives

$$n_e^{II} = 10.0\times10^{16}(\alpha_p\Delta)_{384} - 12.7\times10^{16}(\alpha_p\Delta)_{399} + 25.3\times10^{16}(\alpha_p\Delta)_{367} - 19.0\times10^{16}(\alpha_p\Delta)_{369}.$$

The positive and negative signs for the values of a^{II}, b^{II}, c^{II}, and d^{II} represent their band status as donor and acceptor, respectively. The analysis indicates that the 367-cm^{-1} band is due to a donor defect and the 369-cm^{-1} band to an acceptor. The donor and acceptor nature of the defects responsible for the 384- and 399-cm^{-1} bands, respectively, are reaffirmed.

TABLE III. LPE layers (GaAs : Si).

Sample		Growth Temp. (°C)	Si_{Ga} $(\alpha_p\Delta)_{384}$ (cm^{-2})	Si_{As} $(\alpha_p\Delta)_{399}$ (cm^{-2})	367-cm^{-1} band[c] $(\alpha_p\Delta)_{367}$ (cm^{-2})	n_e (elect. meas.) (cm^{-3})	n_e^I (cm^{-3})	n_e^{II} (cm^{-3})
I[a]	1	750	126.6	80.7	18.5	4.8×10^{18} p[b]	5.3×10^{18} n[b]	7.1×10^{18} n
	2	840	338.4	296.6	52.6	2.1×10^{18} p	6.6×10^{18} n	9.4×10^{18} n
	4	910	165.4	144.7	24.4	2.0×10^{18} p	3.3×10^{18} n	4.3×10^{18} n
II[d]	65	Unknown	288.5	230.8	Unknown[c]	3×10^{18} p	7.7×10^{18} n	Unknown[c]
	67	900–807	538.5	442.3	Unknown[c]	3×10^{18} p	13.3×10^{18} n	Unknown[c]
	68	902–824	961.5	769.2	Unknown[c]	3×10^{18} p	25.6×10^{18} n	Unknown[c]
	79	882–802	111.5	88.5	Unknown[c]	3×10^{17} p	3.0×10^{18} n	Unknown[c]
	80	883–798	96.2	69.2	Unknown[c]	3×10^{17} p	3.3×10^{18} n	Unknown[c]
	77 (No Si)	884–802	0	0	Unknown[c]	0	0	Unknown[c]
	89	920–885	69.2	50.0	Unknown[c]	4.4×10^{18} n	2.3×10^{18} n	Unknown[c]
	90	919–880	215.4	123.1	Unknown[c]	4.2×10^{18} n	10.3×10^{18} n	Unknown[c]
	128	875	153.9	123.1	Unknown[c]	10^{17} p	4.1×10^{18} n	Unknown[c]
	24	900	92.3	61.5	Unknown[c]	10^{18} n	3.6×10^{18} n	Unknown[c]

[a]Data quoted from Kachare *et al.*[13]
[b]Majority-carrier type.
[c]Strengths of the 367-cm^{-1} bands are not given by L-N.[4]
[d]Data quoted from L-N[4] after 30% α_p correction—see text.
[e]No. 369-cm^{-1} band is found in LPE samples.

The values of n_e^{II} calculated in this way are also given in Table II with n_e^{I}. In almost all cases the optical value of n_e^{II} is within 15% of the measured value of n_e. The relative chi value for $N = 18$ samples and $n = 4$ parameters is 0.88×10^{18} cm^{-3} which is a considerable improvement over the first model. However, this result may be simply the effect of increasing the number of variables. The value for a^{II} is very close to a^{I}, however, b^{II} is about 30% larger than b^{I}. The values given here still differ significantly from the modified values of L-N. Although this four-band least-squares-fitting process gives a better fitting result than the previous model with only two bands, its validity still requires further investigation, especially the identification of the 367- and 369-cm^{-1} bands. It should also be pointed out that our calculated n_e^{I} and n_e^{II} values for two KM-26 samples in Tables I and II are much higher than the measured n_e values. This result was not unexpected as significant concentrations of other acceptors were found in these samples as was noted previously.

C. LPE samples

It was described previously that heavily Si-doped GaAs crystals grown from a nearly stoichiometric melt near the melt temperature of 1238 °C are always n type. However, GaAs having similar Si concentrations but grown at lower temperature, frequently between 750 °C and 1000 °C and from a Ga-rich solution containing dissolved Si, is frequently p type.[12,13] The conditions which determine whether a solution-grown LPE layer will be p type include the Si concentration, growth temperature, and crystallographic orientation of the substrate on which the layer is grown.[24] Some major differences in the characteristics of LPE and melt-grown GaAs : Si samples have been reported.[7,13,17] Infrared absorption results of these two types of materials indicate that only bands also seen in melt-grown samples compensated by e^- irradiation are observed in similarly compensated LPE samples. However, the 369-cm^{-1} band which is present in melt-grown samples is absent in the LPE samples. The infrared absorption results from previous studies indicate that $(\alpha_p \Delta)_{384} > (\alpha_p \Delta)_{399}$ even though the LPE layers were all p type before irradiation. If these defects were the only electrically active ones and the cross section of the Si_{A_s} band is approximately equal to that of Si_{G_a} band, the samples should have been n type prior to irradiation. So a model, in which an additional acceptor, which is not observed in the infrared absorption spectra, must be present in significant concentrations was proposed in some of the previous studies.[12,13] Table III shows integrated absorption data for the LPE layers quoted from the Kachare *et al.*[13] and the L-N[4] studies and also their calculated n_e^{I} and n_e^{II} by using the two sets of cross sections. A comparison of measured n_e value and calculated n_e^{I} or n_e^{II} value for each p type or even n type LPE sample seems to reafirm this previously reported model in which an additional Si-related acceptor defect of unknown nature is required.

ACKNOWLEDGMENTS

The authors are pleased to express their appreciation to Professor R.C. Newman for supplying three samples and helpful communications, and to Professor D.B. Wittry for useful discussions during electron microprobe analysis. The authors would also like to thank L. Lowe and D. Morris for their help with the electron irradiations and their hospitality to one of authors (W.G.S.) during his stay at Hanscom Field, Mass. This work was supported by the Air Force Office of Scientific Research (AFSC) under Grant/Contract 76-2990.

[1] W.G. Spitzer and W. Allred, J. Appl. Phys. 39, 4999 (1968).
[2] P.C. Leung, J. Fredrickson, W.G. Spitzer, A. Kahan, and L. Bouthillette, J. Appl. Phys. 45, 1009 (1974).
[3] W.G. Spitzer, *Advances in Solid State Physics XI*, edited by O. Madelung (Pergamon. New York, 1971), p. 1.
[4] K. Laithwaite and R.C. Newman, J. Phys. C 9, 4503 (1976).
[5] K. Laithwaite and R.C. Newman, Philos. Mag. 35, 1689 (1977).
[6] J.K. Kung and W.G. Spitzer, J. Appl. Phys. 44, 912 (1973).
[7] J.K. Kung and W.G. Spitzer, J. Appl. Phys. 45, 4477 (1974).
[8] J.K. Kung and W.G. Spitzer, J. Electrochem. Soc. 121, 1482 (1974).
[9] J.K. Kung and W.G. Spitzer, J. Appl. Phys. 45, 2254 (1974).
[10] L.H. Skolnik, W.G. Spitzer, A.H. Kahan, F. Euler, and R.G. Hunsperger, J. Appl. Phys. 43, 2146 (1972).
[11] K. Laithwaite, R.C. Newman, J.F. Angress, and G.A. Gledhill, *Sixth International Symposium on Gallium Arsenide and Related Compound*, Edinburgh, 1976, Inst. Phys. Conf. 33a (Institute of Physics, London, 1977), p. 133.
[12] W.G. Spitzer and M.B. Panish, J. Appl. Phys. 40, 4200 (1969).
[13] A.H. Kachare, W.G. Spitzer, J.M. Whelan, and G.H. Narayanan, J. Appl. Phys. 47, 5022 (1976).
[14] L. Skolnik, W.P. Allred, and W.G. Spitzer, J. Phys. Chem. Solids 32, 1 (1971).
[15] W.P. Allred, G. Cumming, J. Kung, and W.G. Spitzer, *2nd International Conference on Gallium Arsenide*, Dallas, Texas (Institute of Physics and the Physical Society, London, 1968), p. 66.
[16] W.G. Spitzer and W.P. Allred, Appl. Phys. Lett. 12, 5 (1968).
[17] G.H. Narayanan and A.H. Kachare, Phys. Status Solidi 26, 657 (1974).
[18] *Harshaw optical crystals* (Harshaw Chemical Company, Solon, Ohio 44138, 1967), pp. 38 and 48.
[19] W. Cochran, S.J. Fray, F.A. Johnson, J.E. Quarrington, and N. Williams, J. Appl. Phys. 32, 2101 (1961).
[20] J.R. Aronson, H.G. McLinden, and P.J. Gielisse, Phys. Rev. 135, A785 (1964); R.J. Collins and H.Y. Fan, Phys. Rev. 93, 674 (1953).
[21] R.C. Newman (private communication).
[22] Irving W. Burr, *Applied Statistical Methods*, (Academic New York, 1974), pp. 372–380.
[23] H. Kressel, J.W. Dunse, H. Nelson, and F.Z. Hawrylo, J. Appl. Phys. 39, 2006 (1968).
[24] B H. Ahn, R.R. Shurtz, and C.W. Trussel, J. Appl. Phys. 42, 4512 (1971).

Reprinted from JOURNAL OF THE ELECTROCHEMICAL SOCIETY
Vol. 127, No. 7, July 1980
Printed in U.S.A.

2. # Infrared Absorption and Microstructure of Li-Saturated Si-Doped GaAs

R. T. Chen* and W. G. Spitzer

Departments of Materials Science and Physics, University of Southern California, Los Angeles, California 90007

ABSTRACT

Infrared absorption, free carrier density, and transmission electron microscopy measurements have been correlated for n-type Si-doped GaAs samples with 1×10^{18} cm$^{-3} \lesssim$ [Si] $\lesssim 5 \times 10^{19}$ cm^{-3}. The infrared absorption of the localized vibrational modes was measured after the samples were compensated by e^- irradiation or by ^{6}Li saturation diffusion. Comparisons of the results of the two compensation methods indicate that: (*i*) the Li-native defect acceptor complex is responsible in large part for the compensation after a 750°C Li diffusion; (*ii*) the degree of the Si site transfer from Ga to As lattice sites as a result of the Li saturation diffusion at 950°C is a function of [Si] and the Li-native defect donor is probably responsible for this transfer; (*iii*) samples that are heavily Si-doped have Si-rich faulted loops produced by a heat-treatment or Li diffusion at 750°C and this excess Si transfers to As sites if Li is diffused at 950°C; (*iv*) absorption cross sections of the Li-native defect donor and acceptor bands can be determined which account for the compensation of the Li-diffused Si-doped samples and also fit previously published data for Li-saturated pure GaAs. There is also the suggestion that, at least in the nondiffused, nonannealed more heavily Si-doped material, not all of the Si shows up in the localized mode measurements even though there is no observable microstructure.

Results are presented here of an investigation of the behavior of Si and Li when they are simultaneously present as impurities in GaAs. This system is a complicated one since the behavior of either Si or Li when individually present as an impurity in GaAs is complex. However, a combination of optical, electrical, and microstructural measurements yields considerable insight into the nature of this double-doped system. In this study one observes clearly the influence of Li saturation diffusions in GaAs:Si at various temperatures on the concentrations of both Li and Si defects for a variety of Si concentrations. The presence of the Si inhibits the formation of certain Li-native defect complexes while the presence of the Li can cause the transfer of Si from one type of lattice site (Ga) to another (As). The measurements of compensated samples permit an estimate of the infrared absorption cross sections of the prominent localized vibrational mode (LVM) bands previously attributed to the two most important electrically active Li-native defect complexes.

The Si site transfer effect in Li-diffused GaAs:Si has been observed previously but was not studied in any detail (1). The present investigation demonstrates that the site redistribution is a function of Si concentration. It also shows that the observed LVM absorption bands produced by Si-related defects in low temperature Li-diffused, heavily Si-doped samples do not account for all the Si. Transmission electron microscope (TEM) measurements of the heavily doped samples after Li diffusion reveal some microstructure which could account for the unobserved Si.

* Electrochemical Society Active Member.
Key words: infrared absorption, microstructure, gallium arse[illegible]

Background

Gallium arsenide doped with Si has been of particular interest in a number of studies because of the amphoteric behavior of the Si. Silicon substitution on a Ga site, Si_{Ga}, is a donor and on an As site, Si_{As}, is an acceptor. The distribution of Si on the two sublattices is known to vary with the Si concentration (2-4), the temperature of growth (2-7), the temperature and time of heat-treatment (8-12), the nature and concentration of other impurities (13-15), and the vacancy concentrations (1, 8-11). Electroluminescent (16) and photoluminescent (8-10) characteristics, LVM absorption band strengths (1-7, 11-15), and transport properties (17) of the GaAs:Si are dependent on the distribution of Si on the two lattice sites. Other Si defects such as Si_{Ga}-Si_{As} nearest neighbor pairs and Si_{Ga}-native defect complexes have also been proposed and studied.

Lithium is an electrically active impurity in semiconductors and has been the subject of many investiga-

tions for both technological and scientific reasons. While lithium behaves as an interstitial donor in the elemental semiconductors Si and Ge, it is self-compensating in GaAs. Lithium can form either donor or acceptor defects in GaAs and can be used electrically to compensate either n- or p-type material. The relative concentrations of the different Li defects are controlled by the initial concentrations of electrically active impurities and by the tendency for self-compensation. There has been a considerable volume of literature (2, 18-29) dealing with the detailed behavior of Li in pure and doped GaAs, and as a result of these studies a number of specific defect species involving Li either with native defects or paired with other impurities have been identified.

The earlier studies of the GaAs:Si + Li system arose because of the Li behavior as an electrical compensator. In order to make infrared measurements of the LVM absorption bands in GaAs:Si it is necessary to reduce the free carrier absorption. The free carriers are present because heavily doped GaAs:Si is strongly n-type when grown from a nearly stoichiometric melt. One of the methods used for carrier removal was compensation by Li saturation diffusion at an elevated temperature. For reference Table I summarizes all LVM bands observed in GaAs:Si + Li as deduced from a number of studies (1-7, 11-14, 25, 29-31). Table I gives the peak absorption frequency for each band measured at liquid nitrogen temperature and the defect responsible for the band, where X_A refers to the species X on the A sites. According to the theory of localized vibrational modes the integrated absorption for each band is proportional to the volume concentration of the defect species responsible for the band. We refer to the constant of proportionality as the absorption cross section; $\int_{\text{band}} \alpha \, d\nu/[X_A]$, where α is the absorption coefficient and [ ] means concentration. The $\nu = 384$ and 399 cm^{-1} bands in Table I are due to Si_{Ga} and Si_{As} and their absorption cross sections have been established (3, 4). The $\nu = 389$ and 406 cm^{-1} bands are attributed to two electrically active ^{6}Li-native defect complexes, and the absorption cross sections for these bands are given in a later section of this work. These latter bands do not involve Si as they occur in Li-diffused undoped GaAs samples. The Si concentration does, however, play a significant role in determining the concentrations of these Li defect species. In Table I the band at $\nu = 367$ cm^{-1} has not been assigned to a specific defect. It was previously assigned to the $^{28}Si_{Ga}$-$^{28}Si_{As}$ nearest neighbor pair defect, however, recent experimental evidence has lead to the conclusion that this assignment is not correct (4, 32).

The electrical compensation of GaAs:Si which is necessary for the infrared studies has been accomplished by saturation diffusions of either Li or Cu at elevated temperatures, i.e., 700°C $\lesssim T_D \lesssim$ 1000°C, or by penetrating particle irradiation, i.e., 1 to 2 MeV electrons or by neutrons (31). In a few cases partial compensation was achieved (6, 12) by counterdoping with a compensating impurity such as Zn during crystal growth. If one wants to study the distribution of Si among the various defects then a major difficulty of all the above procedures is that the compensation process may alter the Si distribution and even create Si-related defects which were not present in significant concentration prior to the compensation procedure. Ample evidence exists for such changes. Saturation diffusions of Li or Cu result in the formation of Si_{Ga}-Li_{Ga} or Si_{Ga}-Cu_{Ga} second neighbor pairs, and Li diffusion at $T_D \gtrsim 900$°C can cause the transfer of substitutional Si from Ga to As sites (1). Also Li and Cu diffusions are done at temperatures, i.e., $T_D \gtrsim 400$°C, and times for which major aging effects have been observed (11, 33), and these effects are attributed to changes in Si defect concentrations as well as the formation of new defects. The compensation by electron irradiation is frequently done with the sample maintained near liquid nitrogen temperature during the irradiation to reduce thermal annealing. Subsequently the sample is allowed to warm to room temperature. There is the concern that native defects introduced by the irradiation might pair with some of the Si defects and thus alter the defect concentrations (31). In one study (3) the irradiation was continued to fluences approximately five times that necessary to render the samples transparent at frequencies where there is little lattice or LVM absorption. Essentially no changes were observed in the absorption at the Si_{Ga} or Si_{Ga}-Si_{As} LVM frequencies as a result of this extended irradiation fluence. Further measurements of the removal rate (31) for the Si_{As} band with increases in electron fluence indicate that for the total fluences used in the present study there should be no significant change produced in this band. As will be discussed the present measurements are in accord with this view. From the evidence available the e^--irradiation method of compensation appears to be the least disturbing to the precompensation distribution of Si defects and in the present work it is assumed that the Si defect concentrations are the same as the precompensated values.

The site transfer of substitutional Si from Ga to As sites in GaAs has been inferred in several studies. Two reports (8, 9) describe thermally related photoluminescence changes introduced in n-type Si-doped GaAs. In one case the change was by heating heavily doped crystals ($n_e \simeq 4 \times 10^{18}$ cm^{-3}) in hydrogen at 1050°C and the other case by heating lightly doped material ($n_e \simeq 3 \times 10^{16}$ cm^{-3}) in evacuated quartz ampuls at 900°C. These two studies indicate that Si atoms may transfer from Ga to As sites via an As vacancy mechanism. One more recent photoluminescence measurement (10) of lightly doped GaAs:Si ($n_e \simeq 3.3 \times 10^{16}$ cm^{-3}) which was annealed in vacuum at a temperature of 800°C has also resulted in the same conclusion. It was also reported (13, 15) that for heavily double-doped crystals of GaAs:Si + Te and GaAs:Si + Se, the effect of the Te or Se is to substantially enhance the fraction of the Si concentration, [Si], which resides on As sites and thus to reduce the [Si_{Ga}]. The effect of redistribution of Si between substitutional sites induced by the saturation diffusion of Li at elevated temperatures has been previously observed (1) only for Si-doped GaAs with $n_e \simeq 9.0 \times 10^{17}$ cm^{-3} and was not studied in any detail.

In the present study a comparison is made of the LVM absorption and microstructure for identically doped samples compensated either by ^{6}Li diffusion or by e^- irradiation as well as comparing the influence of different diffusion temperatures on the degree of Si site transfer. These comparisons are made by using sets of identical samples for the different treatments. Different sets of samples are used to cover a range of values for n_e and [Si].

Table I. A list of all observed LVM bands in ^{6}Li-diffused Si-doped GaAs

Mode frequency (cm^{-1})	Electrical character	Impurity	Defect
352			
389	Acceptor	^{6}Li	^{6}Li-native defect complexes
406	Donor		
410			
461			
470		$^6Li_{Ga}$	Si_{Ga}-$^6Li_{Ga}$
480			
487			
374		Si_{Ga}	
379			
405			
384	Donor	Si_{Ga}	Si_{Ga}
399	Acceptor	Si_{As}	Si_{As}
388		Si_{Ga}-Si_{As}	Si_{Ga}-Si_{As}
404			
367	?	—	Si-related defect

Experimental Method

The samples were taken from several horizontal Bridgman-grown ingots which were doped with different Si concentrations. Some ingots were single crystals while others were polycrystalline but with very large single crystal sections, i.e., typical dimensions of centimeters. The samples were always taken from the single crystal regions. The total Si concentration was 1×10^{18} cm^{-3} $\lesssim$ [Si] $\lesssim$ 5×10^{19} cm^{-3} as estimated from the dopant added during crystal growth by using the known segregation coefficient and also from spectrochemical analyses. In a few cases the [Si] was also measured by using an electron probe microanalyzer.

All samples were first heat-treated at 1200°C for 1 hr and then quenched to room temperature, a process hereafter called HT + Q. The HT + Q treatment establishes a common thermodynamic background for all samples. It avoids some of the known and previously mentioned lower temperature aging effects for both the free carrier density, n_e and the Si defect concentrations. These aging effects are generally present in the as-grown material because of a cool-down cycle in the growth process. The carrier densities after HT + Q ranged from 1.0×10^{18} cm^{-3} $\lesssim n_e \lesssim$ 8.0×10^{18} cm^{-3}. The HT + Q procedure has essentially no effect on the n_e for material with [Si] $\lesssim 1 \times 10^{18}$ cm^{-3} but it substantially increases n_e for samples with [Si] $\gtrsim 1 \times 10^{19}$ cm^{-3}. This procedure also significantly improves the microstructural quality of the material, particularly for the heavily Si-doped samples.

After the HT + Q treatment the free electron density of each sample was measured by determining the frequency of the free carrier plasma minimum observed in the infrared reflectivity. This method has been compared previously (34) with Hall measurement results and very good agreement was obtained. Before taking the measured n_e as the bulk value sufficient material was removed from the surfaces, ~0.1 mm, that the infrared reflectivity measurements of the plasma frequency indicated that further removal of material did not change the carrier density.

Several samples with nearly the same free carrier density were cut from the same section of each ingot and were divided into two groups. One group was compensated by e^- irradiation while the other group of samples was saturation diffused with ^{6}Li in an inert atmosphere, some at $T_D = 750$°C for 18 hr and others at $T_D = 950$°C for 2 hr. The diffusions were done with a "sandwich" arrangement in which the sample of interest was placed between two pure GaAs blocks which had previously been surface alloyed with ^{6}Li on the outer surfaces, i.e., the surfaces not in contact with the sample to be diffused. This procedure substantially reduced the loss of material which occurs when the sample of interest is surface alloyed with Li directly. The details of the procedure used for the Li diffusions have been reported elsewhere (22). The samples of the first group were compensated by 1.4 MeV e^- irradiation while at temperatures $\lesssim$ 140°K and with electron fluences of $\sim 1 \times 10^{19}$ e^-/cm^2.

The infrared absorption coefficient at liquid nitrogen temperature of the Li-diffused and the e^--irradiated samples was measured. The spectral range covered was 350 cm^{-1} $\lesssim \nu \lesssim$ 500 cm^{-1} which contains the frequencies of all the absorption bands of interest in this study. The samples were generally about ~0.3 mm thick and had a wedge of ~0.2° to eliminate multiple reflection interference fringes. The absorption coefficient α was calculated from the transmission T by using the usual formula

$$T = I_{Sample}/I_0 = (1 - R)^2 \exp(-\alpha x)/1 - R^2 \exp(-2\alpha x)$$

where R is the reflectivity and x is the sample thickness.

After the infrared transmission measurements all Si-doped samples, as well as some pure GaAs samples which had been saturation diffused with ^{6}Li, were used to prepare specimens for transmission electron microscope measurements (35). The TEM specimens were examined by a Hitachi HU-125C microscope operated at 125 kV. Measurements were also made of the HT + Q, Si-doped materials before Li diffusion as well as undoped samples and they were free of microstructure except for an occasional dislocation loop. In particular the samples showed no stacking faults or precipitates while the Si-doped samples which had not been given the HT + Q treatment, i.e., in the as-grown condition, were found to have frequent extrinsic stacking faults, particularly those samples having the larger [Si] (36).

Results and Discussion

In this section the results are presented in the following order:

1. The changes introduced by Li diffusion into GaAs:Si at 750°C are examined by comparison with e^--irradiated samples. Some of the irradiated samples will have no prior annealing while others were thermally aged at 700°C prior to the irradiation.
2. A comparison is made of samples which have been Li-diffused at two different temperatures and the Li-induced Si transfer from Ga to As sites is examined including the [Si] dependence of the transfer process.
3. The possible role of the known Li-native defect complexes in the Si site transfer process is explored.
4. The LVM absorption measurements of the Li saturation diffused GaAs:Si samples are used with other data to estimate the absorption cross sections of the two bands arising from the two electrically active Li defect complexes. These cross sections are then tested by applying them to previously reported LVM measurements of Li-saturated undoped GaAs.
5. TEM results for the microstructure of the Li-diffused samples are discussed and correlated to the LVM measurements and the Si site transfer observations.

Changes in defect structure and concentration resulting from ^{6}Li saturation diffusion at 750°C.—One of the primary purposes of the present study is to investigate the site transfer of Si in GaAs:Si which results from ^{6}Li saturation diffusions at an elevated temperature, i.e., 950°C. This effect is demonstrated by direct comparisons with samples diffused at a lower temperature of 750°C where the transfer process is found to be negligible. However, before reviewing the data for the above comparison it is of interest to inquire first into the changes introduced by Li diffusion at 750°C as compared to the prediffused state. The LVM spectra of the prediffused state is taken to be that of the e^--irradiated samples. As mentioned previously, the heavily doped GaAs:Si undergoes changes due to thermal aging at temperatures such as 750°C and therefore the effect of the diffusion on Si distribution could be the result of the 750°C diffusion temperature and/or the presence of a large Li concentration.

To demonstrate the changes three absorption curves are used, one for a sample which was Li saturated at 750°C, a second e^- irradiated, and a third annealed near 750°C and then e^- irradiated. These comparisons allow one to attribute the changes as due primarily to Li saturation or due to thermal annealing at the diffusion temperature.

Figure 1 shows the LVM absorption bands for three samples of nearly equivalent [Si] $\simeq 5 \times 10^{18}$ cm^{-3} and $n_e \simeq 8 \times 10^{18}$ cm^{-3} after the HT + Q treatment. Sample 7-a, see curve I, was compensated by ^{6}Li saturation diffusion at 750°C and sample WA-2-3 was electron irradiated, see curve II. The data for these

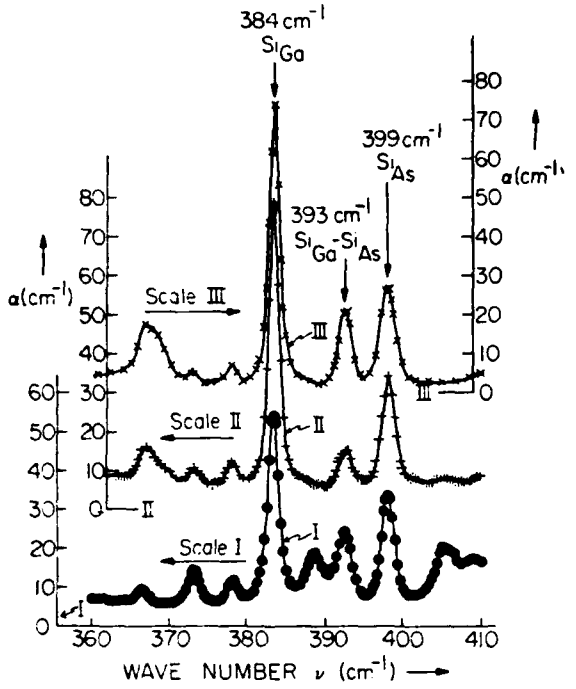

Fig. 1. Infrared absorption spectrum at liquid nitrogen temperature for three GaAs:Si samples having nearly equivalent [Si] ≃ 5 × 10^{19} cm^{-3} and with initial $n_e \simeq 8 \times 10^{18}$ cm^{-3} after 1200°C/1 hr + quench (see Table II). Curve I: sample 7-a, 750°C ^{6}Li diffused. Curve II: sample WA-2-3, compensated by e^- irradiation. Curve III: sample annealed at 700°C then compensated by e^- irradiation.

two samples including the integrated absorption ($\alpha_p\Delta$) of the LVM are among those of Table II, where α_p is the peak LVM absorption coefficient with the background removed and Δ is the bandwidth at half-maximum. Curve III of Fig. 1 is for the third sample which was annealed at 700°C before being compensated by electron irradiation. The $(\alpha_p\Delta)_{399}$ is the same for the three samples indicating that the [Si_{As}] is independent of the compensation method or thermal aging as long as the temperatures involved are ~750°C. The Si_{Ga}-Si_{As} nearest neighbor pair band at 393 cm^{-1} is the same for the annealed sample and the diffused sample but they both are approximately twice the value for the nonannealed, nondiffused sample. This indicates that there is a substantial increase in [Si_{Ga}-Si_{As}] for the diffused and annealed samples, and this increase is clearly a thermal effect rather than the result of the presence of a large [Li]. The $(\alpha_p\Delta)_{384}$ for the Si_{Ga} band of the annealed sample is 102.5 cm^{-2} which is below the 117.3 cm^{-2} of the nonannealed sample, but significantly larger than the 78.3 cm^{-2} of the diffused sample. The decrease of [Si_{Ga}] in the diffused sample therefore appears to be largely a combination of thermal aging and the formation of (Si_{Ga}-Li_{Ga}) pairs which give rise to the bands at 374, 379, and 405 cm^{-1}, see Table I and Fig. 1-curve I. Several other bands are observed in the absorption spectra of Fig. 1. The weak bands near 374 and 379 cm^{-1} in the nondiffused samples are due to the LVM of the $^{30}Si_{Ga}$ and $^{29}Si_{Ga}$ and they superimpose upon two of the $^{28}Si_{Ga}$-Li_{Ga} bands, see curve I. The 367 and 369 cm^{-1} bands are poorly resolved and are related to unknown defects involving Si; see Ref. (4) for a discussion of these modes. The 389 cm^{-1} band in the diffused sample is due to a Li-native defect complex which is not Si related, see Table I.

These results necessitate a reinterpretation of some previously published data in which the samples were not given the HT + Q treatment prior to electron irradiation or ^{7}Li diffusion at 700°C (30). This prior comparison between Li diffusion and e^- irradiation was therefore between samples which had been thermally aged in an unknown temperature profile during the growth process. Therefore, the effective anneal temperature is unknown although a temperature zone of ~800°C was used after the growth zone.

A more complete comparison of the nonannealed, e^--irradiated, and 750°C ^{6}Li-diffused cases for different [Si] is given by the data of Table II. In all cases the absorption was measured at liquid nitrogen temperature. The data of Table II were taken from samples such as those in Fig. 1. The data for the irradiated samples were also used in Ref. (4) where they are discussed in detail. From Table II it is seen that the changes observed in Fig. 1 and the conclusions based on those changes appear to apply generally with larger changes being observed at higher [Si]. In particular, it can be concluded that the saturation diffusion of Li at 750°C produces no change in the concentration of Si_{As} acceptors, significant increases in the concentration of Si_{Ga}-Si_{As} nearest neighbor pairs, and decreases in the concentration of Si_{Ga} donors with all changes being measured relative to the prediffused state. With this information we may now examine the changes which occur when the saturation temperature is increased.

Si site transfer induced by Li saturation diffusion.— Figure 2 and curve I of Fig. 3 show the absorption coefficient of three samples having different [Si] which were ^{6}Li diffused at 950°C. Each of these samples is similar to one of those diffused with ^{6}Li at 750°C. The results of 750° and 950°C saturation diffusions of ^{6}Li are summarized quantitatively in Table III for pairs of initially similar samples. Comparisons indicate that the 384 and 399 cm^{-1} bands of the Si_{Ga} and Si_{As}, respectively, have changed their relative strengths while the other Si-related bands remain essentially unchanged. The 384 cm^{-1} band is reduced and the 399

Table II. Comparisons of LVM results for e^- irradiation and 750°C ^{6}Li diffusion

Sample No.	n_e* (cm^{-3})	Compensation method	$(\alpha_p\Delta)_{384}$ (cm^{-2})	$(\alpha_p\Delta)_{389}$ (cm^{-2})	$(\alpha_p\Delta)_{393}$ (cm^{-2})	$(\alpha_p\Delta)_{399}$† (cm^{-2})	$(\alpha_p\Delta)_{377}$ (cm^{-2})	$(\alpha_p\Delta)_{374}$ (cm^{-2})	$(\alpha_p\Delta)_{379}$ (cm^{-2})
KM-28-1	1.07 × 10^{19}	e^- irradiation	20.8	3.6	0	0	0		
1-a	1.0 × 10^{19}	^{6}Li** diffusion	18.1	5.7	~2	—	0	~1.2	~0.5
KM-16-3	8.4 × 10^{18}	e^-	79.1	31.2	8.4	1.0	6.4		
4-a	8.3 × 10^{18}	^{6}Li**	89.1	30.8	18.5	—	1.8	11.6	8.6
KM-16-4	6.1 × 10^{18}	e^-	91.0	36.0	8.6	1.0	6.4		
5-a	5.7 × 10^{18}	^{6}Li**	61.8	35.6	22.2	—	2.8	11.2	8.0
WA-81-2-2	7.8 × 10^{18}	e^-	129.9	57.2	20.4	1.2	8.6		
6-a	7.7 × 10^{18}	^{6}Li**	82.5	53.2	46.6	—	7.4	17.1	12.8
WA-81-2-3	8.0 × 10^{18}	e^-	117.3	57.4	21.6	7.0	16.4		
7-a	8.0 × 10^{18}	^{6}Li**	78.3	56.2	41.2	—	8.3	15.6	11.6

* Measured.
** ^{6}Li diffusion at 750°C for 18 hr.
† 399 cm^{-1} band only found in e^--irradiated heavily doped sample.
— Not observed.

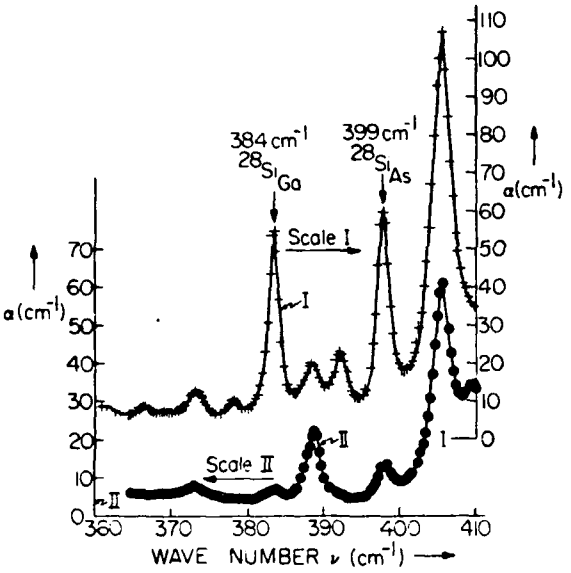

Fig. 2. Infrared absorption spectrum at liquid nitrogen temperature for two GaAs:Si samples having different [Si] and initial n_e; both ^{6}Li diffused at 950°C for 2 hr. Curve I: sample 6-b ($n_e \simeq 7.7 \times 10^{16}$ cm^{-3}). Curve II: sample 1-b ($n_e \simeq 1.0 \times 10^{16}$ cm^{-3}).

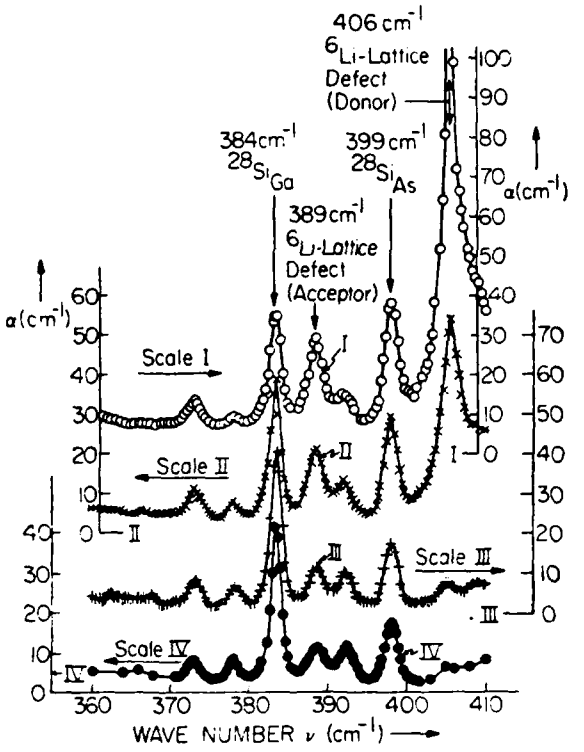

Fig. 3. Infrared absorption spectrum at liquid nitrogen temperature for four GaAs:Si samples having an identical initial $n_e \simeq 5.3 \times 10^{16}$ cm^{-3}. All were ^{6}Li diffused and in one case subsequently outdiffused. Curve I: sample 4-b, 950°C/2 hr ^{6}Li diffused. Curve II: sample 4-c, 900°C/3 hr ^{6}Li diffused. Curve III: sample 4-a, 750°C/18 hr ^{6}Li diffused. Curve IV: sample 4-c', 900°C/3 hr ^{6}Li diffused + 700°C/24 hr ^{6}Li outdiffused.

cm^{-1} band enhanced for the higher diffusion temperature suggesting site transfer of Si from Ga to As sites has been produced. This relative decrease of the 384 cm^{-1} band after the higher temperature diffusion decreases with increasing [Si] while the relative increase for the 399 cm^{-1} band increases. The Si_{Ga}-Si_{As} pair band strengths at 393 cm^{-1} are almost the same for two diffusion temperatures for each set of samples indicating that the large annealing-induced increase observed at 750°C does not continue with increased Li diffusion temperature. There is no consistent pattern of change and the observed changes are small between the two diffusion temperatures for all other bands.

One can examine site transfer hypothesis quantitatively if the absorption cross sections of the Si defect bands are known. In a recent study (4) the cross sections of Si_{Ga}, Si_{As}, and two other Si-related defect bands were measured for a number of melt-grown Bridgman, HT + Q samples having [Si] and n_e in the range of those used here. All samples were compensated by e^- irradiation. Assuming the $^{28}Si_{Ga}$ donor (384 cm^{-1} band), $^{28}Si_{As}$ acceptor (399 cm^{-1} band), and two other Si-related defects (367 and 369 cm^{-1} bands) to be electrically active defects then the reciprocal absorption cross sections were determined to be $a = 10.0 \times 10^{16}$ cm^{-1}, $b = 12.7 \times 10^{16}$ cm^{-1}, $c = 25.3 \times 10^{16}$ cm^{-1}, and $d = 19.0 \times 10^{16}$ cm^{-1}, where

$$n_e = a(\alpha_p\Delta)_{384} - b(\alpha_p\Delta)_{399} + c(\alpha_p\Delta)_{367} - d(\alpha_p\Delta)_{369}$$
$$= [Si_{Ga}] - [Si_{As}] + [Si]_{367} - [Si]_{369}$$

As indicated by the signs the charge status found for 367 and 369 cm^{-1} bands are donor and acceptor, respectively. For all of the Li-diffused samples shown in Table III the 369 cm^{-1} band is not observed and the 367 cm^{-1} band is always small and has almost no change in value at different diffusion temperatures. If one assumes that site transfer of Si_{Ga} to Si_{As} is the only mechanism responsible for the changes in the Si

Table III. Comparisons of LVM results of 750° and 950°C ^{6}Li diffusion measurements

Sample set No.	Sample No./T_D of ^{6}Li (°C)	n_e* (cm^{-3})	$(\alpha_p\Delta)_{384}$ (cm^{-2})	$(\alpha_p\Delta)_{399}$ (cm^{-2})	$(\alpha_p\Delta)_{368}$ (cm^{-2})	$(\alpha_p\Delta)_{367}$ (cm^{-2})	$(\alpha_p\Delta)_{376}$ (cm^{-2})	$(\alpha_p\Delta)_{389}$ (cm^{-2})	$(\alpha_p\Delta)_{401}$ (cm^{-2})
1	1-a/750	1.0×10^{16}	18.1	5.7	~2	0	~1.2	9.6	0
	1-b/950	1.0×10^{16}	6.4	17.8	~2	0	5.5	41.9	187.0
2	2-a/750	1.8×10^{16}	34.8	10.5	4.8	0	5.0	15.1	0
	2-b/950	1.8×10^{16}	26.3	20.0	~4.8	0	3.0	15.5	96.1
3	3-a/750	3.1×10^{16}	43.1	18.9	~8.0	0	9.9	21.6	0
	3-b/950	3.1×10^{16}	24.5	41.8	~8.0	0	6.8	44.5	221.7
4	4-a/750	5.3×10^{16}	89.1	30.8	13.5	1.8	11.6	23.0	0
	4-b/950	5.3×10^{16}	44.2	64.0	18.1	0	13.4	84.2	348.2
5	5-a/750	8.7×10^{16}	61.8	35.6	23.3	2.8	11.2	27.6	0
	5-b/950	8.7×10^{16}	47.0	71.4	22.4	0	12.5	84.2	343.2
6	6-a/750	7.7×10^{16}	82.5	53.2	45.5	7.4	17.1	34.6	0
	6-b/950	7.7×10^{16}	72.4	110.7	38.6	3.5	12.6	35.5	317.1
7	7-a/750	8.0×10^{16}	78.3	56.3	41.2	5.3	15.6	34.8	0
	7-b/950	8.0×10^{16}	58.2	92.0	42.0	6.2	15.9	35.0	194.1

* Measured values.

Table IV. The values of β calculated from Table III as a function of initial n_e

Sample set No.	n_e* (cm^{-3})	$\delta(\alpha_p\Delta)_{384}$** ($cm^{-1}$)	$\delta(\alpha_p\Delta)_{399}$** ($cm^{-1}$)	$\beta = \frac{-\delta(\alpha_p\Delta)_{384}}{\delta(\alpha_p\Delta)_{399}}$
1	1.0×10^{18}	−11.7	+12.1	+0.97
2	1.8×10^{18}	−8.5	+9.5	+0.89
3	3.1×10^{18}	−18.6	+22.9	+0.81
4	5.3×10^{18}	−14.9	+33.2	+0.45
5	5.7×10^{18}	−14.8	+35.8	+0.41
6	7.7×10^{18}	−9.1	+57.5	+0.16
7	8.0×10^{18}	+9.9	+36.8	−0.27

* Measured values.
** $\delta(\alpha_p\Delta)$ = $(\alpha_p\Delta)$ at 950°C − $(\alpha_p\Delta)$ at 750°C.

band strengths of the isolated Si species, then one has $\delta[Si_{Ga}] = -\delta[Si_{As}]$ and thus

$$\beta = \delta(\alpha_p\Delta)_{384}/\delta(\alpha_p\Delta)_{399} = +b/a = +1.27$$

Table IV gives the values for β calculated from Table III and Fig. 4 gives β as a function of n_e. At the lower values of n_e most of the change is indeed accounted for by Si site transfer. However, as n_e and [Si] increase the value of β decreases and the change becomes progressively less due to $Si_{Ga} \rightarrow Si_{As}$. Since the other Si defect concentrations do not appear to change significantly, the large increases in $(\alpha_p\Delta)_{399}$ must be due to transfer of Si to Si_{As} from some state or states not detected by the LVM measurements made after 750°C Li diffusion. For the samples of largest [Si] this latter process dominates the change. From the TEM measurements mentioned previously it is known that there are no precipitates, inclusions, or extrinsic stacking faults in the prediffused samples. Later, TEM measurements will be presented of both 750° and 950°C Li-diffused samples which show that Si-rich loops form at 750°C and disappear at 950°C for the more heavily Si-doped material. Also GaAs:Si samples which were annealed at 900° and 1000°C and then e^- irradiated showed no evidence for the Si site transfer process. The large Li donor concentration present under the conditions of the high temperature saturation diffusion apparently enhances the formation of Si_{As} acceptors. One may thus conclude that site transfer of Si from Ga to As sites is indeed observed for the high temperature Li diffusion. The site transfer is not simply a thermal process, i.e., the presence of the Li is required. Comparisons between low and high temperature Li-saturated samples indicate that at the low [Si] almost all of the $[Si_{As}]$ gain for the high temperature case is the result of Si_{Ga} site transfer while at the highest [Si] almost all the $[Si_{As}]$ gain results from some other source of Si.

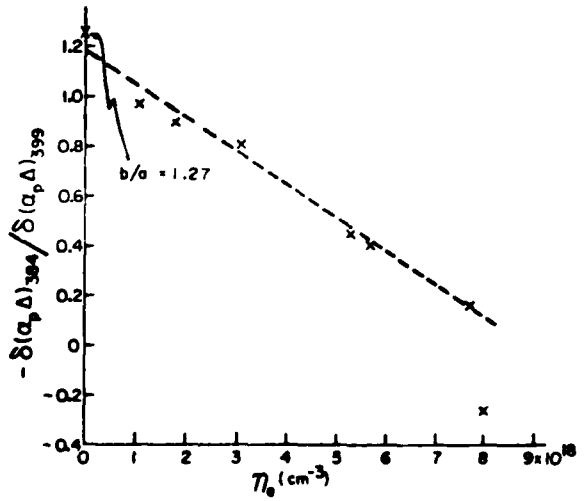

Fig. 4. A plot of $\beta = -\delta(\alpha_p\Delta)_{384}/\delta(\alpha_p\Delta)_{399}$ vs. initial n_e for all of the samples of Table IV. For site transfer only $\beta = 1.27$.

Possible role of Li-native defect complexes in Si site transfer.—From the preceding section we concluded that the presence of the Li was required to produce the site transfer and increase in $[Si_{As}]$. It is of interest to inquire whether one can detail in any way how the Li is instrumental in producing this effect and why the higher diffusion temperature is required.

The strengths of the Li-lattice defect complex bands induced by ^{6}Li diffusion of pure GaAs are very small for a low diffusion temperature (21), i.e., at $T_D \lesssim 750$°C, and they increase *monotonically* with T_D. The 389 cm^{-1} (acceptor) and 406 cm^{-1} (donor) bands are known to be the only two bands induced by Li-lattice defect complexes which are electrically active. For pure GaAs the ratio $(\alpha_p)_{406}/(\alpha_p)_{389}$ is approximately 2 at higher diffusion temperatures, $T_D \gtrsim 800$°C (21, 22).

Examination of all absorption curves for ^{6}Li-diffused, Si-doped GaAs samples with different initial n_e and [Si] which were diffused at lower temperatures, i.e., $T_D \lesssim 750$°C, indicates that the 389 cm^{-1} acceptor band is the only Li-lattice defect band observed with significant strength and it increases in samples with higher n_e and Si values as shown in Table V. This indicates that the growth of the 389 cm^{-1} Li-native defect acceptor band may be a significant factor in the compensation of Si-doped GaAs for the lower temperature diffusions. As a comparison this result is quite different from that of Li-diffused p-type GaAs for a similar diffusion temperature. In this latter case, no Li-lattice defect bands are observed. In particular the 389 cm^{-1} band is absent. The compensation is completely accomplished (28) by forming Li_i-Mg_{Ga} (or -Zn_{Ga}, or -Cd_{Ga}, or -Mn_{Ga}) neutral pairs.

For the high temperature diffusion, $T_D \simeq 950$°C, the Li-lattice defect complex bands in the present samples have increased substantially. To illustrate this Fig. 3 shows the absorption curves for four GaAs:Si samples having a common origin and identical n_e values but ^{6}Li diffused or outdiffused at different temperatures. Comparisons between these curves indicate that the saturation concentration of Li increases due to a higher diffusion temperature, the 389 and 406 cm^{-1} Li-lattice defect bands both increase, however, the growth rate of 406 cm^{-1} Li-lattice donor band is much larger than that of the 389 cm^{-1} acceptor band. It is this donor formation which likely provides the mechanism producing Si acceptor formation by the transfer of Si to As sites from other defects. When Li is outdiffused at a lower temperature the absorption curve tends to return to the curve it would have if indiffused at that temperature; see curve IV of Fig. 3. In particular, the site transfer produced in a 900°C diffusion has reversed and the 406 cm^{-1} band has disappeared. Furthermore, a 950°C ^{6}Li rediffusion after a 750°C diffusion produces Si site transfer with similar LVM curves as a sample diffused initially at 950°C.

Table V. Comparison of the $(\alpha_p)_{389}$ values for all 750°C ^{6}Li-diffused samples

Sample No./ T_D of ^{6}Li (°C)	n_e* (cm^{-3})	$(\alpha_p)_{389}$ (cm^{-1})
Pure GaAs/750	—	~0.5
1-a/750	1.0×10^{18}	4.0
2-a/750	1.8×10^{18}	5.5
3-a/750	3.1×10^{18}	9.0
4-a/750	5.3×10^{18}	10.0
5-a/750	5.7×10^{18}	11.5
6-a/750	7.7×10^{18}	14.4
7-a/750	8.0×10^{18}	14.2

* Measured values.

Table VI. Comparison of the $(\alpha_p)_{406}/(\alpha_p)_{389}$ ratios for all 950°C ^{6}Li-diffused samples

Sample No./ T_D of ^{7}Li (°C)	n_e* (cm^{-3})	$(\alpha_p)_{389}$ (cm^{-1})	$(\alpha_p)_{406}$ (cm^{-1})	$\frac{(\alpha_p)_{406}}{(\alpha_p)_{389}}$
Pure GaAs/950°C	0	~32	~64	~2
1-b/950	1.0×10^{18}	18.2	55.0	~3
2-b/950	1.8×10^{18}	6.2	17.0	~3
3-b/950	3.1×10^{18}	17.8	65.0	~4
4-b/950	5.3×10^{18}	22.6	105.5	~5
5-b/950	5.7×10^{18}	22.6	104.0	~5
6-b/950	7.7×10^{18}	14.2	99.1	~7
7-b/950	8.0×10^{18}	14.6	53.4	~4

* Measured values.

Table VI shows that the $(\alpha_p)_{406}/(\alpha_p)_{389}$ ratio in general increases with increases of n_e for samples which are ^{6}Li diffused at 950°C for 2 hr. This observation is consistent with the result that in more heavily doped samples more Si transfers to As sites producing more acceptors.

The conclusion here is that the primary Li defect responsible for the enhancement of the Si_{As} concentration is the Li donor responsible for the LVM band at 406 cm^{-1} (for ^{6}Li). The increase in the concentration of this Li defect with temperature as measured by the LVM absorption is the reason why the site transfer requires the high diffusion temperature. The concentration of this Li defect and the Si_{As} both increase with the total [Si].

Absorption cross sections of Li-native defect complex bands.—From the discussion in the previous section we see that the electrically active defects in the Li-saturated samples are the Si_{Ga} donor, the Si_{As} acceptor, the Si-related donor responsible for the 367 cm^{-1} band, the Li donor responsible for the 406 cm^{-1} band, and finally the Li acceptor giving the 389 cm^{-1} band. One can now use this information to obtain the absorption cross sections for the Li bands. For all of the 750° and 950°C ^{6}Li-diffused samples of Table III one can use the fact that the samples are highly compensated after diffusion to obtain

$$n_e = 0 = a(\alpha_p\Delta)_{384} - b(\alpha_p\Delta)_{399} + c(\alpha_p\Delta)_{367} + E(\alpha_p\Delta)_{389} + F(\alpha_p\Delta)_{406}$$

where a, b, and c have been previously given. If the two Li defects are singly charged then E and F are the reciprocal cross sections for the Li defect bands. If either Li defect is a doubly charged donor or acceptor then the corresponding coefficient contains a factor of 2. For the 389 and 406 cm^{-1} bands our best estimated values of Δ are 2.4 ± 0.2 and 3.4 ± 0.2 cm^{-1}, respectively. Both of these bands overlap other bands which frequently made determinations of Δ difficult. Figure 5 shows a plot of $(\alpha_p\Delta)_{406}/\eta$ *vs.* $(\alpha_p\Delta)_{389}/\eta$. Here

$$\eta = -[a(\alpha_p\Delta)_{384} - b(\alpha_p\Delta)_{399} + c(\alpha_p\Delta)_{367}] = E(\alpha_p\Delta)_{389} + F(\alpha_p\Delta)_{406}$$

where all samples of Table III except sample 2-b are included. Sample 2-b was omitted because η was orders of magnitude smaller than for the other samples. Also note that $d(\alpha_p\Delta)_{389}$ is omitted as that band does not occur in Li-diffused samples. The line in Fig. 5 is a least squares fit which gives values for E and F of

$$E = -9.7 \times 10^{16}\ cm^{-1}$$

$$F = +2.8 \times 10^{16}\ cm^{-1}$$

where the signs indicate the 389 cm^{-1} band is an acceptor and the one at 406 cm^{-1} is a donor as expected from previous assignments. Application of these values for E and F and the n_e equation given above to the

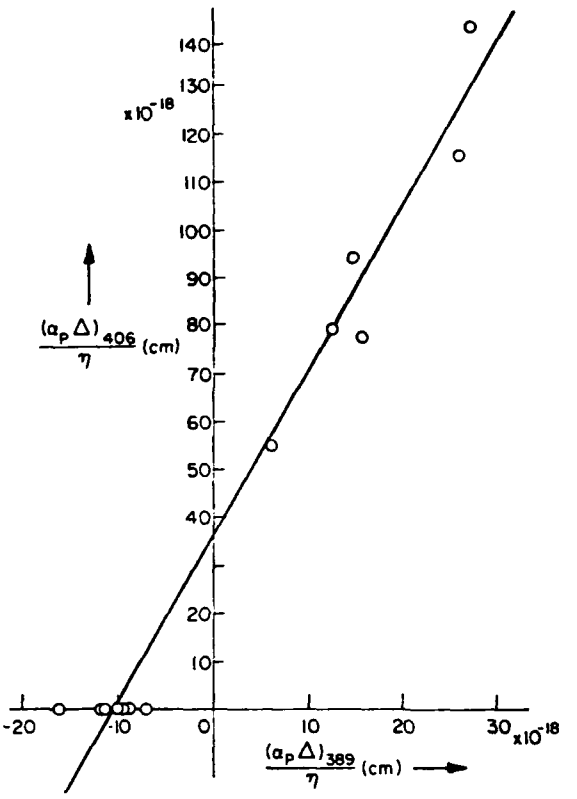

Fig. 5. $(\alpha_p\Delta)_{406}/\eta$ vs. $(\alpha_p\Delta)_{389}/\eta$ for the samples of Table III. The line is a least squares fit which yields values of $E = -9.7 \times 10^{16}$ cm^{-1} and $F = +2.8 \times 10^{16}$ cm^{-1} (see text).

samples of Table III yields n_e values for all cases save one which are <6% of the sum of all the defect concentrations used in the n_e equation. The single exception is sample 2-a where the figure is 11%.

When ^{7}Li is used as the diffusant in place of ^{6}Li then the Li bands have an isotope shift (22) with the 389 $cm^{-1} \rightarrow$ 364 cm^{-1} and the 406 $cm^{-1} \rightarrow$ 379 cm^{-1}. For the same Li concentrations there is also a change in α_p with $(\alpha_p)_{389}/(\alpha_p)_{364} = (\alpha_p)_{406}/(\alpha_p)_{379} = 1.30$. Since the Δ shows almost no change with Li isotope one has

$$E(^7\text{Li}) = 1.30E(^6\text{Li}) = -12.6 \times 10^{16}\ cm^{-1}$$

$$F(^7\text{Li}) = 1.30F(^6\text{Li}) = +3.6 \times 10^{16}\ cm^{-1}$$

As a test of the validity of these values they can be applied to the LVM results previously published (22) for ^{7}Li saturation diffusion in pure GaAs for 700°C $< T_D <$ 950°C. Near 700°C the E and F values with the previous data indicate almost exact compensation in agreement with experiment. However, at 900°C the estimated n_e is approximately 10% of the total Li donor and acceptor charge concentration if one still assumes that the 389 (364) and 406 (379) cm^{-1} defects are the only electrically active ones. Experimentally the samples are highly compensated and high resistivity.

One can also use the above values of E and F to estimate the total [Li] in the saturated pure material. From previous work (22) it is known that the 389 (364) cm^{-1} acceptor complex has 2 Li per defect and the 406 (379) cm^{-1} donor defect has 3 Li. Therefore the total [Li] due to these two defect centers only is

$$N = 2|E(^7\text{Li})|(\alpha_p\Delta)_{364}/n + 3|F(^7\text{Li})|(\alpha_p\Delta)_{379}/m$$

where n and m are the acceptor and donor defect charge states, respectively. Assuming $n = m = 1$ the calculated values for N are the points in Fig. 6 and they can be compared with the total [Li] which is

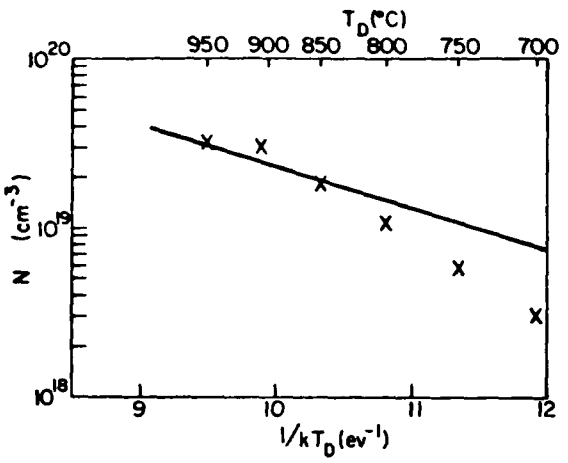

Fig. 6. A plot of ln$N$ vs. $1/kT_D$ for the ^{7}Li diffused pure GaAs samples in Ref. (22). Here $N = 2 \mid E(^7\text{Li}) \mid (\alpha_p\Delta)_{364} + 3 \mid F(^7\text{Li}) \mid (\alpha_p\Delta)_{379}$ which is the total [Li] due to these two defect centers (assuming $n = m = 1$, see text). A straight line is the total [Li] measured by Fuller and Wolfstein [see Ref. (18)].

given by the straight line determined by the flame spectrophotometric analysis measurements of Fuller and Wolfstirn (18). While there is reasonable agreement between the calculated points and the line there are several difficulties. First, there is no independent evidence that $n = m = 1$. Second, the LVM measurements show additional bands due to the other Li defects and they are not included in the calculated N values. Third, the determination of E and F depends on the prior knowledge of a, b, and c which means that the value of N involves a number of parameters known with only limited accuracy. In view of the uncertainties the qualitative agreement in Fig. 6 is considered to be very satisfactory. Therefore the reciprocal cross sections for the Li-donor and Li-acceptor defects are consistent with the data for the compensation of Li-saturated GaAs:Si, the compensation of Li-saturated pure GaAs and the total [Li] in the Li-saturated pure GaAs.

Microstructures of ^{6}Li-diffused samples.—The extent and nature of the microstructure of ^{6}Li-diffused samples depend both on the starting material, particularly the [Si], and on the temperature of the diffusion. It will help to clarify the results if they are discussed by groups of samples as follows:

(i) As previously mentioned nondiffused, nonannealed, HT + Q samples had no significant observable microstructure even for the highest [Si] used in this study.

(ii) Pure GaAs samples ^{6}Li diffused at $T_D \simeq 750°$, 900°, and 950°C were measured and showed Li precipitates and some dislocations which tend to be pinned by the precipitates. Some extrinsic stacking faults on {111} planes which may be related to the Li metastable phase were also observed in the 750°C diffusion. The size and density of Li precipitates decrease with decreases in diffusion temperature. In the case of the 950°C diffused samples, the average size of Li precipitates is approximately 1000Å and their density is approximately 9.5×10^{12} particles/cm^3. These observations are in agreement with those reported previously (24).

(iii) ^{6}Li-diffused samples at $T_D = 750°$C with low [Si] and $n_e \lesssim 3.0 \times 10^{18}$ cm^{-3}, as in sets No. 1 to 3 of Table III, have a microstructure which is similar for the 750°C ^{6}Li-diffused pure GaAs material described in case (ii). There were however, no extrinsic stacking faults observed. Thermal annealing with $T_D \gtrsim 400°$C of nondiffused samples with [Si] $\simeq 1.5 \times 10^{18}$ cm^{-3}, i.e., set No. 1, resulted in no observable microstructure as in the HT + Q state.

(iv) ^{6}Li diffusion at $T_D = 750°$C for the samples with high [Si] $\gtrsim 2 \times 10^{19}$ cm^{-3} and $n_e \gtrsim 5.0 \times 10^{18}$ cm^{-3}, as in sets No. 4 to 7 of Table III, induces a high concentration of defects. Samples 4-a and 5-a with [Si] $\simeq 2 \times 10^{19}$ cm^{-3} show a microstructure with primarily triangular-shaped faulted loops, as shown in Fig. 7a. The loops are on four {111} planes of a tetrahedron and have the displacement vector $\vec{R}_F = a/3$ [111]. To the best of our knowledge this kind of defect has not been reported previously. Similar defects are also observed in the material with similar [Si] $\simeq 2 \times 10^{19}$ cm^{-3} when annealed at 750°C without ^{6}Li diffusion, and their density is similar to that of 750°C ^{6}Li-diffused samples, but they are about three time smaller in linear dimension. By using two different and independent TEM analyses (37, 38) we have established that these triangular loops are extrinsic faults and microanalysis with a scanning electron microscope (SEM) shows that they have a large Si content. We therefore conclude that these triangular loops are due to Si precipitation from GaAs:Si solution, however, the mechanism of their formation is unknown as is the reason for the observed morphology. The microstructure of samples 6-a and 7-a which have the highest [Si] $\simeq 5 \times 10^{19}$ cm^{-3} show primarily circular loops which are also on four {111} planes of a tetrahedron as shown in Fig. 7b. The TEM analysis (38) has established that these circular loops are also of the extrinsic type. As seen in Fig. 7b the loops here are much smaller than those in Fig. 7a making the SEM measurement difficult. However it seems reasonable to assume that the circular loops are due to Si precipitation from GaAs:Si solution as in the case of the triangular loops. Typical dimension of these loops is ~2500Å for the sample with [Si] $\simeq 2 \times 10^{19}$ cm^{-3} (Fig. 7a), decreasing to ~450Å for the sample with the largest [Si] $\simeq 5 \times 10^{19}$ cm^{-3} (Fig. 7b). The loop density in the former case is $\sim 8.0 \times 10^{12}$ cm^{-3} and is roughly thirty-five times higher or $\sim 2.9 \times 10^{14}$ cm^{-3} in the latter case. This indicates that the amount of Si precipitation through the formation of these triangular or circular loops increases with increasing [Si] in the 750°C ^{6}Li-diffused samples. Assuming that these extrinsic triangular or circular loops are forming completely by Si with double interstitial layers on {111} planes, one can estimate [Si] $\simeq 3.2 \times 10^{18}$ cm^{-3} for the triangular loops observed in sample 4-a (Fig. 7a) and [Si] $\simeq 6.6 \times 10^{18}$ cm^{-3} for the circular loops observed in sample 7-a (Fig. 7b).

(v) ^{6}Li-diffused samples at $T_D = 950°$C, all sets in Table III, all had similiar microstructure, i.e., Li precipitates and some dislocations which tend to be pinned by the precipitates. This is similar to the 950°C ^{6}Li-diffused pure GaAs material. However, the size ~700Å and density $\lesssim 3.3 \times 10^{12}$ particles/cm^3 of precipitates is small compared to that of the pure GaAs. One previous study (18) concluded that the solid solubility of Li in doped GaAs is frequently larger than that in pure GaAs which can account for the reduction in precipitates in the Si-doped material. A few large dislocation loops are also observed in samples with high [Si] $\gtrsim 2 \times 10^{19}$ cm^{-3} as in sets No. 4-7 in Table III. The character of these large loops is not known, however, they would account for only a very small amount of [Si] even if one assumes their origin is due to Si precipitation. As previously mentioned ^{6}Li rediffusion at 950°C of sample 7-a after it was ^{6}Li diffused at 750°C, also induces site transfer and shows a similar LVM curve as that of sample 7-b with only 950°C diffusion. After this double diffusion the microstructure does not show the high density of circular loops seen after the first lower temperature diffusion.

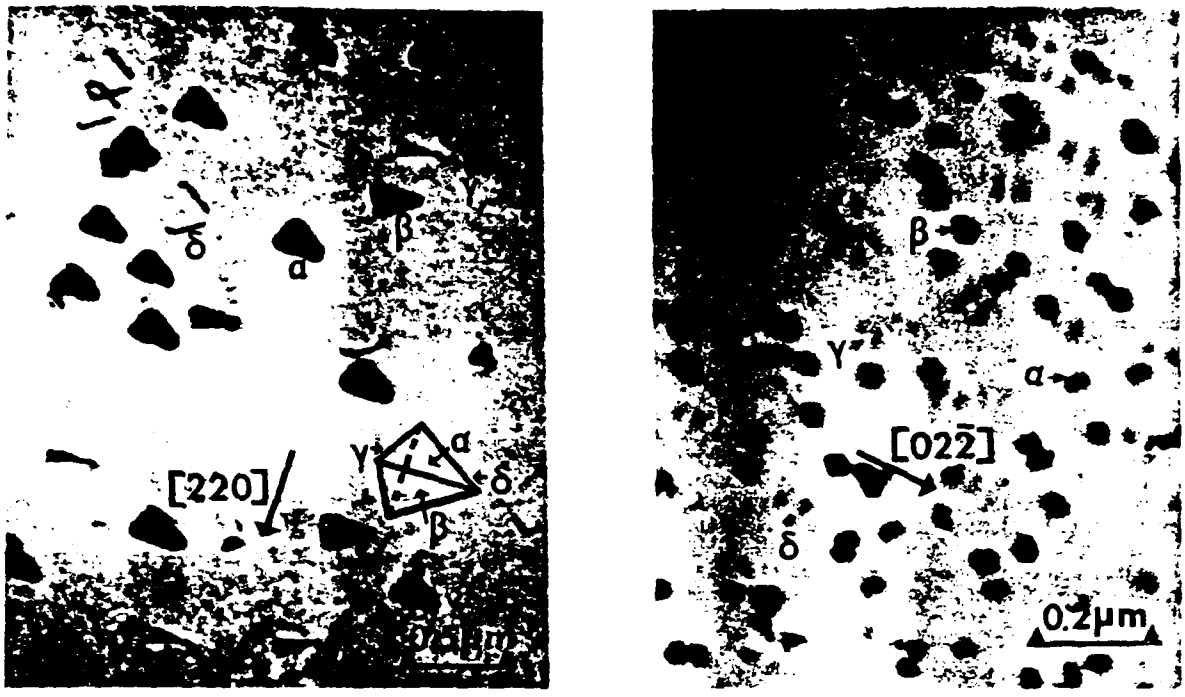

Fig. 7. Bright field micrographs showing the presence of a high concentration of loops which are extrinsic and on four {111} planes of a tetrahedron and observed after 750°C ^{6}Li diffusion. (a, left) Sample 4-a, $n_e \simeq 5.3 \times 10^{18}$ cm^{-3} shows triangular-shaped faulted loops with density $\sim 8.0 \times 10^{12}$ cm^{-3} and the displacement vector $\vec{R_F} = a/3$ [111]. Half of these triangular faulted loops (γ, δ) do not show fringe contrast under the deflection condition being used here. Foil orientation $\sim\langle\bar{1}14\rangle$. (b, right) Sample 7-a, initial $n_e \simeq 8.0 \times 10^{18}$ cm^{-3} shows circular loops with density $\sim 2.9 \times 10^{14}$ cm^{-3}. Foil orientation $\sim\langle\bar{1}12\rangle$.

The resulting final microstructure of sample 7-a is very similar to that of sample 7-b.

The microstructural results described above can be correlated with the LVM measurements and some of the results discussed in the four preceding sections. For the samples of lower [Si] no Si-rich loops are observed at any point in the study and the gain in $(\alpha_p\Delta)$ for the 399 cm^{-1} band for Si_{As} is largely the result of Si site transfer from Si_{Ga} defects, i.e., β values of +0.97, +0.89, and +0.81 for sets No. 1-3 of Table IV as compared to the predicted value of +1.27. On the other hand, the higher [Si] samples show the Si-rich loops after the 750°C diffusion, but essentially none after a 950°C diffusion. These same materials have very low β values indicating that the increases in $[Si_{As}]$ come largely from a source other than the Si_{Ga} defect concentration observed at 750°C. Since no other Si-related LVM bands show significant changes between the two temperatures it is reasonable to inquire into the possibility that the Si-rich loops could be the source of the high temperature increases in $[Si_{As}]$. By using the reciprocal cross sections a and b given earlier, one can estimate the net changes in [Si] in the 399 and 384 cm^{-1} band jointly from the data of Table IV. For sample 4-b the increase in [Si] is 2.7×10^{18} cm^{-3} and 5.7×10^{18} cm^{-3} for sample 7-b. These values are quite close to the estimated [Si] in the loops, 3.2×10^{18} cm^{-3} and 6.6×10^{18} cm^{-3}, respectively, obtained in the previous section. Therefore we conclude that the Si in the loops formed at 750°C is indeed the source of the additional Si observed after the 950°C diffusion.

There remains the fundamental question of the original source of the Si which appears as the Si-rich loops after a 750°C Li diffusion and as enhanced $[Si_{As}]$ after 950°C Li diffusion. We know from the data of Table II that the 750°C Li diffusion causes a reduction of $[Si_{Ga}]$, a reduction of both the 367 and 369 cm^{-1} Si-related defects and a substantial increase in the $[Si_{Ga}\text{-}Si_{As}]$. Also the $Si_{Ga}\text{-}Li_{Ga}$ bands are created by the diffusion. The $[Si_{As}]$ is unaffected. Since the cross sections of the $Si_{Ga}\text{-}Si_{As}$ band and the $Si_{Ga}\text{-}Li_{Ga}$ bands are not known one cannot quantitatively determine whether the total [Si] represented by the bands remains constant. It is conceivable that the Si in the loops and the enhanced $[Si_{As}]$ comes from net decreases of Si in the Si bands observed in the prediffused samples. If this is the case then the source must be either the Si_{Ga} or the Si-related defects causing the 367 and 369 cm^{-1} bands and cannot be the $Si_{Ga}\text{-}Si_{As}$ defect. Also the Si in the loops cannot come from the Si_{As} defects.

An alternate explanation for the original source of the Si in the loops or enhanced $[Si_{As}]$ for the more heavily doped samples is the possibility that some of the Si dopant does not give rise to LVM spectra in the prediffused (e^--irradiated) samples. An indication of this possibility comes from a comparison of the measured total [Si] with that calculated from LVM spectra by using the known absorption cross sections. It is reasonable to estimate Si concentration by assuming $[Si]_{calculated} \simeq [Si_{Ga}] + [Si_{As}] + [Si_{Ga}\text{-}Si_{As}] + [Si]_{367} + [Si]_{369} \simeq a(\alpha_p\Delta)_{384} + b(\alpha_p\Delta)_{399} + 2a(\alpha_p\Delta)_{393} + c(\alpha_p\Delta)_{367} + d(\alpha_p\Delta)_{369}$ for e^--irradiated samples in Table II. The results for KM-16-3,4 and WA-Si-2-2,3 show that values for $[Si]_{calculated}$ account for only 60%-70% of the total [Si] values measured by electron microprobe analysis which were 2.3×10^{19} cm^{-3} and $\sim 5 \times 10^{19}$ cm^{-3}, respectively. In addition, Newman (37) and co-workers have recently studied irradiated samples simultaneously doped with Si and a group VI donor. The $(\alpha_p\Delta)_{384}$ band of Si_{Ga} is about the same as $(\alpha_p\Delta)_{399}$ for Si_{As}. Prolonged irradiation (31) can reduce the $(\alpha_p\Delta)_{399}$. They have found that after such an irradiation and upon annealing, $[Si_{As}]$ recovers and $(\alpha_p\Delta)_{399}$ can overshoot its original value by as much as a factor of five even though the $[Si_{Ga}]$ does

not change. Furthermore in a most recent communication, they have also observed that annealing Si-doped GaAs samples ($[Si] \simeq 2 \times 10^{18}$ cm^{-3}) after being irradiated with fast neutrons, the strength of the Si_{As} band also increases and may overshoot its original value by a factor of three but without any measurable change in the strength of other LVM bands involving silicon. They have also concluded that there is some silicon in as-grown crystals which does not give rise to LVM absorption.

Conclusions

The use of measurements of the carrier density, the LVM absorption, and the microstructure of GaAs:Si samples has provided information which allows one to describe in considerable detail the behavior of a number of defects in Li-saturated material. Specifically the conclusions which have been made from the present study are:

1. The effect of a saturation diffusion of Li at a temperature (750°C) which is below that at which Si transfers from Ga to As sites results in significant changes in the Si defect concentrations as compared to the prediffused state. These changes are: (i) a decrease in $[Si_{Ga}]$; (ii) an increase in $[Si_{Ga}$-$Si_{As}]$; and (iii) the creation of Si_{Ga}-Li_{Ga} defects. There is no change in $[Si_{As}]$. The changes increase with increases in [Si].

2. For samples of lower [Si], i.e., $[Si] \lesssim 5 \times 10^{18}$ cm^{-3} and $n_e \lesssim 3 \times 10^{18}$ cm^{-3}, saturation diffusion of Li at a temperature of 950°C does result in $Si_{Ga} \rightarrow Si_{As}$ and most of the increase in $[Si_{As}]$ is attributable to the decrease in $[Si_{Ga}]$. The Li defect responsible for inducing the Si site transfer is the Li donor which has an LVM band at 406 cm^{-1} (for ^{6}Li). The microstructure of these lower [Si] samples includes some Li precipitates and some dislocations which tend to be pinned by the precipitates. There is no evidence of Si precipitation or extrinsic faults.

3. For samples of higher [Si], i.e., $[Si] \gtrsim 2 \times 10^{19}$ cm^{-3} and $n_e \gtrsim 5 \times 10^{18}$ cm^{-3}, the comparisons of Li saturation diffusion at 750° and 950°C are more complicated. The $[Si_{Ga}]$ generally decreases and $[Si_{As}]$ increases for the higher temperature case, however, $Si_{Ga} \rightarrow Si_{As}$ site transfer is no longer the dominant process. After the 750°C saturation, TEM measurements show faulted {111} extrinsic loops which are Si rich. These loops are not present after a 950°C saturation diffusion. Semiquantitative comparisons indicate that the large increase in $[Si_{As}]$ at the higher temperature could come from the Si content of these loops. The question of the origin of the Si in the loops could not be answered unambiguously although two possible sources were identified and discussed.

4. By using the fact that the Li-saturated samples are electrically compensated and using the known values of the absorption cross sections of the electrically active Si defects, the absorption cross sections of the bands for the principal Li-donor and -acceptor defects were determined. These cross sections were used with the knowledge that there are 3 Li per donor defect and 2 Li per acceptor and some previously published data for Li-saturated undoped GaAs to estimate the total [Li] as a function of saturation temperature. The results are in reasonable agreement with earlier quantitative analysis data.

Acknowledgments

This work was supported by the Air Force Office of Scientific Research (AFSC) under Grant/Contract 76-2990. The authors wish to express their gratitude to Dr. G. H. Narayanan for his helpful advice on the TEM results and to Professor D. B. Wittry for useful discussions during the electron microprobe analysis. The authors would also like to thank L. Lowe and D. Morris for their help with the electron irradiations and their hospitality to one of the authors (W.G.S.) during his stay at Hanscom Field, Massachusetts. The authors also wish to express their appreciation to Professor R. C. Newman and his co-workers for their comments and communication of their results prior to publication.

Manuscript submitted Oct. 29, 1979; revised manuscript received Feb. 13, 1980. This was Paper 578 presented at the Los Angeles, California, Meeting of the Society, Oct. 14-19, 1979.

Any discussion of this paper will appear in a Discussion Section to be published in the June 1981 JOURNAL. All discussions for the June 1981 Discussion Section should be submitted by Feb. 1, 1981.

Publication costs of this article were assisted by the University of Southern California.

REFERENCES

1. W. G. Spitzer and W. Allred, *Appl. Phys. Lett.*, **12**, 5 (1968).
2. W. G. Spitzer and W. Allred, *J. Appl. Phys.*, **39**, 4999 (1968).
3. K. Laithwaite and R. C. Newman, *J. Phys. C: Solid State Phys.*, **9**, 4503 (1976).
4. R. T. Chen and W. G. Spitzer, Private communication.
5. W. G. Spitzer and M. B. Panish, *J. Appl. Phys*, **40**, 4200 (1969)
6. A. H. Kachare, W. G. Spitzer, J. M. Whelan, and G. H. Narayanan, ibid., **47**, 5022 (1976).
7. W. G. Spitzer, in "Advances in Solid State Physics," Vol. XI, O. Madelung, Editor, p. 1, Pergamon Press (1971).
8. H. J. Queisser, *J. Appl. Phys.*, **37**, 2909 (1966).
9. C. J. Hwang, ibid., **39**, 3347 (1968).
10. W. Y. Lum and H. H. Wieder, ibid., **49**, 6187 (1978).
11. J. K. Kung and W. G. Spitzer, ibid., **45**, 4477 (1974).
12. L. H. Skolnik, W. G. Spitzer, A. Kahan, F. Eules, and R. G. Hunsperger, ibid., **43**, 2146 (1972).
13. W. P. Allred, G. Cumming, J. Kung, and W. G. Spitzer, in Second International Conference on Gallium Arsenide, Dallas, Texas, p. 66, Institute of Physics and the Physical Society (1968).
14. K. Laithwaite, R. C. Newman, J. F. Angress, and G. A. Gledhill, in Sixth International Symposium on Gallium Arsenide and Related Compound, Edinburgh, Sept. 20, 1976, p. 133, Institute Phys. Conf. 33a, Institute of Physics, London (1977).
15. J. K. Kung and W. G. Spitzer, *J. Appl. Phys.*, **45**, 2254 (1974).
16. H. Rupprecht, J. M Woodall, K. Konnerth, and D. G. Pettit, *Appl. Phys. Lett.*, **9**, 221 (1966).
17. J. M. Whelan, J. D. Struthers, and J. A. Ditzenberger, in Proceedings of International Conference on Semi-conductor Physics, Prague, p. 943 (1960).
18. C. S. Fuller and K. B. Wolfstirn, *J. Appl. Phys.*, **33**, 745 (1962a); *J. Appl. Phys.*, **33**, 2507 (1962b); in Proceedings of International Conference on Physics of Semiconductors, Exeter, p. 745, The Institute of Physics and The Physical Society, London (1962c); *Appl. Phys. Lett.*, **2**, 45 (1963a); *J. Appl. Phys.*, **34**, 1914 (1963b); Radiation Damage in Semiconductors, Report of 7th International Conference on Physics of Semiconductors, Paris, Vol. 3, p. 187, Academic Press, New York (1964).
19. C. S. Fuller and H. W. Allison, *J. Appl. Phys.*, **35**, 1227 (1964).
20. W. Hayes, *Phys. Rev.*, **138**, A1227 (1965).
21. M. Levy, O. Lorimor, and W. G. Spitzer, *J. Appl. Phys.*, **39**, 1914 (1968).
22. M. E. Levy and W. G. Spitzer, *J. Phys. C: Solid State Phys.*, **6**, 3223 (1973).
23. M. E. Levy, Ph.D. Dissertation, University of Southern California, 1973, Unpublished.
24. B. Norris and G. H. Narayanan, *J. Appl. Phys.*, **48**, 2784 (1977).
25. O. G. Lorimor and W. G. Spitzer, ibid., **37**, 3687 (1966).
26. O. G. Lorimor and W. G. Spitzer, ibid., **38**, 2713 (1967).
27. O. G. Lorimor and W. G. Spitzer, ibid., **38**, 3008 (1967).
28. P. C. Leung, L. H. Skolnik, W. P. Allred, and

W. G. Spitzer, ibid., 43, 4096 (1972).
29. P. C. Leung, J. Fredrickson, W. G. Spitzer, A. Kahan, and L. Bouthillette, ibid., 45, 1009 (1974).
30. W. G. Spitzer, A. Kahan, and J. Bouthillette, *ibid.*, 40, 3398 (1969).
31. K. Laithwaite and R. C. Newman, *Philos. Mag.*, 35, 1689 (1977).
32. R. C. Newman, Private communication.
33. J. K. Kung and W. G. Spitzer, *J. Appl. Phys.*, 44, 912 (1973).
34. J. K. Kung and W. G Spitzer, *This Journal*, 121, 1482 (1974)
35. G. H. Narayanan and S. M. Copley, *Phys. Status Solidi A*, 23, 123 (1974).
36. G. H Narayanan and A. H. Kachare, ibid., 26, 657 (1974).
37. R. C. Newman, Private communication.
38. R. Gevers, A. Art, and S. Amelinckx, *Phys. Status Solidi*, 3, 1563 (1963).
39. J. W. Edington, "Practical Electron Microscopy in Materials Science," pp. 134-136, Van Nostrand Reinhold, New York (1976).

3. Si-DEFECT CONCENTRATIONS IN HEAVILY Si-DOPED GaAs: ANNEALING-INDUCED CHANGES-II

by

R.T. Chen[a] and W.G. Spitzer
Departments and Materials Science and Physics
University of Southern California
Los Angeles, California 90007

ABSTRACT

Isothermal annealing produces changes in the free carrier density, defect-induced localized vibrational mode (LVM) infrared absorption, microstructure as measured by transmission electron microscopy (TEM), and critical resolved shear stress of heavily Si-doped GaAs. The changes have been measured and correlated for three different Si concentrations for several annealing temperatures. The measurements reveal temperature dependent annealing-induced changes in several specific defect concentrations. The observations indicate the following behavior for two ingots with $[Si] \geq 2 \times 10^{19} cm^{-3}$: (1) When the anneal temperature, $T_A = 400^{o}C$, the concentration of Si_{Ga} donors, as determined from LVM spectra decreases probably due to the generation of V_{Ga} defects followed by the formation of Si_{Ga}-V_{Ga} pairs. This change is responsible for observed decreases in carrier density and the large increase in yield stress. The yield stress shows a dependence of the form $\sigma - \sigma_o^{\alpha} [Si_{Ga}-V_{Ga}]^{1/4}$. (2) When $T_A = 500^{o}C$, the LVM spectra indicate that all of the observed Si defect concentrations change . The decrease in $[Si_{Ga}]$ alone cannot explain the decrease in carrier density, and a previous suggestion that a new acceptor is required is confirmed. Both the LVM measurements and the shear stress indicate that only a small fraction of the $[Si_{Ga}]$ reduction is by the formation of Si_{Ga}-V_{Ga} pairs. (3) When $T_A = 700^{o}C$, a new acceptor is still required and the other experimental

observations at T_A = 500°C are also still seen here. There is a large decrease in $[Si_{Ga}]$ and $[Si_{As}]$ observed for short anneal times which coincides with the formation of Si-rich extrinsic loops and the loop area/vol increases with [Si]. (4) When T_A > 700°C, all of the changes become smaller as T_A increases. For lower [Si] ~ 1.5×10^{18} cm^{-3}, no significant annealing-induced changes are observed for any of the T_A given above.

a) Present address: Electronic Research Center, Rockwell International, Thousand Oaks, CA 91360.

I. Introduction

There have been a number of studies[1-7] of annealing-induced effects on the properties of heavily Si-doped GaAs. Annealing produces changes in several properties including the free carrier density,[3,4] the photoluminescence,[1-4] the defect-induced infrared localized vibrational mode (LVM) absorption,[2,4] the microstructural characteristics as determined by transmission electron microscopy[5] (TEM), and the critical resolved shear stress.[6,7] The studies have suggested that the observed changes in these various properties are related. The present work is an extension of some of these prior investigations, particularly the earlier work of Kung and Spitzer in Ref.4, hereafter referred to as Part I. The present work is a detailed and systematic study of the annealing-induced changes in specific defect concentrations and the influence of these changes on several diverse physical properties of heavily Si-doped GaAs. Measurements are reported here of the carrier density, the infrared LVM absorption, the dislocation loop size and density, and the yield stress as functions of annealing for samples from the same material. The concentration of Si is varied by about two orders of magnitude, and the annealing temperatures T_A cover the range from 400°C to 1000°C. The results of all measurements for the same material are correlated and are interpreted on the basis of common defect models. Specifically, the present work extends the previous studies including those of Part I in the following ways:

(1) A detailed study is presented which covers a variety of annealing temperatures and times as well as three different Si concentrations (hereafter concentration is indicated by [ ]).

(2) Four different physical measurements are made for essentially all temperatures and times by using samples with the same origin and identical [Si]. The common origin facilitates detailed comparisons

of the different data. The previous studies did not use material of a common origin and properties were measured for only a very limited set of annealing conditions.

(3) The study is a semi-quantitative one in that specific defect and microstructure concentrations are calculated. The previous studies are largely qualitative.

(4) Annealing-induced changes in the carrier densities, LVM, TEM, and yield stress are discussed quantitatively in terms of the changes of the specific defect concentrations. It is found that the changes in defect concentrations indicated by the LVM spectra can largely explain the changes in the other measured properties.

The subject of annealing-induced changes in physical properties of GaAs has a long history and the results of these different studies are often seemingly contradictory. Most of these studies have involved relatively lightly doped, low carrier density material or doped layers on the surface of the samples. For this reason one might draw the conclusion that measurements such as those reported here are indications of the behavior of the particular samples studied but would not apply to randomly chosen samples. It should be realized that the three principal studies of the annealing-induced bulk changes in heavily Si-doped GaAs have been quite consistent, see references 3 and 4 as well as the present work. These studies involve over 200 samples taken from 7 different ingots grown by two different methods in two different laboratories. Of even greater significance is that all samples having a high Si doping level, $[Si] \geq 2 \times 10^{18} cm^{-3}$, and grown from a nearly-stochiometric melt show the annealing effects to be described. As will be discussed, attempts at quantification and modeling these changes does require that all samples start from the same thermodynamic equilibrium state.

The mechanical measurements for the material used here have already been reported,[7] and therefore much of the experimental detail concerning these measurements is omitted in the present discussion.

II. Background

The amphoteric nature of Si in GaAs is well known, and it has made this impurity of particular interest in a number of studies. It is known that Si substitutes on a Ga site, Si_{Ga}, producing a shallow donor state and on an As site, Si_{As}, producing an acceptor state. If GaAs:Si is grown from a nearly stochiometric GaAs melt then the resulting material is always n-type, and the behavior of the Si is reasonably well understood. At low Si concentrations, $[Si] \lesssim 1 \times 10^{18}$ cm^{-3}, the Si preferentially occupies the Ga sites,[8-11] and the room temperature free electron density, n_e, approximately equals the [Si]. If the [Si] increases to larger values then n_e does not increase proportionally.[3,8-11] The Si forms significant concentrations of other defects such as Si_{As} acceptors, Si_{Ga}-Si_{As} nearest neighbor pairs,[2,4,10-14] and Si-native defect

complexes.[1,4,6,9-11,13-16] Generally, for as-grown samples with $[Si] \gtrsim 10^{19}$ cm^{-3}, the value of n_e becomes almost independent of [Si] and $n_e \sim 5\times10^{18}$ cm^{-3}.[8] The exact saturation value for n_e is dependent upon growth method and thermal history. The high temperature solid solubility limit for Si in GaAs is ~0.5 at.% or $\sim2\times10^{20}$ atoms cm^{-3}.[17]

Heat treatments at elevated temperatures are frequently a part of the procedure of processing GaAs materials and devices. Examples where the heat treatment is important include expitaxial growth, impurity diffusion, and annealing of implanted layers. When GaAs crystals are annealed at high temperature, i.e. $T_A \gtrsim 700^oC$, large concentrations of lattice defects are frequently introduced near the surfaces. There have been several studies which reported that annealing n-type GaAs increases the acceptor concentration and changes the photoluminescent characteristics near the sample surface. These changes depend on the As pressure during annealing. Different explanations have been proposed for this behavior including contamination by Cu[18,19] or Si[20,21], the creation of Ga or As vacancies,[21-29] the transfer of Si between types of lattice sites,[11,20,30-33] and the formation of complex defects involving both impurity atoms and lattice defects.[30-34] In some of these studies the diffusion coefficients for Ga and As vacancies have been estimated. Muñoz et al.[25] estimated the diffusion coefficients at 850°C to be 10^{-12} cm^2 sec^{-1} for Ga vacancies and 10^{-10} cm^2 sec^{-1} for As vacancies. In a more detailed study Chiang and Pearson[27] determined the temperature dependent relations for the diffusion coefficients which give values at 850°C of 8×10^{-13} and 1×10^{-14} cm^2 sec^{-1} for Ga and As vacancies, respectively. Because the present work involved thermal anneals at temperatures as high as 1000°C and our primary interest is in bulk properties, a sufficient

amount of material will be removed from the surfaces to insure that the effects of the changes in the surface layer properties on the measurements are eliminated.

As previously mentioned, the present work is an extension of some earlier studies,and for the sake of clarity a brief review of these prior studies will be given here. In particular some previous LVM studies of GaAs:Si are considered which involve annealing effects on the carrier density, the microstructure, and the yield stress. For further details, including more extensive reviews of the early studies, the reader is referred to the literature.[3-6]

A. Localized Vibrational Mode (LVM) Absorption

Because of the amphoteric behavior of Si in GaAs a number of studies have used LVM frequencies obtained from infrared absorption measurements for the identification of defect species and estimates of their concentrations. Infrared measurements[11,13,35] have been used with electrical data and expected defect symmetry properties to identify the Si defects responsible for the observed absorption bands. Several of the observed LVM bands have been assigned to specific point defects. The bands having liquid nitrogen temperature peak absorption frequencies at 384 and 399 cm^{-1} are due to $^{28}Si_{Ga}$ and $^{28}Si_{As}$ defects, respectively. The bands at 464 and 393 cm^{-1} are assigned to $^{28}Si_{Ga}$ - $^{28}Si_{As}$, where the Ga and As sites are nearest neighbors. These pairs are presumed to be electrically neutral. Two other bands located at 367 and 369 cm^{-1} have been attributed to two other unidentified but Si-related defects. It has been suggested[14] that the 369 cm^{-1} band which is seen only in electron-irradiated, Si-doped samples and the 367 cm^{-1} band which was

previously incorrectly assigned to the $^{28}Si_{Ga}$ - $^{28}Si_{As}$ nearest neighbor pair defect, are both caused by defects involving Si paired with native lattice imperfections. The bands and their assignments are given in Table I.

All of the above LVM results have been obtained from electrically compensated material. The compensation is necessary to reduce the density and hence the absorption due to free carriers which would otherwise effectively obscure the LVM absorption. For GaAs:Si grown from a nearly stochiometric melt, which is always n-type, saturation diffusion of Li or Cu at an elevated temperature, i.e. $700^{o}C \lesssim T_{D} \lesssim 1000^{o}C$, and penetrating particle irradiation, i.e. 1 to 2 MeV electrons, have been used as compensation techniques. If however one wishes to study the pre-compensation distribution of Si among the various possible defects then one difficulty of these procedures is that the compensation process may alter the distribution of Si defects and even create Si related defects which were not present in significant concentration prior to the compensation procedure. Ample evidence exists for such changes[13,36,37] where the compensation is produced by saturation diffusions of Li or Cu, and the effect of this compensation process on the Si distribution has been previously discussed.[11] From the evidence available[10,11,37,38] the e^{-}-irradiation method of compensation appears to be the least disturbing to the pre-compensation distribution of Si defects, and it has been used to compensate all the samples in this study as well as in many of the previous studies. This compensation method has the further advantage of reducing the number of defect bands compared to those in the Li or Cu compensation cases and thus reducing the complexity of the interpretation.

According to the theory of localized vibrational modes[39] the integration of the linear absorption coefficient over frequency for each band is proportional to the volume concentration of the defect species responsible for the band. We refer to the constant of proportionality as the absorption cross section; $\int_{band} \alpha d\nu / [Defect]$, where α is the LVM absorption coefficient and ν is the frequency. In the present study the integrated absorption, $\int_{band} \alpha d\nu$, is replaced by $(\alpha_p \Delta)_{band}$, where α_p is the peak LVM absorption less background and Δ is the bandwidth in cm^{-1} at half-maximum.

The LVM absorption cross section for each of the Si defect bands must be known if the bands are to be used to determine the changes in defect concentrations. In a recent study[11] the cross sections of Si_{Ga}, Si_{As}, and the two Si-related defect bands of Table I were measured for a number of samples from Bridgman, melt-grown ingots. The samples had all been subjected to the same initial treatment of annealing for 1h at 1200°C followed by quenching to room temperature. The purpose of this treatment was to remove any thermal aging effects produced by temperatures in the 400°C to 900°C range during the growth period. The importance of this procedure will be discussed later in the present work. The samples had concentrations of $1x10^{18}\ cm^{-3} \lesssim [Si] \lesssim 1x10^{20}\ cm^{-3}$ and $1x10^{18}\ cm^{-2} \lesssim n_e \lesssim 1x10^{19}\ cm^{-3}$ and were compensated by e^--irradiation. The $^{28}Si_{Ga}$ donor (384 cm^{-1} band), $^{28}Si_{As}$ acceptor (399 cm^{-1} band) and two other Si related defects (367 and 369 cm^{-1} bands) were assumed to be the only electrically-active defects prior to the irradiation and thus, they determine the carrier density after the high temperature plus quench treatment. With this assumption the reciprocal absorption cross sections were found to be $a=10.0x10^{16}cm^{-1}$, $b=12.7x10^{16}cm^{-1}$, $c=25.3x10^{16}cm^{-1}$,

and $d = 19.0 \times 10^{16}$ cm^{-1}, where

$$n_e = a(\alpha_p\Delta)_{384} - b(\alpha_p\Delta)_{399} + c(\alpha_p\Delta)_{367} - d(\alpha_p\Delta)_{369}$$

$$= [Si_{Ga}] - [Si_{As}] + [Si]_{367} - [Si]_{369}.$$

The electrical behavior of the defects responsible for the 367 and 369 cm^{-1} bands are donor and acceptor, respectively. These values of the constants will be used in the quantitative analysis of the LVM results in the present work.

B. Carrier Concentration

Kung and Spitzer (KS) were the first to report[3] the annealing effects in heavily Si-doped GaAs. The effects are qualitatively similar to those reported earlier[40-43] for GaAs doped with Te and Se impurities. It was observed by KS that the n_e could be decreased by as much as a factor of 6 by annealing GaAs:Si with $[Si] \sim 4 \times 10^{19}$ cm^{-3} at temperatures between 400 and 900°C. In a later study called Part I,[4] KS attempted to determine the source of the annealing-induced decrease in n_e by measuring the LVM infrared absorption and low temperature photoluminescence for samples similar to those that were employed in the n_e investigation. It was concluded that the decrease in n_e was related to the decrease in the $[Si_{Ga}]$ donors. After annealing at 400°C the loss in $[Si_{Ga}]$ could quantitatively account for the decrease in n_e while after annealing at 600 or 750°C, the decrease in $[Si_{Ga}]$ was insufficient to account for the n_e change and thus, an additional unknown acceptor species was postulated. After the 600 and 750°C anneals, the growth of a new photoluminescence band near 1.0 ev was attributed to this new acceptor defect. It was also observed at all annealing temperatures that the concentrations of Si_{As}

and Si_{Ga} - Si_{As} pairs as determined by strengths of the LVM absorption bands, remained essentially constant. This observation indicated that neither site transfer nor Si-Si association reactions involving these Si defects were related to the decrease in strength of the Si_{Ga} band. Based on these results, KS tentatively suggested that the observed decrease in the strength of the Si_{Ga} band might be due to the formation of Si_{Ga} - V_{Ga} pairs, where V_{Ga} represents a vacancy on the Ga site which is a second neighbor of the Si_{Ga}. This suggestion of the Si_{Ga} - V_{Ga} defect was based largely on earlier studies of photoluminescence spectra.

It is clear that if V_{Ga} is an acceptor species as is generally assumed, then pairing Si_{Ga} donors with pre-existing V_{Ga} acceptors will not result in a decrease in n_e. The decrease in n_e must result from the generation of V_{Ga} defects from internal sources and these vacancies can then pair with the Si_{Ga} and are observed by the decrease in $[Si_{Ga}]$. The generation must involve internal vacancy sources since for the anneal temperature and the sample thicknesses used, the vacancy diffusion rate is far too small for the interior of the samples to be in equilibrium with the surface. The bulk generation of acceptor vacancies during annealing is favored by the fact that the samples are strongly extrinsic and n-type at the anneal temperature employed. Although this explanation is attractive it must be emphasized that there is no direct experimental LVM evidence that Si_{Ga}-V_{Ga} formation is responsible for the decrease in $[Si_{Ga}]$ and therefore, the mechanism is regarded as speculative.

C. Microstructural Studies

The effects of annealing on the defect structure of heavily Si-doped GaAs have been examined by Narayanan and Kachare[5] who used thin foil transmission electron microscopy (TEM) for samples taken from different regions of the same GaAs ingot as was used by KS.[4] In brief, this study revealed that the annealing treatments are accompanied by pronounced changes in the microstructure of the material. Annealing at 1100°C followed by quenching to room temperature produced a homogeneous solid solution which was free of observed microstructure; however, subsequent annealing of these samples at a temperature in the range of 600 to 850°C induced prismatic dislocation loops of the vacancy type. It was found that the density, size, and distribution of the loops exhibited an anomalous temperature dependence. Samples annealed at 750°C had a high density of small loops while those annealed at 600°C exhibited a smaller density of larger loops. Samples annealed at 400°C contained no dislocation loops. In order to explain this behavior it was postulated that an appreciable fraction of the quenched-in vacancies become trapped by the Si_{Ga} defects to form $Si_{Ga} - V_{Ga}$ at the lower

annealing temperature so that the vacancies are not available for the nucleation of prismatic loops.

Qualitatively similar microstructural observations have been reported for heavily Te-,[44-49] Se-,[50] and S-doped[49] GaAs. In a detailed study[47] of heavily Te-doped material, dislocation loops were observed after annealing at a temperature as low as 400°C. The loop area per unit volume was found to be constant for all annealing temperatures between 400 and 1000°C. The conclusions of the various investigations regarding the nature of the prismatic loops in heavily Te-doped samples are not mutually consistent. Interstitial-type[46,49] and vacancy-type[44,45] loops have been reported by different investigators. Thermal annealing does not produce dislocation loops in heavily Zn-doped,[49-51] in undoped, or in lightly Si-[4] or Te-doped GaAs samples.

D. Yield Stress

Swaminathan and Copley (SC)[54] investigated the mechanical behavior of GaAs single crystals doped with various impurities. The temperature range used was 420 to 680°K. As observed in earlier studies,[52,53] doping with a donor impurity increased the yield stress, while an acceptor decreased the yield stress relative to the undoped state. To explain the donor behavior, it had been previously proposed that dislocations were pinned by the impurity atmosphere. Because of the absence of either abrupt or serrated yield behavior in their stress-strain experiments, SC[54] claimed this explanation was unacceptable, and they proposed that the observed hardening was due to the interaction of moving dislocations with static defect complexes. To explain the magnitude of hardening, they proposed that the defect complexes were solute-vacancy pairs similar to those known to strengthen alkali halide crystals.[55]

If the solute-vacancy pair consists of a Si atom and a vacancy located on a second nearest neighbor site, i.e. $Si_{Ga} - V_{Ga}$, then the elastic distortion resulting from the pair has deviatoric as well as hydrostatic components, and there will be an elastic interaction between the pair and both edge and screw components of the glide dislocations. A $Si_{Ga} - V_{As}$ pair would not have the type of elastic distortion necessary for the interaction. Also, in GaAs, a Si atom occupying a Ga site is a single donor,[8] and there is evidence suggesting that a gallium vacancy may be a single acceptor.[56] Thus, there may be a short range electrostatic interaction between pairs and dislocations associated with the displacement of the oppositely charged defects relative to each other, while they are at the dislocation core, produced by the shearing action of the gliding dislocations. An interaction of this type has been proposed to explain impurity hardening in ionic crystals.[57]

The effect of various thermal treatments on the yield stress and dislocation substructure of heavily Si-doped GaAs have also been investigated by SC.[6] The material they investigated was taken from a source ingot which had a somewhat higher [Si] than the material investigated by KS[3,4] and by Narayanan and Kachare.[5] SC measured samples which were first annealed at 1100°C and then quenched to room temperature. The samples were subsequently aged at different temperatures. They found that the yield stress measured at 400°C increased with aging time and approached a saturation value. The saturation value decreased with increasing aging temperature. This behavior is consistent with the proposed interaction between moving dislocations and static $Si_{Ga} - V_{Ga}$ pairs. The yield stress would be expected to increase during isothermal aging because of the formation of the pairs and to approach a saturation value corresponding to the establishment of the steady-state concentration

of pairs at the aging temperature. This concentration of pairs is expected to decrease with increasing aging temperature because the thermal energy increases relative to the energy bonding the Si atoms to the vacancies. Thus the saturation value of the yield stress also would be expected to decrease. This interpretation was qualitatively consistent with the LVM and microstructural behavior just discussed.

III. Experimental Methods

Figure 1 is a flow diagram which indicates the measurements made in the present study and their sequence. The [Si] range indicated at the top of this figure includes the values for three different horizontal Bridgman-grown ingots which were doped with different [Si] as indicated by the second column of Table II. The [Si] in Table II are those in the first portion of the ingot solidified. Since the equilibrium segregation coefficient[58] for Si in GaAs is 0.14, samples with different [Si] can be obtained by cutting them from different parts of the ingot. In the present experiments a large number of samples of each of three different [Si] were desired. Therefore ingots of several hundred grams were grown in long boats and approximately the first one-third of each ingot was used. In this portion the [Si] should change slowly with the fraction solidified if nearly ideal growth conditions are approximated. Thus samples taken from the same region in the front portion of the same ingot should have nearly identical values of [Si].

The total [Si] was estimated in three ways. The first estimate was based on the dopant added to the melt and the known segregation coefficient. The second method was by using spectrochemical analyses. The third and most reliable method for the more heavily doped samples

was a measurement made by using an electron probe microanalyzer. The two ingots having the lower [Si] were single crystals and were grown by the authors. The ingot of highest [Si] was obtained from Crystal Specialties, Inc.[59] and was polycrystalline but with very large single crystal sections, i.e. typical crystallite dimensions were centimeters. In this latter case groups of samples having nearly the same [Si] were always taken from the same region of the same crystallite.

The total number of samples required from all three ingots for all of the measurements indicated in Fig. 1 is quite large, approximately 140 samples not including those used for mechanical measurements by Ganesan and Copley[7]. The latter will not be discussed in this section as they have already been described.[6,7]

To obtain the samples for the n_e, LVM, and TEM measurements, wafers approximately 1.5 mm thick were cut from the ingots with the large area surfaces perpendicular to the ingot axis. Each wafer was then divided into a number of individual samples having typical large area surface dimensions of 3x10 mm^2. For the KM-16 ingot the measurements of [Si] indicated that the values within a given wafer were essentially identical. The most heavily doped ingot, WA-Si, had a factor of $\sim$2 change between the [Si] value near the bottom of a wafer, i.e. next to the boat, and the top. This meant that for the WA-Si ingot, samples of the same [Si] had to be taken from the same regions of adjacent wafers. Fortunately this ingot was the largest one and frequently more than 15 samples could be cut from a single wafer.

As indicated in Fig. 1 a few samples were measured in the as-grown state. Except for these cases all samples were heat treated in small evacuated quartz ampoules at 1200°C for 1h and then quenched to room

temperature (a process hereafter called HT+Q) prior to making any measurement or proceeding with the isothermal anneals. Both the quartz and samples were subjected to special washing and cleaning procedures to reduce the possibility of Cu contamination during HT+Q. As mentioned earlier the HT+Q treatment establishes a common thermodynamic background for all samples. Also, as will be discussed, this process significantly improves the microstructural quality of the material, particularly for the most heavily Si-doped samples. The carrier densities after HT+Q ranged from 1.0×10^{18} cm^{-3} to 1.0×10^{19} cm^{-3}. The HT+Q procedure has essentially no effect on n_e for material with [Si] $\lesssim 2 \times 10^{18}$ cm^{-3} and $n_e \lesssim 1.5 \times 10^{18}$ cm^{-3}, but it substantially increases n_e for as-grown samples with [Si] $\gtrsim 1 \times 10^{19}$ cm^{-3}. In some cases the as-grown n_e almost doubled as a result of the HT+Q treatment.

After the HT+Q treatment the n_e for each sample was measured by determining the frequency of the free carrier plasma minimum observed in the infrared reflectivity. This method has been compared in detail previously[3,60] with Hall measurement results and very good agreement was obtained. In making these measurements it was necessary to remove surface material from each sample after the HT+Q treatment to insure that the measured n_e was the bulk value. It was found that removal of $\sim$0.1 mm by lapping and chemical polishing gave n_e values which did not change with further removal of material. A similar removal of at least 0.1 mm sample surface layer is also performed after annealing.

Since a large number of samples of essentially identical [Si] and n_e were needed from each ingot, the samples from the same wafer or neighboring wafers were formed into groups identified by their common

origin, the post HT+Q value of n_e, and the [Si]. Again following Fig. 1, a few samples from each group were used for TEM and liquid nitrogen temperature infrared LVM measurements. These and all other samples used for the infrared measurements were e^--irradiated with 1.4 MeV electrons prior to the measurements. The sample temperature was kept below 140°K during the irradiation and the e^--fluence $\lesssim 1 \times 10^{19}$ e^-/cm^2. The LVM measurements of these HT+Q samples, which were not subsequently isothermally annealed, have been used[11] to obtain the absorption cross sections for the four different Si defects as mentioned previously. The TEM measurements were made for both e^--irradiated and non-irradiated samples, and no changes in microstructure attributable to the irradiation were observed.

The remaining samples were sealed in quartz ampoules as described previously and taken through the isothermal anneals indicated in Fig. 1. The groups were arranged so that several samples of each group could be annealed for different times at each temperature. The detailed schedule used is given in Table II. Unless otherwise indicated each anneal time and temperature combination required two samples, one for the post-annealing measurement of n_e and then to be electron irradiated and measured for the LVM absorption, the other for TEM analysis. Again additional samples were required for mechanical measurements, and they have not been included in this description. In a few cases the annealed samples used for n_e and infrared measurements were subsequently TEM analyzed to determine if the e^--irradiation produced changes in the annealed sample microstructure. As in the non-annealed samples the comparisons made here and those made previously[61] for the annealed and irradiated samples with those annealed but non-irradiated showed that no

TEM sensitive microstructural differences occurred.

The infrared absorption measurements were made with a single-beam grating spectrometer equipped with a set of transmission filters to isolate the first order spectrum. The transmission was measured in a low temperature optical dewar by using the sample in-sample out method with the sample mounted over one of a pair of matched aperatures. The spectral range covered was 350 $cm^{-1} \lesssim \nu \lesssim 500\ cm^{-1}$ which contains all of the absorption bands of interest.

In a few cases, larger frequency ranges were covered to ensure that no new bands were being introduced. The samples used for the infrared measurements were generally about 0.3 mm thick and had a wedge of $\sim 0.2^{o}$ to eliminate multiple reflection interference fringes. The absorption coefficient α was calculated from the transmission T by using the standard expression:

$$T = I_{sample}/I_{o} = (1-R)^{2}\exp(-\alpha x)/1-R^{2}\exp(-2\alpha x),$$

where R is the reflectivity and x is the sample thickness.

All of the samples for TEM studies were lapped and polished on both surfaces to a thickness of ~ 0.2 mm. Specimens of $\sim 3 \times 3\ mm^{2}$ were cut and were thinned by using a chemical jet polishing technique[62] to obtain samples suitable for the TEM measurements. The specimens were examined by a Hitachi HU-125C transmission electron microscope operated at 125 KV. TEM measurements of the HT+Q, Si-doped samples as well as undoped samples showed them to be free of microstructure except for an occasional dislocation loop. In particular the samples showed no stacking faults or precipitates while Si-doped samples which

had not been given the HT+Q treatment, i.e. in the as-grown condition, were found to have frequent extrinsic stacking faults, particularly those samples having the largest [Si], i.e. WA-Si.

IV. Results

The body of experimental data to be presented here is organized in sections as follows:

A. Annealing-induced changes in n_e

B. Annealing-induced changes in LVM absorption

C. Annealing-induced effects in the TEM measured microstructure.

In each case the data will include the results for the three [Si] and for all anneal temperatures. The results of mechanical measurements will be discussed later.

A. Annealing-induced changes in n_e:

Ingot KM-26, [Si] $\sim 1.5\times10^{18}$ cm^{-3}, $n_e \sim 1.0\times10^{18}$ cm^{3}

Measurements of samples cut from this ingot and given the HT+Q treatment showed no change in n_e after annealing at 400, 500, and 700°C.

Ingot KM-16, [Si] $\simeq 2.5\times10^{19}$ cm^{-3}, $n_e \simeq 5\text{-}7\times10^{18}$ cm^{-3} and

Ingot WA-Si, [Si] $\simeq 3\text{-}6\times10^{19}$ cm^{-3}, $n_e \simeq 7\text{-}9\times10^{18}$ cm^{3}.

Samples from these ingots show dramatic annealing-induced changes in n_e, and the results are shown in Figs. 2, 3, and 4. The $T_A \gtrsim 600$°C anneal curves appear to have reached equilibrium by approximately 150h while the 400 and 500°C curves have not reached equilibrium for the longest anneal times used. Decreases in n_e approaching an order of magnitude are observed. Even though the equilibrium values are not reached at the lower temperatures, it appears from the data that the

equilibrium value for n_e increases with increasing T_A. From previously reported measurements[4] it is known that the annealing-induced changes are reversible, i.e. a HT+Q treatment restores n_e to the pre-annealed value.

B. Annealing-Induced Changes in LVM Absorption:

Ingot KM-26

Because of the relatively low [Si] in this ingot, only the Si_{Ga} and Si_{As} bands at 384 and 399 cm^{-1} were observed. These absorption bands showed no measureable change in integrated strength, $\alpha_p\Delta$, as a result of annealing at any of the temperatures. The n_e values calculated from the free carrier plasma minimum in the reflectivity before e^--irradiation are known to be close to those obtained from Hall measurements and are referred to as "measured" values. By using $n_e(\text{optical}) = a(\alpha_p\Delta)_{384} - b(\alpha_p\Delta)_{399}$, where $a = 10.0\times10^{16}$ cm^{-1} and $b = 12.7\times10^{16}$ cm^{-1}, values of n_e (optical) can be calculated from the LVM data and they are in good agreement with the measured values. The comparison will be discussed later. Hereafter n_e(optical) refers to the n_e calculated from the LVM data. It may also be noted that $[Si_{Ga}]=a(\alpha_p\Delta)_{384}$ and $[Si_{As}] = b(\alpha_p\Delta)_{399}$, and thus, the LVM results can be presented in terms of the concentrations of the related defects.

Ingot KM-16 and Ingot WA-Si

The LVM measurements were made with the same samples used for the n_e measurements described above. As an illustrative example, the infrared absorption specturm of a 500°C/1200h annealed sample from KM-16 is shown in Fig. 5 along with the spectrum for an identical but non-annealed sample. The band frequencies observed in Fig.5 are the same as those observed previously and given in Table I. In this illustrative case it

is seen that the anneal causes changes in all of the LVM bands and hence in the concentrations of the related defects. One can calculate n_e(optical) from

$$n_e(\text{optical}) = a(\alpha_p\Delta)_{384} - b(\alpha_p\Delta)_{399} + c(\alpha_p\Delta)_{367} - d(\alpha_p\Delta)_{369}$$

$$= [Si_{Ga}] - [Si_{As}] + [367\ cm^{-1}\text{defect}] - [369\ cm^{-1}\text{defect}],$$

where a and b are the same as above, c = 25.3×10^{16} cm^{-1}, and d = 19.0×10^{16} cm^{-1}. Again,each term on the right is the concentration of the related defect. The LVM strengths for all annealing conditions have been measured and some of the results are given in terms of defect concentrations in Figs.6 through 9. Since the constant of proportionality between $[Si_{Ga}\text{-}Si_{As}]$ and $(\alpha_p\Delta)_{393}$ is not known, the $[Si_{Ga}\text{-}Si_{As}]$ in these figures is not the actual concentration but proportional to it. Figures 6 through 8 give the results for ingot KM-16 and Fig.9 is for WA-Si after 700°C annealing.

The relationship between n_e (optical) and n_e (measured) for all non-annealed samples is shown in Fig. 10. The straight line of slope one indicates n_e (optical) = n_e (measured), and as it is seen in this figure all non-annealed samples lie close to this line. In one sense this agreement is not surprising since the LVM measurements for these samples are those which were used[11] to determine a, b, c, and d which yielded n_e (optical). However, the close fit of all 18 points is significant when one realizes that there were only 4 adjustable parameters. The changes in n_e (optical) with annealing time are illustrated for 2 different values of T_A in Fig. 11 and compared with the annealing curves for n_e (measured) for the same samples and conditions. The two

400°C anneal curves are very close to one another while those for 500°C strongly diverge. The results of similar measurements for all ingots and annealing conditions are summarized in Figs. 12 and 13, where n_e (optical) is plotted against n_e (measured). In all cases where the points do not lie close to the lines of slope one they are high because the decrease in n_e (optical) is too small to account for the observed decrease in n_e (measured).

C. TEM Measured Microstructure:

As mentioned previously, the HT+Q treated samples which were not annealed all had no significant microstructure for all three ingots. Only a few dislocations were observed. In particular there were no stacking faults, no dislocation loops and no precipitates. After annealing, some significant changes were seen for the more heavily doped samples.

Ingot KM-26

Similar to the n_e and LVM results for this ingot of lowest [Si], there were no microstructural changes observed for any of the annealing temperatures or times. The samples remained essentially featureless.

Ingot KM-16 and Ingot WA-Si

Figure 14 shows a set of micrographs for samples from Ingot KM-16 which were given the HT+Q treatment and then annealed at different temperatures. No dislocation loops were observed for annealing temperatures of 400 and 500°C. As $T_A \gtrsim 600$°C a high density of loops is observed. In general the loop size increases and the loop density decreases for increasing T_A. Ingot WA-Si has a similar behavior except that the total loop area per unit volume is larger. Tables III and IV summarize the TEM results for the annealed samples from the two ingots.

The loop densities and areas are rough estimates from micrographs. For $600^{o}C \lesssim T_A \lesssim 800^{o}C$ anneals, increasing the anneal time increases the loop size and decreases the density. For each ingot the total loop area shows some increase for short anneal times and then tends to remain essentially constant for longer annealing times at 600, 700, and $800^{o}C$. The total loop area appears to start to decrease at $900^{o}C$ and by $1000^{o}C$ is significantly decreased for both ingots.

The effect of the anneal temperature and time on the habit planes of the loops is also indicated in Tables III and IV. A short term anneal produces small loops lying on {111} planes with $\vec{b} = a/3[111]$. Increasing the anneal time increased the loop size and the loops were increasing on {110} planes with $\vec{b} = a/2[110]$. For annealing temperatures $T_A \gtrsim 800^{o}C$ and times $\geq$ 150h the {111} loops had disappeared and the {110} loops increased in size and decreased in density.

All of the above TEM results are similar to those previously reported for annealed, heavily Te-doped GaAs.[47] The primary differences are that the loops in the Te-doped material are formed at T_A as low as $380^{o}C$ and the loop area is constant for all T_A up to $1000^{o}C$ and for all times.

An analysis[63] of the TEM results has been made for different T_A by using 12 of the annealed samples from both ingots in order to determine the nature of the loops. In all cases the loops were found to be of the extrinsic type. This result differs from that previously given by Narayanan and Kachare[5] for annealing-induced loops in similar material. They found the loops were of the intrinsic type, i.e. vacancy loops. In order to check the present results, a different and independent TEM analysis[64] was doubly conducted on some of the above 12 annealed samples, which show faulted loops on {111}. Moreover, two additional annealed samples

were sent to the Boeing Aerospace Corp. (Seattle, Wash.) for a second analysis with a different microscope (EM300) and operator. The results all confirmed the conclusion that the loops are of the extrinsic type.

In an attempt to resolve the differences between the present results and the previous work samples from KM-16 and samples from the ingot used by the previous authors were given the same HT+Q treatment employed in the previous study (1100^{o}C/15 min) and then annealed at exactly the same condition, i.e. 750^{o}C/320h which was an annealing condition of the previous study. The TEM analysis[63] were carefully conducted and the results confirmed that the loops are indeed of the extrinsic type. We have therefore been unable to reproduce the results of the previous study even when the experimental conditions are the same as those specified by the previous authors. In all of the present work for all heavily-Si doped ingots the thermal annealing-induced loops are always extrinsic.

In a previous study[37] of Li-saturated GaAs:Si, where the Li saturation was done at temperatures in the range of the T_A values used here and where the same material used here was also used for that study, extrinsic loops were also observed and scanning electron microscope measurements employing an energy resolution system established that the loops were Si-rich. By assuming the loops in the present study contain double layers of Si interstitial atoms, one can roughly estimate the Si content in the loops, i.e. $[Si]_{loop}$, for each annealed sample. These estimates are also given in Tables III and IV. Further justification of this assumption was supplied by one KM-16 sample which was double annealed at 950°/2h+700°C/65h. Large extrinsic and triangular loops having a size of approximate 7000 Å were observed. The loop size is similar but even larger than that observed for the 900°C annealed case. Microanalysis of these large loops with a scanning electron microscope showed that they have a large Si content similar to the loops in the Li saturated GaAs:Si. We therefore assume that all the observed extrinsic loops are due to Si precipitation from the GaAs:Si solution.

V. Discussion

The first part of this section examines the conclusions which can be drawn from the results of the previous section and the relationships between the different measurements. As will be seen the rather extensive

body of experimental data permits one to examine the behavior of a relatively complicated system. The discussion is unusual in that the measurements allow conclusions to be formed on the basis of the knowledge of the changes of individual defect concentrations rather than considerations only in terms of quantities such as n_e which depend upon the net behavior of two or more defect concentrations. The second part of this section will utilize the results in an attempt to interpret the annealing-induced changes in mechanical properties.

A. Carrier Density, LVM, and Microstructure:

Ingot KM-26

In this relatively lightly Si-doped ingot there appears to be no detectable effect of annealing. The values of n_e, $[Si_{Ga}]$, $[Si_{As}]$ and the microstructure are all unchanged by the longest annealing times at all temperatures. This result is in agreement with the previous less detailed results for n_e by KS[3] for GaAs:Si with a similar [Si].

Ingot KM-16 and WA-Si

In the more heavily doped ingots there are a large number of annealing-induced changes. In general, the pattern of the changes are similar for both ingots. The results will be examined for each annealing temperature.

(400°C) After annealing at this temperature there are essentially no loops or other microstructural features although both $[Si_{Ga}]$ and n_e showed large decreases. The other Si defect concentrations including $[Si_{As}]$, $[Si_{Ga}\text{-}Si_{As}]$, [367 cm^{-1} defect], and [369 cm^{-1} defect] all remained constant or showed relatively small changes even for the samples with the highest [Si]. It is also noted in Figs. 12 and 13 that all of

the 400°C points are close to the straight lines of slope one indicating that n_e(optical) is essentially equal to n_e(measured) for all anneal times and for both ingots. This conclusion can also be reached by considering Fig.11. Therefore the decrease in n_e(measured) with anneal time is attributable entirely to the decrease in $[Si_{Ga}]$ donors. It is also observed that the decrease in Si_{Ga} defect concentration cannot be allocated to increases in any of the other observed defect concentrations in Fig.6 and similarly for WA-Si for the same anneal conditions unless one assumes that each defect involves several Si atoms. The latter possibly can be rejected since earlier Si isotopic studies[16] showed that the 367 and 369 cm^{-1} bands involve one Si atom per defect. Since no precipitates or extrinsic loops are observed in the 400°C annealed material we attribute the change in $[Si_{Ga}]$ to the formation of a new neutral point defect. It has been proposed previously[4-6] that this new point defect results from the generation of V_{Ga} acceptors followed by a pairing reaction to forms Si_{Ga}-V_{Ga}. It is clear that this new defect cannot be responsible for either the 367 or 369 cm^{-1} bands, and it is therefore disturbing that no new bands attributable to the LVM of this defect are observed. It is possible that the presence of the second neighbor vacancy lowers the effective force constants at the Si site and the LVM frequencies shift down into the region of high lattice absorption of the GaAs and hence are not observable. For the purposes of the present study the formation of Si_{Ga}-V_{Ga} defects is regarded as the mechanism responsible for the decrease in $[Si_{Ga}]$. There is however no evidence here that the Si_{Ga}-V_{Ga} formation is indeed responsible for the changes in $[Si_{Ga}]$.

(500°C) As after annealing at 400°C the samples have no observable microstructural features and in particular, no loops or faults. The defect

behavior is much more complicated than that at 400°C in that all of the defects change concentration in significant amounts. The [Si_{Ga}], [Si_{As}], and n_e (measured) decrease while all of the other defects show increases, especially for the longest anneal times. Of particular interest is the increase in [Si_{Ga}-Si_{As}] after 1200h which indicates that there is detectable Si diffusion at this temperature. Of the 3 temperatures studied in detail, 400, 500, and 700°C the only temperature at which changes in Si_{Ga}-Si_{As} pair concentrations are observed is at 500°C. KS[4] have previously reported this effect for 600°C annealing. Assuming the [Si] to be uniform and the diffusion length to be equal to the distance between two nearest Si atoms, a diffusion constant of about 3×10^{-20} cm^2 sec^{-1} at 500°C is obtained. This value is in reasonable agreement with that estimated by KS[4] from earlier data.

As indicated in Figs. 11, 12, and 13, n_e (optical) does not equal n_e (measured) after annealing at 500°C. In particular the n_e (measured) decreases substantially while n_e (optical) has very little decrease. The n_e (optical) decreases about 10% for KM-16 and about 30% for WA-Si while n_e (measured) decreases by a factor of six to eight for the longest anneal times for both materials. Therefore one must postulate the formation of a new "unknown acceptor" which is not observed in the LVM spectra and is not the Si_{Ga}-V_{Ga} center proposed to explain the 400°C change in [Si_{Ga}]. The concentration of the new acceptor is given by n_e (optical) - n_e (measured) for the longest anneal times and this quantity is plotted in Fig. 15 as a function of the anneal temperature. The curves on the figure have no significance other than to smoothly connect the experimental points. If the loss in [Si_{Ga}] plus the loss in [Si_{As}] is compared with the gains in the [367 cm^{-1} defect] and

[369 cm^{-1} defect] and if one assumes one Si/defect for the latter two cases as indicated by the prior isotropic studies,[16] then there could be a sufficient net [Si] loss to account for both the increase in [Si_{Ga}-Si_{As}] and the [unknown acceptor], again assuming the latter has one Si/defect. Therefore after annealing at 500°C one does not have to postulate the presence of any Si in the system other than that present or proposed for the point defects discussed. A major uncertainty here is the lack of information on changes in [Si_{Ga}] due to Si_{Ga}-V_{Ga} formation. Moreover, as will be seen a different conclusion seems to be required from the 700°C annealing data.

(700°C) At this annealing temperature microstructure is introduced in the form of loops. The loops density decrease and the average loop size increases with time, see Tables III and IV. The loops are of the extrinsic type. There is no listing[65] of any Ga_xSi_y or Si_xAs_y compounds, and therefore equal numbers of Ga and As interstitials or of Si interstitials are the only two likely possibilities for the extrinsic loops. As previously reported in the study of the annealing effect for GaAs:Te material, the loops consisting of Ga and As interstitials started to form even for an annealing temperature as low as 380°C while in the present study the loops formed only for $T_A \gtrsim 600°C$. Because of the lower diffusion coefficient for Si in GaAs for the temperature range of concern, it is not unreasonable to find a larger T_A is required for extrinsic loops formed of Si interstitials.[47] Silicon has a diamond structure with a lattice parameter of 5.43 Å which is close to that of GaAs and hence layers of Si could be easily accomodated in the GaAs lattice.

As observed in Figs. 12, 13,and 15,the n_e (optical) and n_e (measured) behave in a manner similar to that observed at 500°C. Again a large [unknown acceptor] is necessary to account for the fact that n_e (optical) $\gg$ n_e (measured) after prolonged annealing. However, the individual defect concentrations showed a significantly different behavior at 700°C than at 500°C. The [Si_{Ga}-Si_{As}] remained constant, the [Si_{Ga}] and [Si_{As}] both decreased in the first 0.5 h and were essentially constant thereafter and the 367 and 369 cm^{-1} defects increased somewhat,particularly in WA-Si. Again, if it is assumed that there is one Si/defect, then the total loss of Si from Si_{Ga} and Si_{As} defects and the total gain in the 367 and 369 cm^{-1} defects are both approximately $10x10^{18}$ cm^{-3}. The 2 to $3x10^{18}$ cm^{-3} Si atoms in the loops is relatively small compared to these changes (see Table IV for WA-Si) and the loops could come from the net changes in these defect concentrations. This is an attractive explanation since the large decreases in the Si_{Ga} and Si_{As} concentrations and the loop formation both take place in the first 0.5h of annealing. However, it is very unlikely that the changes in these same point defect concentrations could also supply the $5x10^{18}$ cm^{-3} Si atoms in the "unknown acceptor". Therefore if the "unknown acceptor" does involve Si it would appear to require a Si source beyond those considered here. Other studies[14,37] have suggested that in heavily Si-doped GaAs, not all the Si is in the defects responsible for the LVM spectra.

(800,900,1000°C) In this temperature range all of the annealing-induced changes reduce as one increases T_A. The n_e (measured) comes closer to the pre-annealed HT+Q value, n_e (optical) becomes nearly equal to n_e (measured) so that the [unknown acceptor] becomes small,

the individual defect concentration changes are reduced, and the loop area and hence Si in the loops is also reduced.

B. Relationship of Yield Stress to n_e, LVM, and TEM Results.

Recently, Ganesan and Copley[7] reported yield stress measurements at 400°C on two sets of samples with different [Si] which were taken from two of the ingots (KM-16 and WA-Si) used for the present study. The samples for the stress measurements were prepared from regions of each ingot adjacent to those from which samples were taken for the measurements reported here. Figures 16 and 17 show the yield stress as a function of annealing time for these samples for T_A = 400, 500, and 700°C. The results given in these two figures are similar to those of previous measurements.[6] An unusual feature seen in Fig. 17 is the T_A = 700°C curve for samples with the largest [Si]. They seem to have reached saturation even before the annealing. Although the crystal orientation of the samples from two ingots were shown to be different, the Schmidt factors[66] turn out to be identical. Hence it can be inferred that the difference in yield stress values arises from the [Si] difference between the ingots rather than an orientation effect. In general, the yield stress values before annealing increase with increasing [Si].

One primary conclusion of the previous section is that the decrease of $[Si_{Ga}]$ after T_A = 400°C annealing is produced by the generation of V_{Ga} and the formation of neutral Si_{Ga}-V_{Ga} pair defects. This process is also responsible for the decrease in n_e. As previously discussed it has been concluded[6] that these Si_{Ga}-V_{Ga} pair defects are responsible for the dramatic increase in yield stress after annealing. If one were to

assume for all T_A the decrease in $[Si_{Ga}] = \delta[Si_{Ga}]$ arises completely from the formation of Si_{Ga}-V_{Ga} pairs, i.e. $\delta[Si_{Ga}] = -\delta[Si_{Ga}\text{-}V_{Ga}]$ one can attempt to correlate the LVM results for $\delta[Si_{Ga}]$ to yield stress changes shown in Figs. 16 and 17. A customary relation is of the form[57] $\sigma-\sigma_o = A(N_0+\delta[Si_{Ga}])^m$, where σ is the yield stress, σ_o is the yield stress for undoped GaAs, N_o is the pre-anneal, HT+Q $[Si_{Ga}\text{-}V_{Ga}]$, $\delta[Si_{Ga}]$ is the assumed change in $[Si_{Ga}\text{-}V_{Ga}]$, and A and m are constants. Fig. 18 shows that a good correlation for both ingots is obtained for $T_A = 400^oC$ anneals and requires that m = 1/4. The value of A and the two N_o values, one for each ingot, are determined by the data of three samples: one non-annealed sample from each ingot and a $400^oC/1200h$ annealed sample from KM-16. The calculated N_o value is $1x10^{15}$ cm^{-3} for KM-16 and $3.8x10^{17}$ cm^{-3} for WA-Si. The plot of the resulting equation is shown by the straight line in Fig. 18. For crystals of NaCl, NaBr, KCl, and KBr, Chin et al.[55] experimentally showed that the yield stress measurements give m = 1/2. The defect density was assumed to be equal to the doping concentrations of divalent impurity ions such as Ca^{2+}, Sr^{2+}, Ba^{2+} added during crystal growth.

If however, the defect responsible for altering the yield stress is a vacancy-impurity pair similar to that proposed here then a likely process for pair formation involving the Ca^{2+} is $Ca^{\bullet}_{Na} + V^{\prime}_{Na} \rightarrow (Ca_{Na}\text{-}V_{Na})^x$, where $\bullet$, $\prime$, and x mean singly positive, singly negative, and uncharged species with respect to the charge normally present at the lattice site. If the $V^{\prime}_{Na}$ concentration is determined by the Ca^{2+} concentration then mass action gives $[(Ca_{Na}\text{-}V_{Na})^x] = k_p[Ca^{\bullet}_{Na}]\,[V^{\prime}_{Na}] = k_p[Ca^{\bullet}_{Na}]^2$. If most of the Ca impurity is present as $Ca^{\bullet}_{Na}$ then $[Ca^{\bullet}_{Na}] \approx [Ca^{2+}]$, and $\sigma-\sigma_o \propto [Ca^{2+}]^{\frac{1}{2}} \propto [(Ca_{Na}\text{-}V_{Na})^x]^{\frac{1}{2}}$. Thus the result becomes identical to that determined here where the Si_{Ga}-V_{Ga} pair concentration is measured in a much more direct manner.

Indeed, the results reported here show the first experimental data for the dependence of the yield stress on the measured concentration of the specific defect responsible for strengthening.

As indicated in Fig.18, the data of the long term annealed samples at 500 and 700°C for both ingots are not in agreement with the results of the T_A = 400°C anneals. This indicates that the assumption that decrease in $[Si_{Ga}]$ for these samples after 500°C or 700°C annealing comes completely from the formation of the Si_{Ga}-V_{Ga} defect is not valid.

From the data in Fig. 18 it is clear that the yield stress indicates that only a small fraction of the decrease of $[Si_{Ga}]$ can be resulting from Si_{Ga}-V_{Ga} formation for these T_A cases. This conclusion is consistent with the LVM results for both ingots which show that Si_{Ga}-Si_{As} pair defect and other Si related defects grow after T_A = 500°C anneal, and the Si-rich loops as well as the other Si related defects grow after the T_A = 700°C anneal. Indeed, we have already concluded for the same T_A values that almost all the decrease in $[Si_{Ga}]$ as well as that for the $[Si_{As}]$ was required to explain the observed increases in the other Si point defects and microstructure. The most striking example of the correlation of the different results is for the T_A = 700°C annealing of WA-Si. The large decrease of $[Si_{Ga}]$ in the first 0.5h was required to explain the extrinsic loop formation. If the decrease in $[Si_{Ga}]$ were all by the formation of $[Si_{Ga}$-$V_{Ga}]$ then the final σ-σ_o should have been a factor of $\sim$2 higher than the observed value. The constancy of $[Si_{Ga}]$ after this initial decrease is also consistent with the constancy of the yield stress for different annealing times.

VI. Summary

Measurements of the isothermal annealing-induced changes in the carrier density, LVM spectra, TEM microstructure and critical resolved shear stress of GaAs:Si have been compared for three different [Si] ingots at several annealing temperatures. The principal results of this study are that for $[Si] \simeq 1$ to 2×10^{18} cm^{-3} there are no significant annealing-induced changes in any of the measured properties while for $[Si] \gtrsim 2$ to 6×10^{19} cm^{-3} there are major changes in all of the properties. The detailed nature of the changes depends upon the anneal temperature and time. The following conclusions all pertain to the

heavily doped material:

(1) For 400°C annealing, the decrease observed in n_e can be accounted for quantitatively by the decrease in the Si_{Ga} donor concentration as measured by the LVM spectra. None of the other Si defects observed in the LVM spectra change concentration significantly. The mechanism suggested to account for the decrease in Si donors is pairing with vacancies to form the Si_{Ga}-V_{Ga} pair defects.

(2) For 500°C annealing, the decrease in n_e cannot be attributed to changes in any or all of the LVM defects, and it is necessary to proposed to an "unknown acceptor" of concentration comparable to that of the other defects. Si defect concentrations change with prolonged annealing times, however these changes can be largely attributed to redistribution of the Si among the various defect species.

(3) For 700°C annealing, extrinsic Si-rich loops are observed after the shortest annealing times, and the Si in these loops appears to come from decreases in the Si_{Ga} and Si_{As} concentrations which are also observed after the shortest annealing times. Again a large concentration of "unknown acceptors" is necessary to account for the decrease in the measured n_e. If these acceptors involve Si then this Si must come from a source other than those defects observed in the LVM spectra, i.e. the Si_{Ga}, Si_{As}, Si_{Ga}-Si_{As} pairs or two other unidentified Si defects.

(4) For annealing temperatures above 700°C the changes in all of the properties reduce as T_A increases. The concentration of unknown acceptors is essentially zero by $T_A \approx 1000°C$.

(5) The previous measurements of the critical resolved shear stress are consistent with the results of the annealing-induced changes in the other physical properties if one assumes a shear stress dependence of the form $\sigma-\sigma_o = A(N_o+\delta[Si_{Ga}])^{1/4}$. The data indicate that the decrease in $[Si_{Ga}]$ at $T_A = 400^oC$ is likely due to V_{Ga} generation followed by Si_{Ga}-V_{Ga} pair formation while at higher T_A values the formation of this defect pair can account for only a small fraction of the decrease in the Si_{Ga} concentration.

VII. ACKNOWLEDGMENTS

This work was supported by the Air Force Office of Scientific Research (AFSC) under Contract 76-2990. The authors wish to express their appreciation to Dr. G. H. Narayanan of the Boeing Aerospace Corporation for performing electron microscopy measurements on a pair of samples which helped confirm the nature of the dislocation loops, and also for his advice on the TEM results. Drs. O. K. Kim, V. Rana and P. S. Vijayakumar were of considerable help during the early phases of this study. The authors would also like to thank L. Lowe and D. Morris for their aid with the electron irradiations and their hospitality of one of the authors (W.G.S.) during his stay at Hanscom Field, Massachusetts. The authors are also grateful to Professor D. B. Wittry for useful discussions during the electron microanalysis, to Professor S. M. Copley for his advice on mechanical results,and to George Mueller for his help with sample preparation and his helpful advice throughout this work.

REFERENCES

1. C. J. Hwang, J. Appl. Phys. 40, 4591 (1969).
2. L. H. Skolnik, W. G. Spitzer, A. Kahan, H. Euler, and R. G. Hunsperger, J. Appl. Phys. 43, 2146 (1972).
3. J. K. Kung and W. G. Spitzer, J. Appl. Phys. 44, 912 (1973).
4. J. K.Kung and W. G. Spitzer, J. Appl. Phys. 45, 4477 (1974).
5. G. H. Narayanan and A.H. Kachare, Phys. Stat. Sol. (a) 23, 657 (1974).
6. V.Swaminathan and S. M. Copley, J. Appl. Phys. 47, 4405 (1976).
7. V. Ganesan, Master Degree Thesis, University of Southern California, January, 1979. V. Ganesan and S. M. Copley (Private Communication).
8. J. M. Whelan, J. D. Struthers, and J. A. Ditzenberger, Proceedings of the International Conference on Semiconductor Physics (Czechoslovak Academy of Science, Prague, 1960), p. 943.
9. M. N. Kamalov, L. I. Kolesnik, M. G. Mil'vidskii, V. V. Rakov, and I. N. Shershakova, Sov. Phys. Semicond. 12, 340 (1978).
10. K. Laithwaite and R. C. Newman, J. Phys. C: Solid State Phys. 9, 4503 (1976).
11. R. T. Chen, V. Rana, and W. G. Spitzer (Private Communication).
12. H. J. Queisser, J. Appl. Phys. 37, 2909 (1966).
13. W. G. Spitzer and W. Allred, J. Appl. Phys. 39, 4999 (1968).
14. M. R. Brozel, R. C. Newman, and B. Ozbay (Private Communication).
15. C. M. Wolfe and G. E. Stillman, Appl. Phys. letters 27, 564 (1975).
16. P. C. Leung, J. Fredrickson, W. G. Spitzer, A. Kahan, and L. Bouthillette, J. Appl. Phys. 45, 1009 (1974).
17. C. Kolm, S. A. Kulin, and B. L. Averbach, Phys. Rev. 108, 965 (1957).
18. J. T. Edmund, J. Appl. Phys. 31, 1428 (1960).
19. J. J. Wysocki, J. Appl. Phys. 31, 1686 (1960).

20. C. J. Huang, J. Appl. Phys. 39, 5347 (1968).

21. M. E. Weiner and A. S. Jordan, J. Appl. Phys. 43, 1767 (1972).

22. M. Toyama, Jap. J. Appl. Phys. 8, 1000 (1969).

23. S. Marie and M. Stogic, Phys. Stat. Sol. (a) 32, K63 (1975).

24. J. S. Harris, Y. Nannichi, G. L. Pearson, and G. M. Day, J.Appl.Phys. 40, 4575 (1969).

25. E. Mũnoz, W. L. Snyder, and J. L. Moll, Appl. Phys. Letters 16, 262 (1970).

26. P. K. Chatterjee, K. V. Vaidyanathan, M. S. Durschlag, and B. G. Streetman, Solid State Communications 17, 1421 (1975).

27. S. Y. Chiang and G. L. Pearson, J. Appl. Phys. 46, 2986 (1975).

28. S. Y. Chiang and G. L. Pearson, J. of Photoluminescence 10, 313 (1975).

29. L. L. Chang, L. Esaki, and R. Tsu, Appl. Phys. Letters 19, 143 (1971).

30. W. Y. Lum and H. H. Wieder, J. Appl. Phys. 49, 6187 (1978).

31. W. H. Koschel, B. G. Bishop, B. D. McCombe, W. Y. Lum, and H. H. Wieder, Sixth International Symposium on Gallium Arsenide and Related Compound, Edinburgh, Sept. 20, 1976 (Institute Phys. Conf. 33a, Inst. of Physics, London, 1977), p. 98.

32. Tadatsugu Itoh and Masami Takeuchi, Japanese J. of Appl. Phys. 16, 227 (1977).

33. E. V. K. Rao and N. Duhamel, J. Appl. Phys. 49, 3458 (1978).

34. Jun-ichi Nichizawa, Hideo Otsuka, Shizenobu Yamakoshi, and Katsuhiko Ishida, Jap. J. of Appl. Phys. 13, 46 (1974).

35. W. G. Spitzer, Adv. in Solid State Phys. XI (Edited by O. Madelung, Pergamon Press, March 22-26, 1971) p. 1.

36. W. G. Spitzer and W. P. Allred, Appl. Phys. Letters 12, 5 (1968).

37. R. T. Chen and W. G. Spitzer (Private Communication).

38. K. Laithawaite and R. C. Newman, Phil. Mag. 35, 1689 (1977).

39. P. G. Dawber and R. J. Elliott, Proc. Phys. Soc. 81, 453 (1963).

40. C. S. Fuller and K. B. Wolfstirn, J. Appl. Phys. 34, 2287 (1963).

41. P. M. Grinshtein, M. Ya. Lipkes, N. S. Rytora, and V. I. Fistul', Sov. Phys.-Semiconductors 9, 725 (1975).

42. S. P. Grishina, M. G. Mil'vidskii, V. B. Osvenskii, and V. I. Fistul Sov. Phys.-Semiconductors 4, 240 (1970).

43. M. G. Mil'vidskii, V. B. Osvenskii, V. I. Fistul, E. M. Omel'yanovskii, and S. P. Grishima Sov. Phys.-Semiconductors 1, 813 (1968).

44. B. Hughes and G. H. Narayanan, Phys. Stat. Sol. (a) 46, 627 (1978).

45. D. Laister and G. M. Jenkins, Phil. Mag. 23, 1077, (1971).

46. P. W. Hutchinson and P. S. Dobson, Phil Mag. 30, 65 (1974).

47. P. W. Hutchinson and P. S. Dobson, J. Materials Science 10, 1636-1641 (1975).

48. L. M. Morgulis, M. G. Mil'vidskii, and V. B. Osevenskii, Sov. Phys.-Solid State 16, 784 (1974).

49. Taibun Kamejima, Junji Matsui, Yasuo Seki, and Hiso Wantanbe, J. Appl. Phys. 50, 3312 (1979).

50. M. S. Abrahams, J. Blanc, and C. J. Buiocchi, J. Appl. Phys. 45, 3277 (1974).

51. Brian Norris and G. H. Narayanan, J. Appl. Phys. 48, 2784 (1977).

52. N. P. Sazhin, M. G. Mil'vidiskii, V. B. Osvenskii, and O. G. Stolyarov, Sov. Phys.-Solid State 8, 1223 (1966).

53. D. Laister and G. M. Jenkins, J. Mater. Sci. 8, 1218 (1973).

54. V. Swaminathan and S. M. Copley, J. Am. Ceram. Soc. 58, 482 (1975).

55. G. Y. Chin, L. G. Van Uitert, M. L. Green, G. J. Zydjik, and T. K. Kometani, J. Am. Ceram. Soc. 56, 369 (1973).

56. F. A. Kröger, Ann. Rev. Mater. Sci. 7, 449-475 (1977).

57. J. J. Gilman, J. Appl. Phys 45, 508 (1974).

58. R. K. Willardson and W. P. Allred, Symp. on GaAs, 35 (1966).

59. Crystal Specialties Inc., 419 W. Maple Street, Monrovia, Calif.

60. K. Okada and T. Oku, Jap. J. Appl. Phys. 6, 276 (1967).

61. G. H. Narayanan (Private Communication).

62. G. H. Narayanan and S. M. Copley, Phys. Stat. Sol. (a) 23, 123 (1974).

63. J. W. Edington, Practical Electron Microscopy in Materials Science (Van Nostrand Reinhold, New York, 1976), p. 134-136.

64. R. Gevers, A. Art, and S. Amelinckx, Phys. Status Solidi, 3, 1563 (1963).

65. Handbook of Chemistry and Physics, 60th Edition (1979-1980), CRC Press, Inc., Boca Roton, Florida.

66. Robert E. Reed-Hill, Physical Metallurgy Principles (Van Nostrand, N. J., 2nd Edition, 1973), p. 173-177.

Table I. Observed LVM Band Frequencies at Liquid Nitrogen Temperature in Si-Doped GaAs Compensated by e-Irradiation.

MODE FREQUENCY (cm^{-1})	ELECTRICAL CHARACTER	DEFECT
384	Donor	Si_{Ga}
399	Acceptor	Si_{As}
393	}	Si_{Ga}-Si_{As}
464	}	
367	Donor[a]	Si Related
369	Acceptor[a]	Si Related

[a]See text for explanation of this assignment.

Table II. Isothermal Annealing Schedule for all Samples.

Ingot	[Si] (cm^{-3})	n_e[a] (cm^{-3})	Isothermal Annealing Schedule (After HT+Q)
KM-26	$\sim 1.5 \times 10^{18}$	$\sim 1 \times 10^{18}$	400°C/153h, 500°C/153h, 700°C/1.5h,153h
KM-16	$\sim 2.5 \times 10^{19}$	5.65×10^{18}	400°C/0.5h,1.5h,15h,400h,1200h,2000h
		$5.65\text{-}6.1 \times 10^{18}$	500°C/0.5h,1.5h,50h,1200h
		$\sim 5.9 \times 10^{18}$	600°C/1.5h[b],64h[b],300h[b]
		6.7×10^{18}	700°C/0.5h,1.5h,15h,150h,600h[b]
		6.1×10^{18}	750°C/1.5h[b],9h[b],64h[b],600h[b]
		$7.3 \times 10^{18}, 6.1 \times 10^{18}$	800°C/1.5h[b],18h[b],46h[b],400h
		7.4×10^{18}	900°C/1.5h[b],19h[b],150h
		7.3×10^{18}	1000°C/150h
WA-Si	$3 \sim 6 \times 10^{19}$	$8.3\text{-}9.0 \times 10^{18}$	400°C/0.5h,1.5h,15h[b],400h,2000h
		$7.8\text{-}8.8 \times 10^{18}$	500°C/0.5h,50h,1200h
		$8.3\text{-}8.8 \times 10^{18}$	700°C/0.5h,1.5h,15h,50h,150h,168h,400h,992h[b]
		$\sim 8.0 \times 10^{18}$	750°C/1.5h[b],18h[b],618h[b]
		8.0×10^{18}	800°C/1.5h[b],20h[b],150h[b],400h
		7.6×10^{18}	900°C/150h
		8.0×10^{18}	1000°C/150h

Note: a. n_e values before isothermal annealing but after HT+Q.

b. n_e and TEM measurements and no LVM measurements.

Table III. TEM Results of Isothermal Annealing of Si-Doped GaAs Samples from the Ingot KM-16 ($[Si] \simeq 2.5 \times 10^{19}$ cm^{-3}).

ANNEAL TEMPERATURE	ANNEAL TIME	AVERAGE LOOP DENSITY (cm^{-3})	AVERAGE LOOP SIZE (A)	APPROXIMATE LOOP AREA PER UNIT VOLUME (cm^{-1})	ESTIMATED[a] $[Si]_{loop}$ (cm^{-3})	COMMENTS[b]
400°C	0.5~2000h	0	0	0	0	No Loops Observed
500°C	0.5~1200h	0	0	0	0	No Loops Observed
600°C	1.5h	120×10^{12}	220	470	0.8×10^{18}	Circular Loops
	15h	98	260	520	0.9	Circular Loops
	64h	95	310	720	1.2	Circular Loops
	306h	90	340	840	1.4	Circular Loops
700°C	0.5h	160	230	670	1.2	Circular Loops
	1.5h	100	280	630	1.1	Circular Loops
	15h	43	460	730	1.2	Circular Loops on {111}
	150h	75	400	950	1.6	Circular Loops on {110} (a few on {111})
800°C	1.5h	9.3	980	380	0.5	Triangular Faulted Loops on {111}
	18h	9.3	980	690	1.1	Circular Faulted Loops on {111}
	42h	12	820	630	1.1	Circular Loops on {111}, {110} (faulted or unfaulted)
	400h	5.8	1300	770	1.2	Circular Loops on {110}
900°C	1.5h,19h	0	0	0	0	No Loops Observed
	150h	0.5	4000	610	1.1	Circular Loops on {110} (a few parallelogram shaped loops)
1000°	150h	0.3	3500	370	0.6	Parallelogram Shaped Loops on {110}

[a] Estimates assuming the loops contain a double layer of Si interstitials.

[b] All loops observed are extrinsic (interstitial)

Table IV. TEM Results of Isothermal Annealing of Si-Doped GaAs Samples from the Ingot WA-Si ([Si] $\sim$ 3-6x10^{19} cm^{-3})

Anneal Temperature	Anneal Time	Average Loop Density (cm^{-3})	Average Loop Size (Å)	Approximate Loop Area Per Unit Volume (cm^{-1})	Estimated[a] $[Si]_{loop}$ (cm^{-3})	Comments[b]
400°C	0.5 2000h	0	0	0	0	No Loop Observed
500°C	0.5 1200h	0	0	0	0	No Loop Observed
700°C	0.5h	390x10^{12}	170	850	1.5x10^{18}	Circular Loops
	1.5h	440	190	1260	2.2	Circular Loops
	15h	370	240	1710	2.9	Circular Loops
	50h	220	310	1630	2.8	Circular Loops
	168h	90	420	1240	2.2	Circular Loops on {110} (a few on {111})
	400h	50	580	1300	2.3	
800°C	400h	3	2100	1170	2.1	Circular loops on {110}
900°C	150h	0.5	4800	850	1.5	Circular loops on {110}
1000°C	150h	0.7	1590	180	0.3	Parallelogram shaped Loop on {110}

[a]Estimates assuming the loops contain a double layer of Si interstitials.

[b]All loops observed are extrinsic (interstitial).

FIGURE CAPTIONS

Figure 1. Flow diagram showing the sequence of the measurements.

Figure 2. Isothermal annealing curves for GaAs:Si samples from ingot KM-16 where [Si] $\simeq$ 2.5 x 10^{19} cm^{-3}. Samples having the same number and the same symbol have the same initial n_e given by the t=0 value.

Figure 3. Isothermal annealing curves for GaAs:Si samples from ingot WA-Si where [Si] $\simeq$ 3 6x10^{19} cm^{-3}.

Figure 4. Isothermal annealing curves for GaAs:Si samples from the ingot WA-Si where [Si] $\simeq$ 3-6x10^{19} cm^{-3}.

Figure 5. Infrared abosrption spectrum at liquid nitrogen temperature for two identical GaAs:Si samples having [Si] $\simeq$ 2.5x10^{19} cm^{-3}. -•- designates non-annealed, HT+Q sample, -+- designates 500°/1200h annealed sample. Both samples were compensated by e^--irradiation at 77°K.

Figure 6. 400°C isothermal annealing curves giving defect or measured carrier concentrations for GaAs:Si samples with [Si] $\simeq$ 2.5x10^{19} cm^{-3}. For convenience, the value of a = 10.0x10^{16} cm^{-1} is used as the constant of proportionality in calculating [Si_{Ga}-Si_{As}]. See text for the other [defect] calculations.

Figure 7. 500°C isothermal annealing curves giving defect or measured carrier concentrations for GaAs:Si samples with [Si]$\simeq$2.5x10^{19} cm^{-3}. For convenience, the value of a = 10.0x10^{16} cm^{-1} is used as the constant of proportionality in calculating [Si_{Ga}-Si_{As}]. See text for the othe [defect] calculations.

Figure 8. $700^{o}C$ isothermal annealing curves giving defect or measured carrier concentrations for GaAs:Si samples with [Si] $\simeq 2.5 \times 10^{19}$ cm^{-3}. For convenience, the value of $a = 10.0 \times 10^{16}$ cm^{-1} is used as the constant of proportionality in calculating $[Si_{Ga}\text{-}Si_{As}]$. See text for the other [defect] calculations.

Figure 9. $700^{o}C$ isothermal annealing curves giving defect or carrier concentrations for GaAs:Si samples with [Si] $\simeq 3\text{-}6 \times 10^{19} cm^{-3}$. For convenience, the value of $a = 10.0 \times 10^{16}$ cm^{-1} is used as the constant of pro portionality in calculating $[Si_{Ga}\text{-}Si_{As}]$. See text for the other [defect] calculations.

Figure 10. n_e (optical) calculated from LVM data vs n_e (measured) for all HT+Q, non-annealed GaAs:Si samples. The straight line indicates n_e (optical) = n_e (measured).

Figure 11. The annealing-induced changes in n_e (optical) for [Si] $\simeq 2.5 \times 10^{19}$. For comparison the annealing curves for n_e (measured) for the same samples and conditions are also shown.

Figure 12. n_e (optical) vs n_e (measured) for all annealed samples where [Si] $\simeq 1.5 \times 10^{18}$ cm^{-3} and 2.5×10^{19} cm^{-3} for samples from KM-26 and KM-16, respectively. The straight line indicates n_e (optical) = n_e (measured).

Figure 13. n_e (optical) vs n_e (measured) for all annealed samples with [Si] $\simeq 3\text{-}6 \times 10^{19}$ cm^{-3}. The straight line indicates n_e (optical) = n_e (measured).

Figure 14. Bright Field micrographs for samples for Ingot KM-16 which were annealed at different temperatures after HT+Q. $\vec{g}$ = [220] for all operative reflections.

(a) 400°C/2000h anneal.

(b) 500°C/1200h anneal. A low angle grain boundary contrast is shown.

(c) 600°C/306h anneal, dislocation loops are observed.

(d) 700°C/400h anneal, loops.

(e) 800°C/400h anneal, loops.

(f) 900°C/150h anneal, loops.

(g) 1000°C/150h anneal, loops.

(h) 1200°C/1h (i.e. HT+Q), no loops.

Figure 15. The concentration of the "unknown acceptor" for the longest anneal times as a function of anneal temperature.

Figure 16. Yield stress vs. annealing time for samples from ingot KM-16 for various annealing temperatures. • designated yield stress σ_o of undoped GaAs.

Figure 17. Yield stress vs. annealing time for samples from ingot WA-Si for various annealing temperature. • designates yield stress σ_o of undoped GaAs.

Figure 18. $\sigma-\sigma_o$ vs. $(N_0+\delta[Si_{Ga}])^{1/4}$ for the annealed samples with T_A = 400, 500 and 700°C. The straight line was obtained as described in the text. The calculated N_o value is 1×10^{15} cm^{-3} for KM-16 and 3.8×10^{17} cm^{-3} for WA-Si.

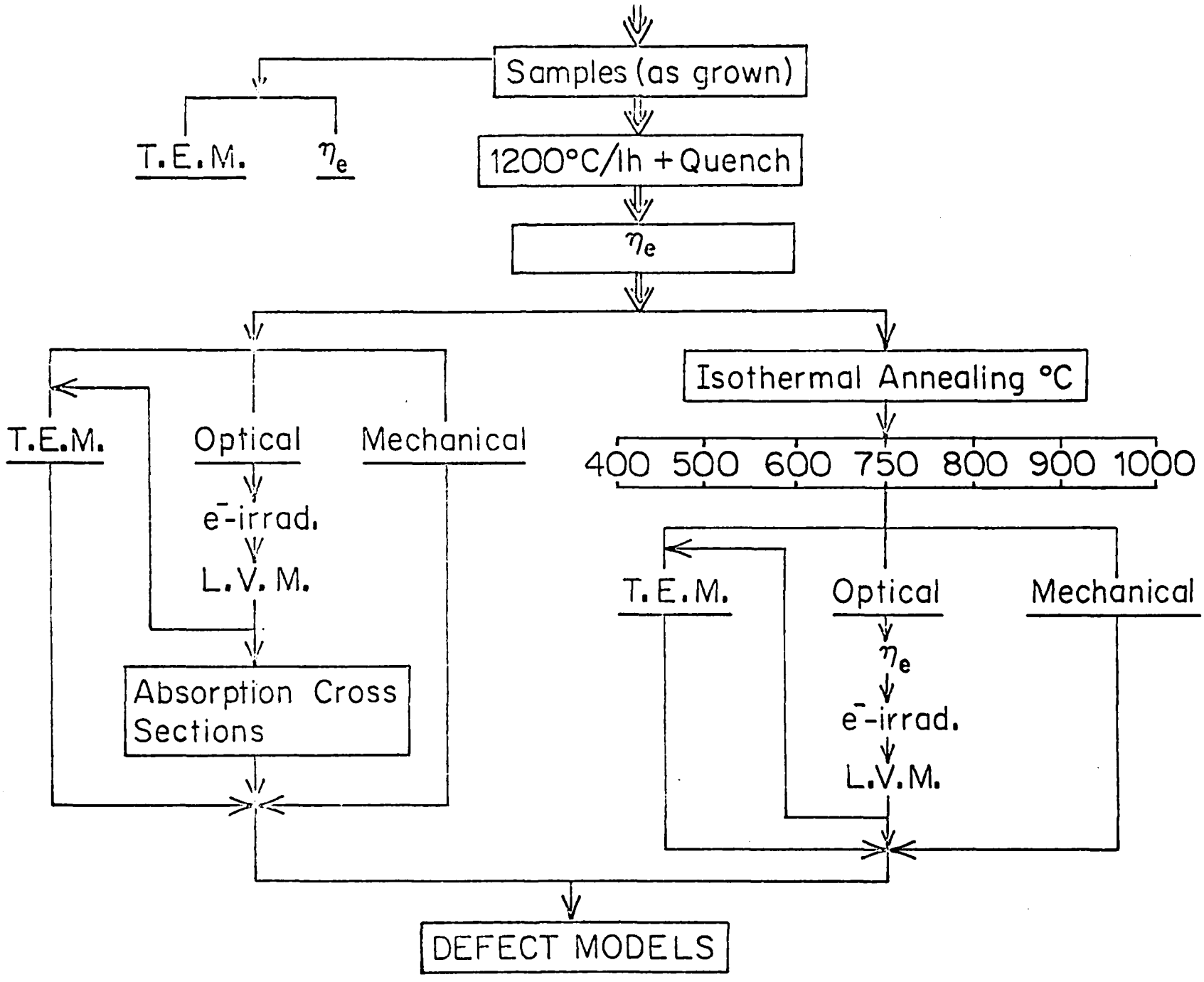
Samples (as grown)
T.E.M.
η_e
1200°C/1h + Quench
η_e
T.E.M.
Optical
Mechanical
e⁻-irrad.
L.V.M.
Absorption Cross Sections
Isothermal Annealing °C
400 500 600 750 800 900 1000
T.E.M.
Optical
Mechanical
η_e
e⁻-irrad.
L.V.M.
DEFECT MODELS

Fig 2

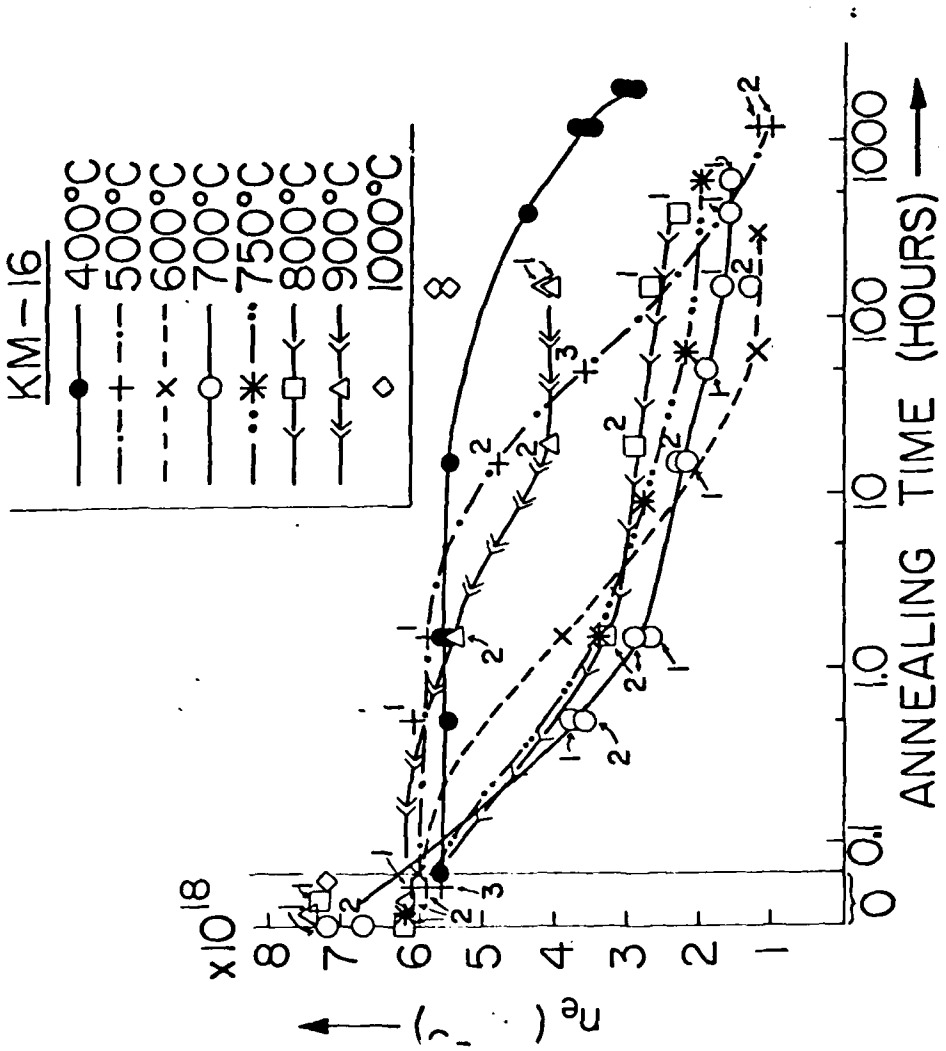
KM-16
400°C
500°C
600°C
700°C
750°C
800°C
900°C
1000°C
n_e ( )
$\times 10^{18}$
8
7
6
5
4
3
2
1
0
0.1
1.0
10
100
1000
ANNEALING TIME (HOURS)

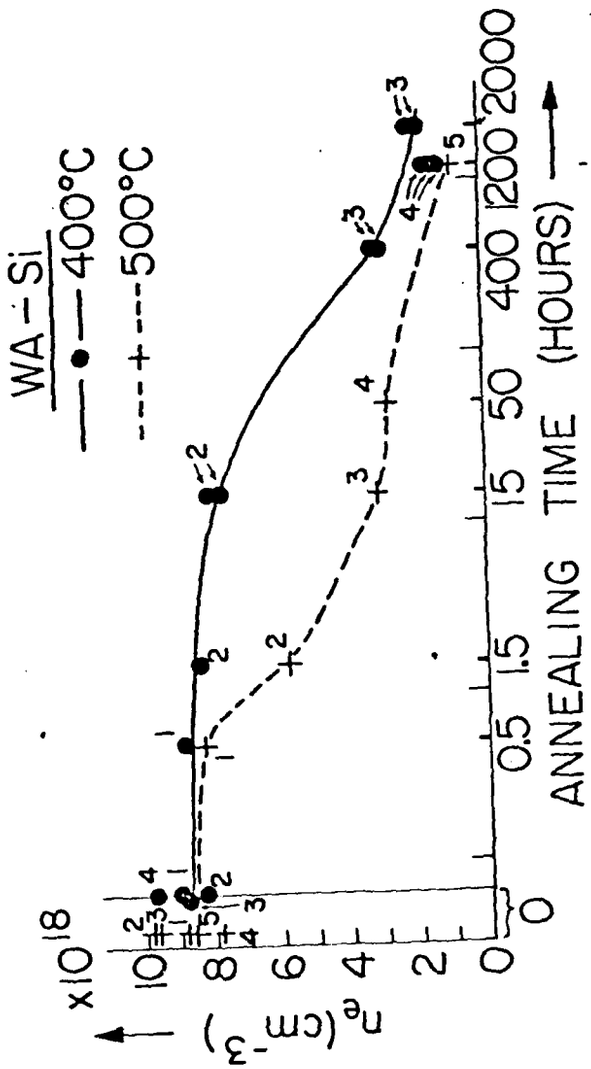
WA-Si
400°C
500°C
n_e (cm^{-3})
x10^{18}
10
8
6
4
2
0
0
0.5
1.5
15
50
400
1200
2000
ANNEALING TIME (HOURS)

Fig 3

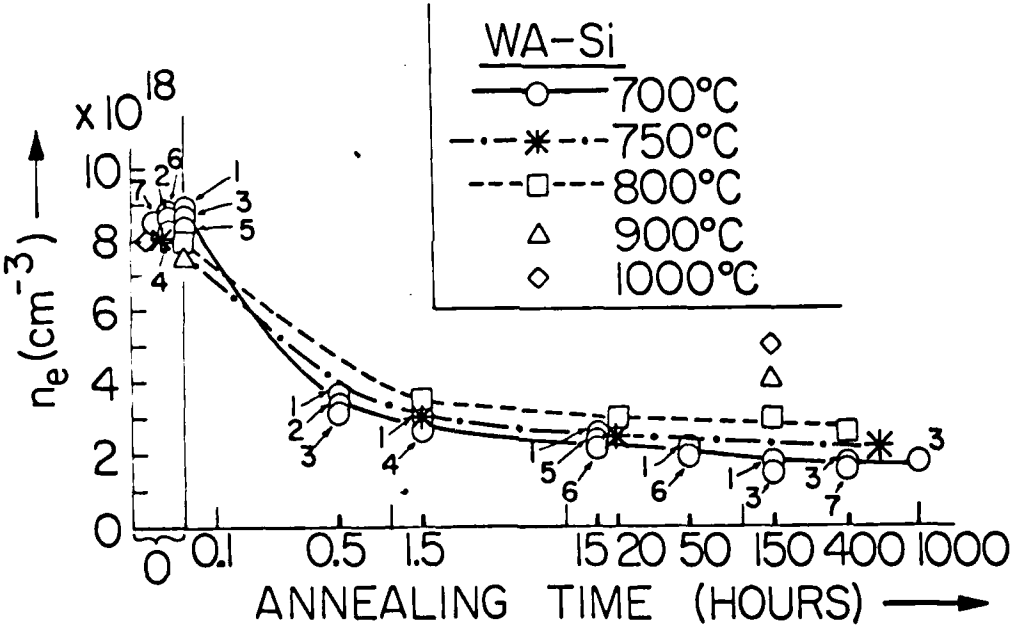
WA-Si
700°C
750°C
800°C
900°C
1000°C
x 10^18
n_e (cm^-3)
0
2
4
6
8
10
0
0.1
0.5
1.5
15
20
50
150
400
1000
ANNEALING TIME (HOURS)

Fig 4

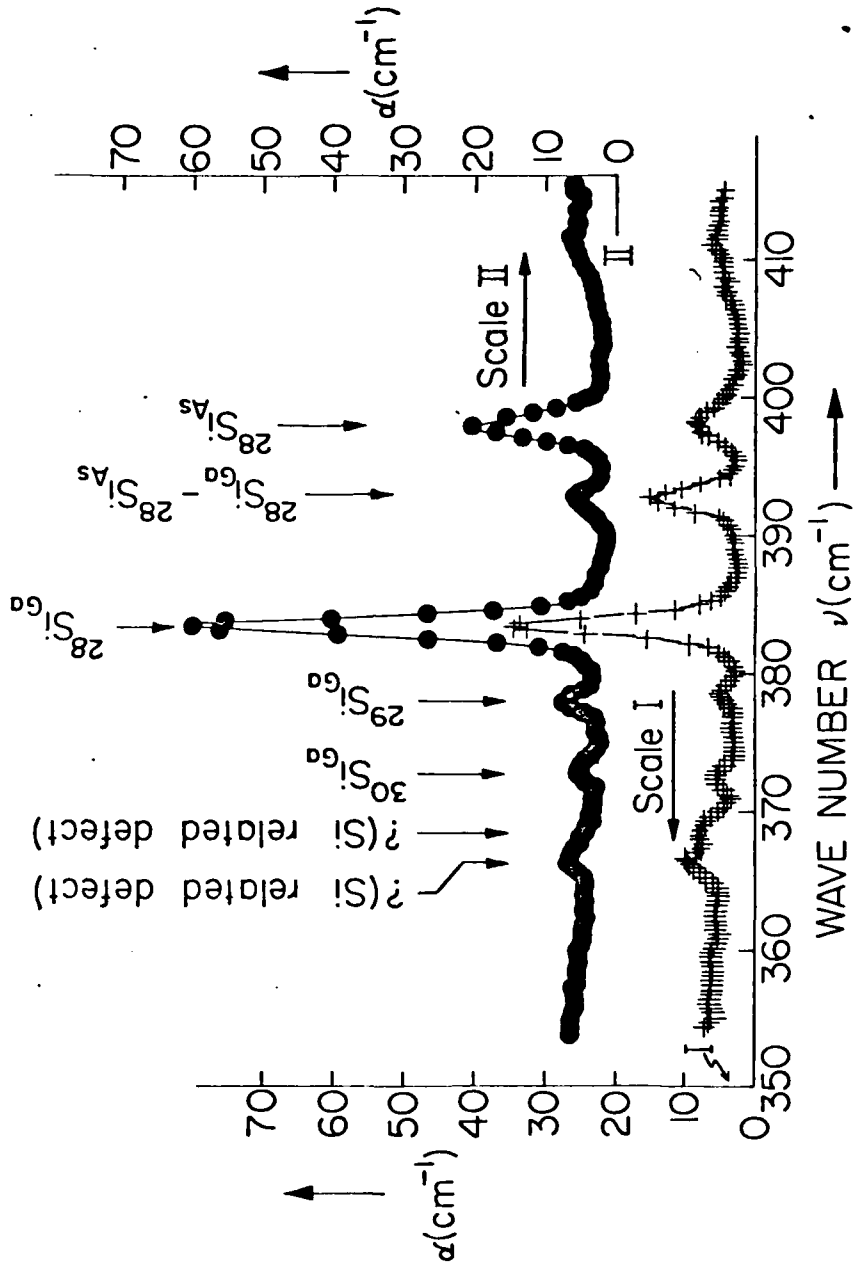
α(cm⁻¹)
70
60
50
40
30
20
10
0
350
360
370
380
390
400
410
WAVE NUMBER ν(cm⁻¹)
Scale I
Scale II
II
28SiGa
29SiGa
30SiGa
?(Si related defect)
?(Si related defect)
28SiGa − 28SiAs
28SiAs

Fig 5

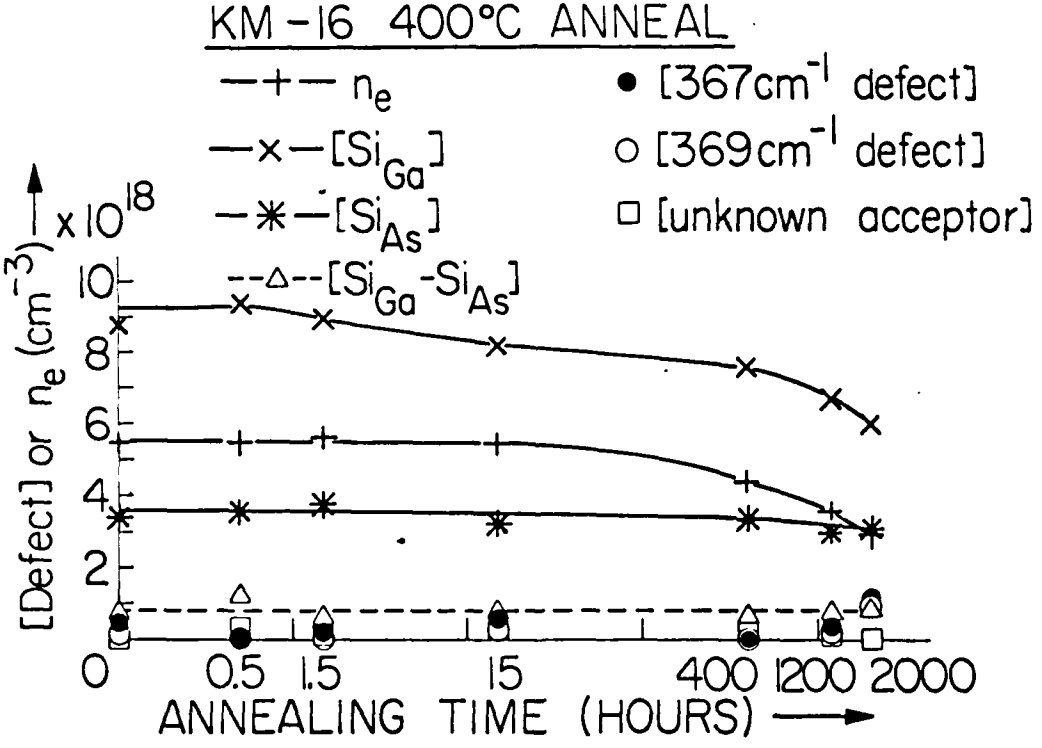
KM-16 400°C ANNEAL
—+— n_e
—x—[Si_{Ga}]
—*—[Si_{As}]
--△--[Si_{Ga}-Si_{As}]
● [367cm^{-1} defect]
○ [369cm^{-1} defect]
□ [unknown acceptor]
[Defect] or n_e (cm^{-3}) x 10^{18}
10
8
6
4
2
0
0.5
1.5
15
400
1200
2000
ANNEALING TIME (HOURS)

II-83-50

Fig 6

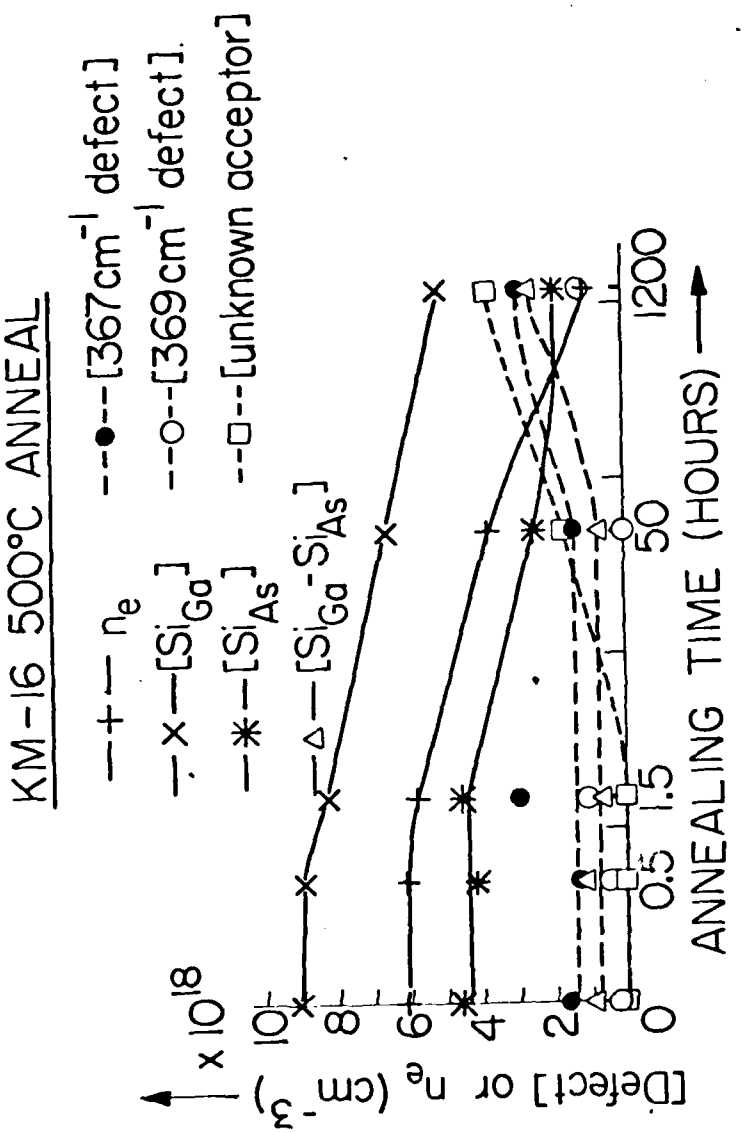
KM-16 500°C ANNEAL
—+— n_e
—x—[Si_{Ga}]
—*—[Si_{As}]
—Δ—[Si_{Ga}-Si_{As}]
--●--[367cm^{-1} defect]
--○--[369cm^{-1} defect]
--□--[unknown acceptor]
[Defect] or n_e (cm^{-3}) → x 10^{18}
10
8
6
4
2
0
0
0.5
1.5
50
1200
ANNEALING TIME (HOURS) →

Fig 7

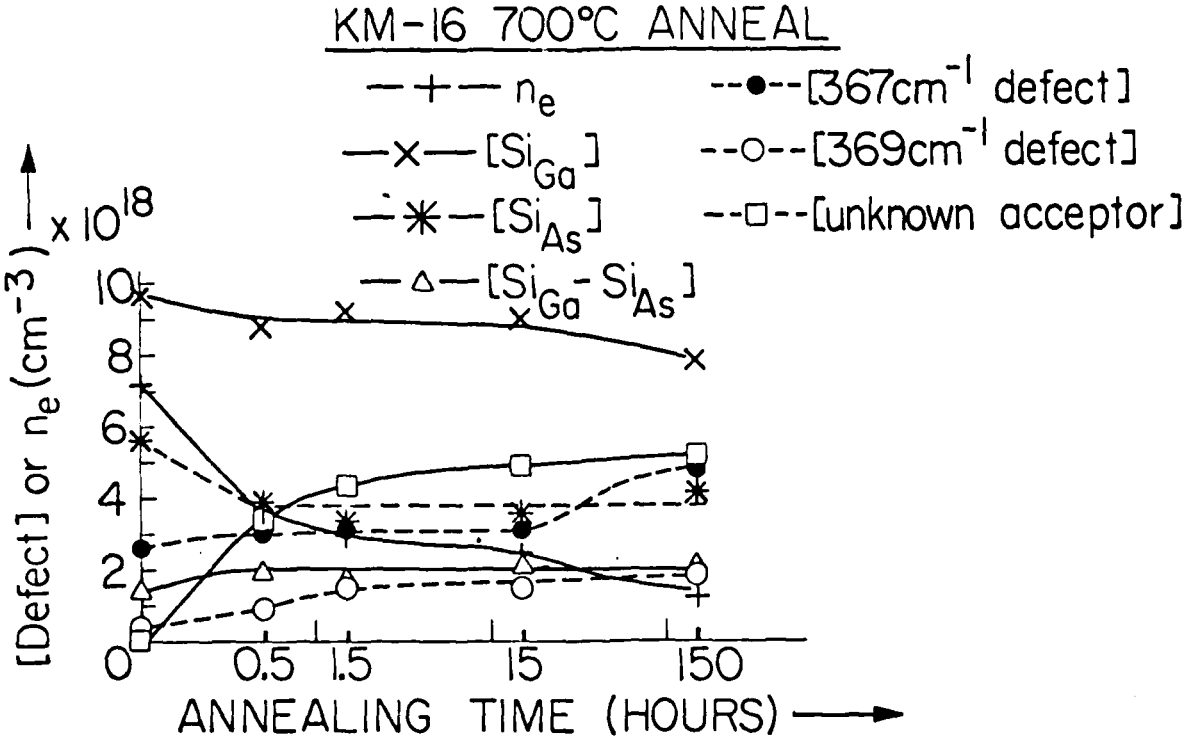
KM-16 700°C ANNEAL
—+— n_e
—x— [Si_{Ga}]
—✳— [Si_{As}]
—△— [Si_{Ga} - Si_{As}]
--●-- [367cm^{-1} defect]
--○-- [369cm^{-1} defect]
--□-- [unknown acceptor]
[Defect] or n_e (cm^{-3}) x 10^{18}
0
2
4
6
8
10
0.5
1.5
15
150
ANNEALING TIME (HOURS)

Fig 8

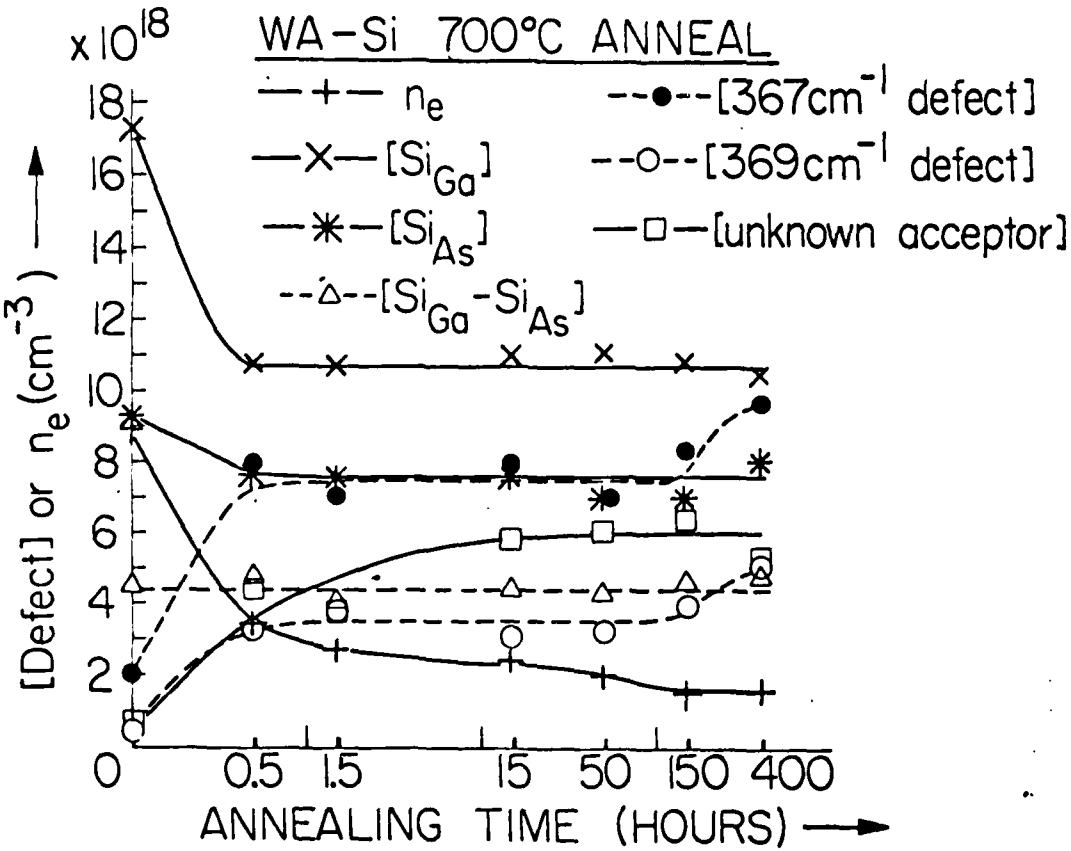
WA-Si 700°C ANNEAL
x 10^18
[Defect] or n_e (cm^-3)
n_e
[Si_Ga]
[Si_As]
[Si_Ga - Si_As]
[367cm^-1 defect]
[369cm^-1 defect]
[unknown acceptor]
0
2
4
6
8
10
12
14
16
18
0.5
1.5
15
50
150
400
ANNEALING TIME (HOURS)

Fig 9

Fig 10

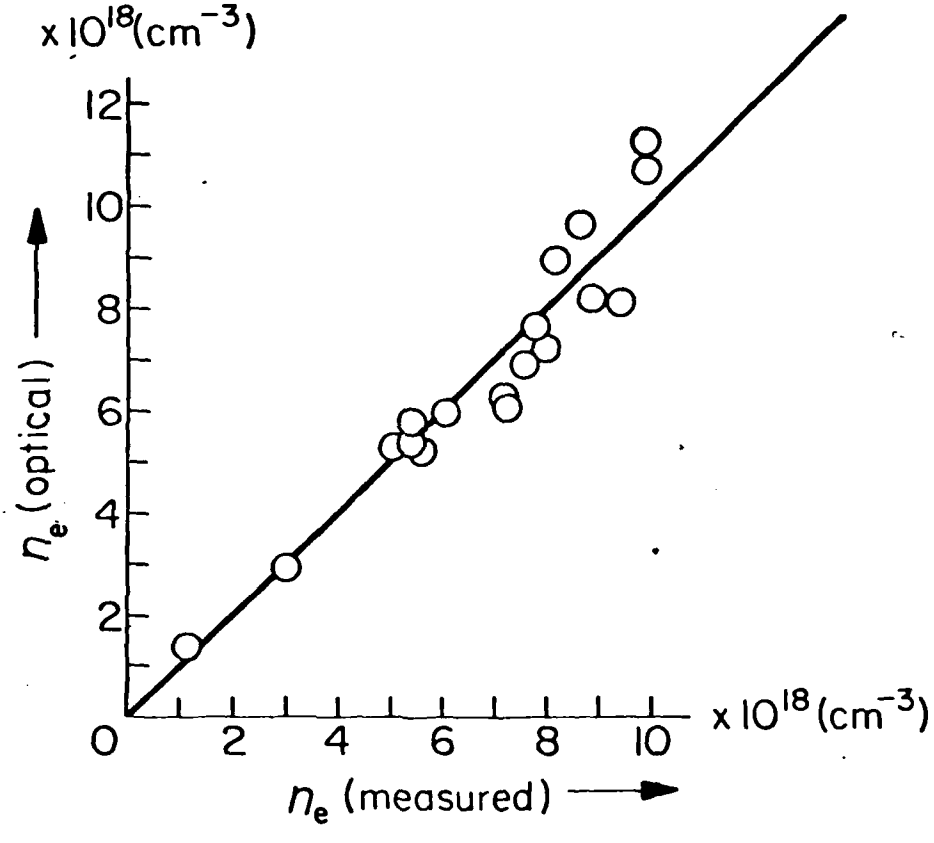
x 10^18(cm^-3)
12
10
8
6
4
2
0
2
4
6
8
10
x 10^18(cm^-3)
n_e (optical)
n_e (measured)

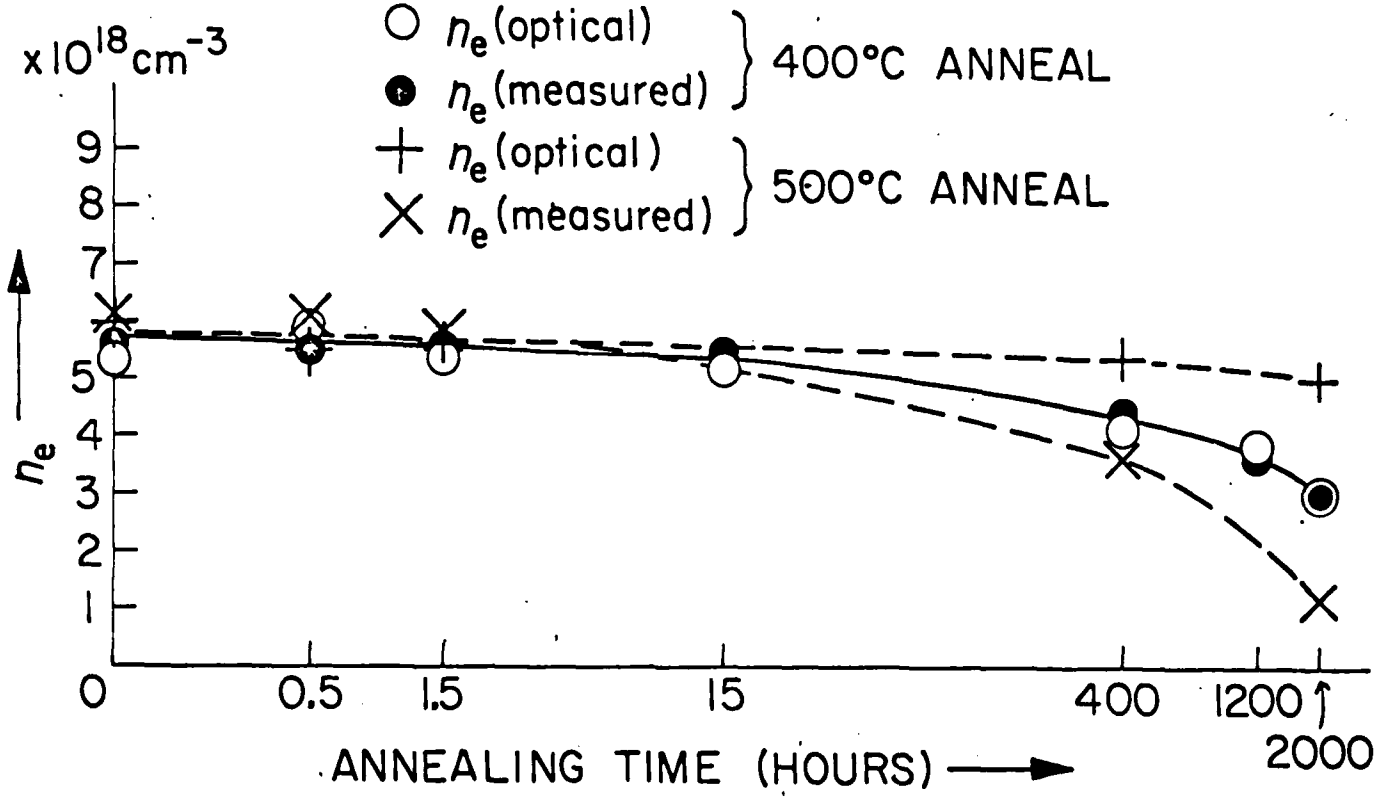

II-B3-55

Fig. 11

Fig 12

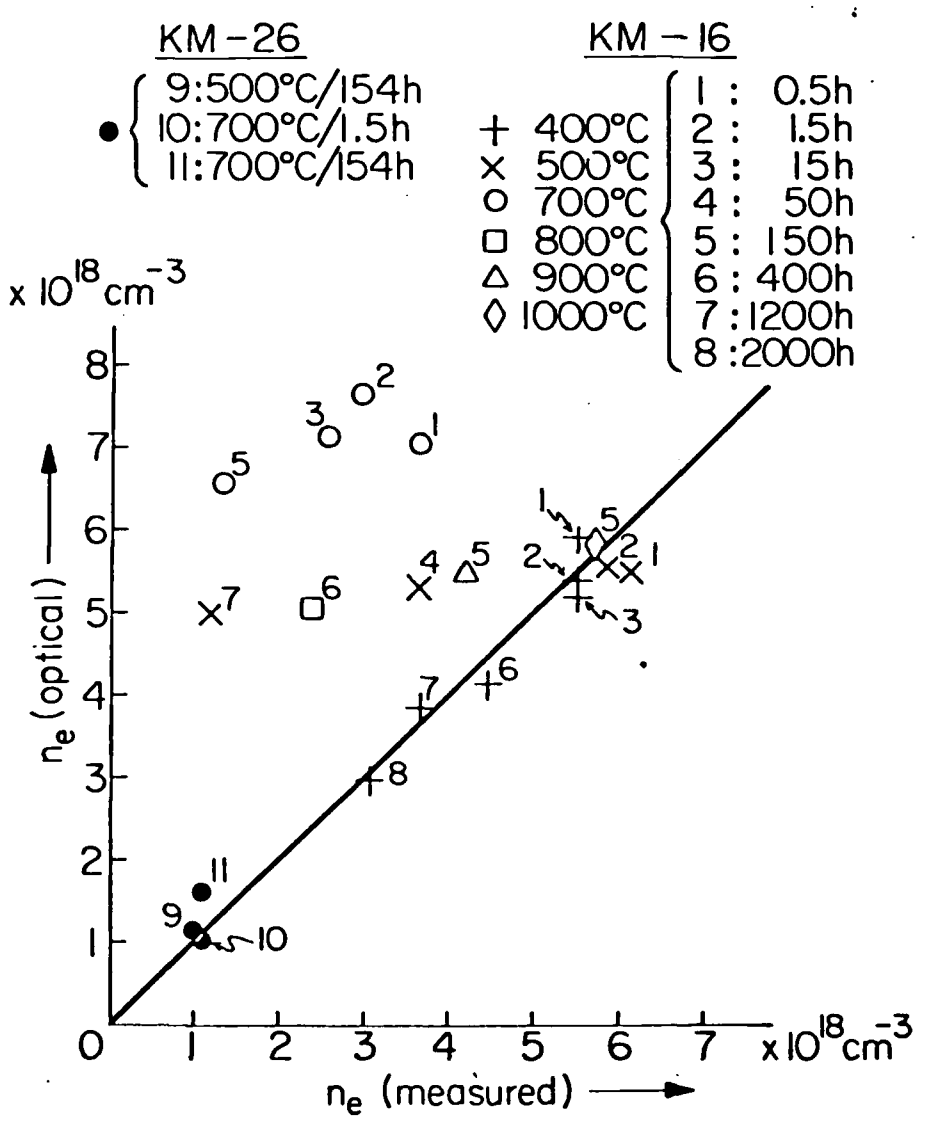
KM-26
9:500°C/154h
10:700°C/1.5h
11:700°C/154h
KM-16
+ 400°C
× 500°C
○ 700°C
□ 800°C
△ 900°C
◇ 1000°C
1 : 0.5h
2 : 1.5h
3 : 15h
4 : 50h
5 : 150h
6 : 400h
7 : 1200h
8 : 2000h
x 10^18 cm^-3
n_e (optical)
n_e (measured)
x 10^18 cm^-3

Fig 13

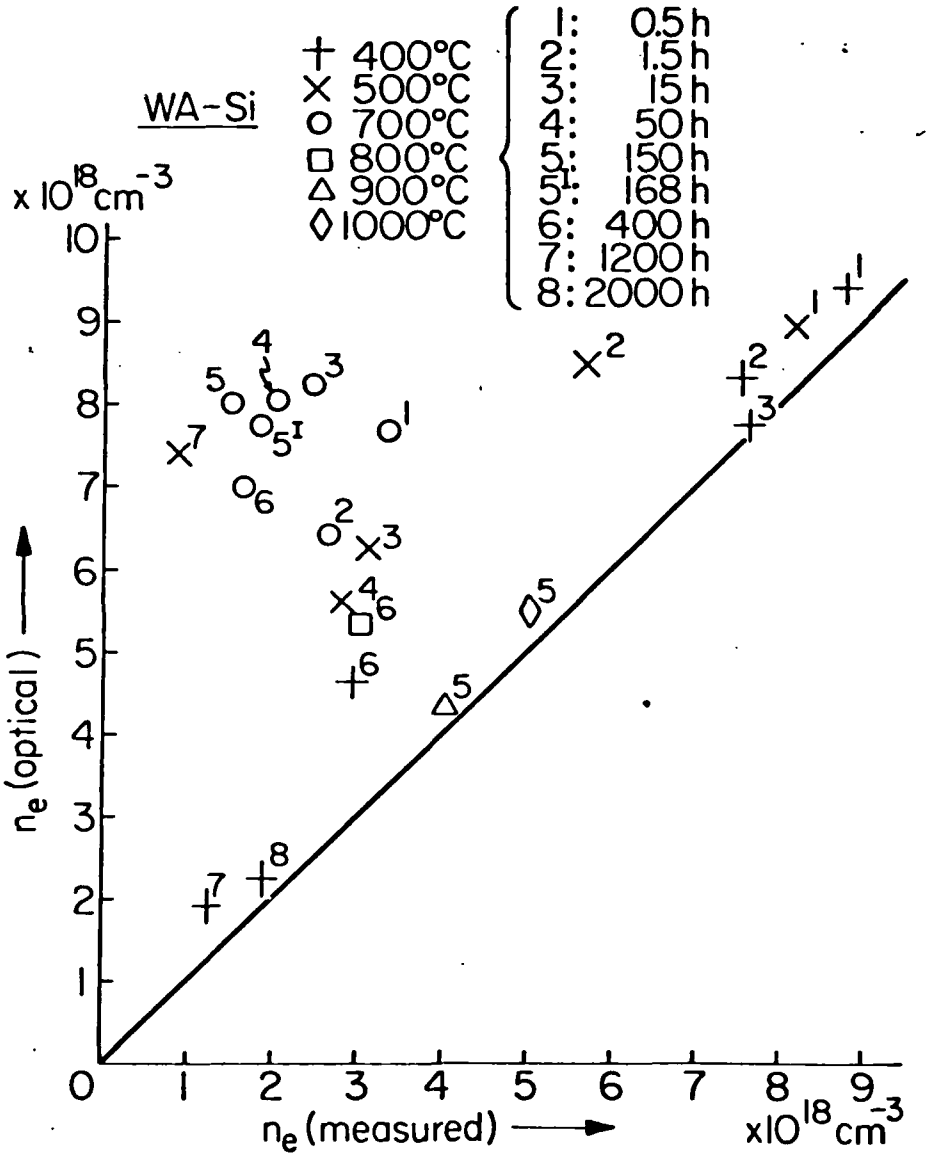
WA-Si
+ 400°C
× 500°C
o 700°C
□ 800°C
△ 900°C
◇ 1000°C
1: 0.5 h
2: 1.5 h
3: 15 h
4: 50 h
5: 150 h
5': 168 h
6: 400 h
7: 1200 h
8: 2000 h
x 10^18 cm^-3
n_e (optical)
n_e (measured)
x10^18 cm^-3
0
1
2
3
4
5
6
7
8
9
10

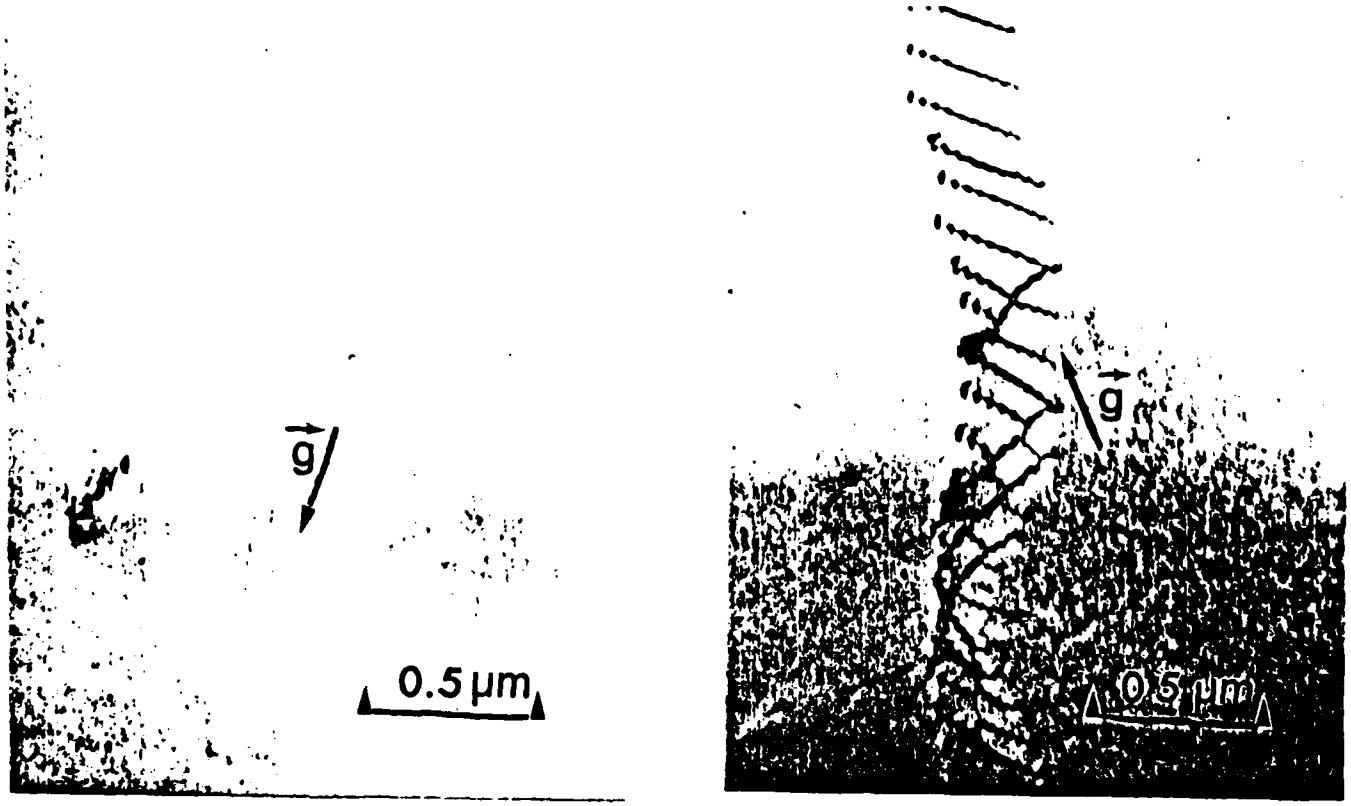

Fig 14(a)+(b)

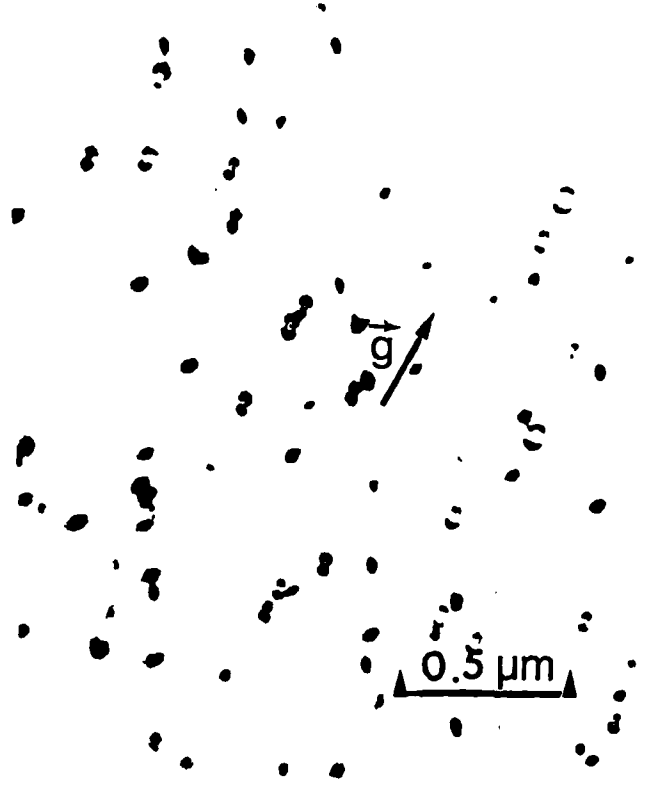

(c)

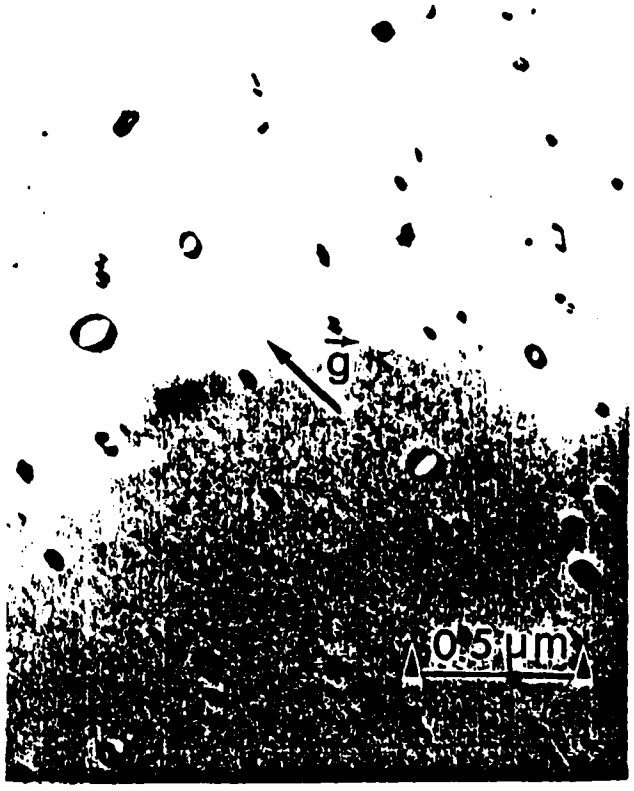

(d)

Fig 14(c) + (d)

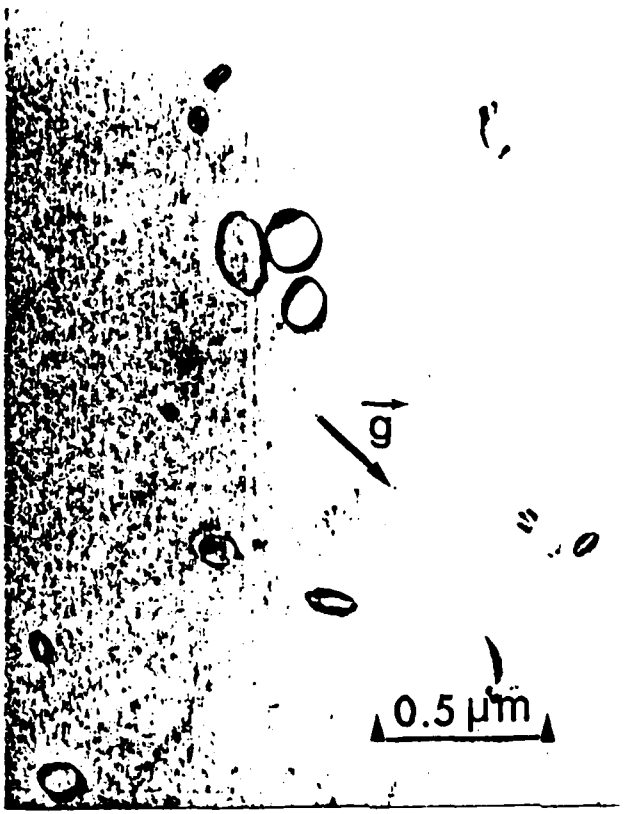

(e)

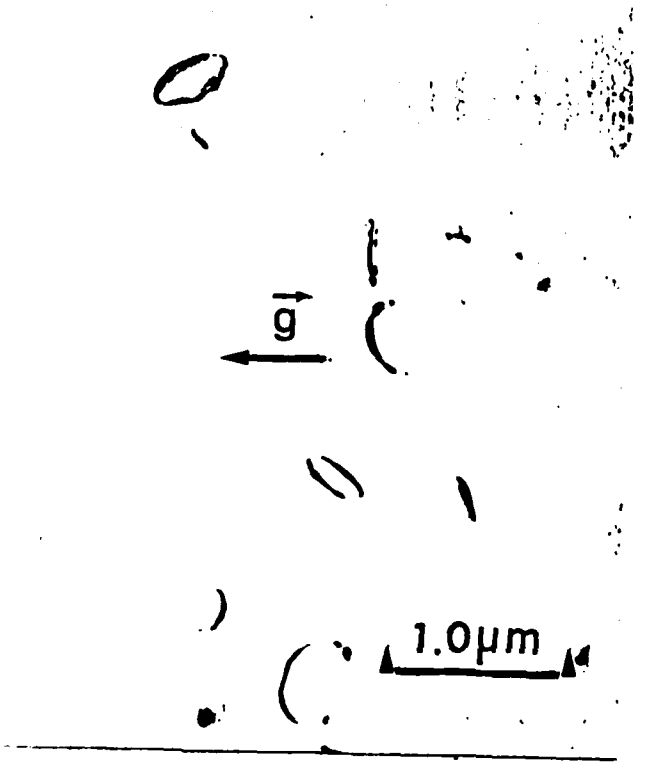

(f)

Fig 14 (e) + (f)

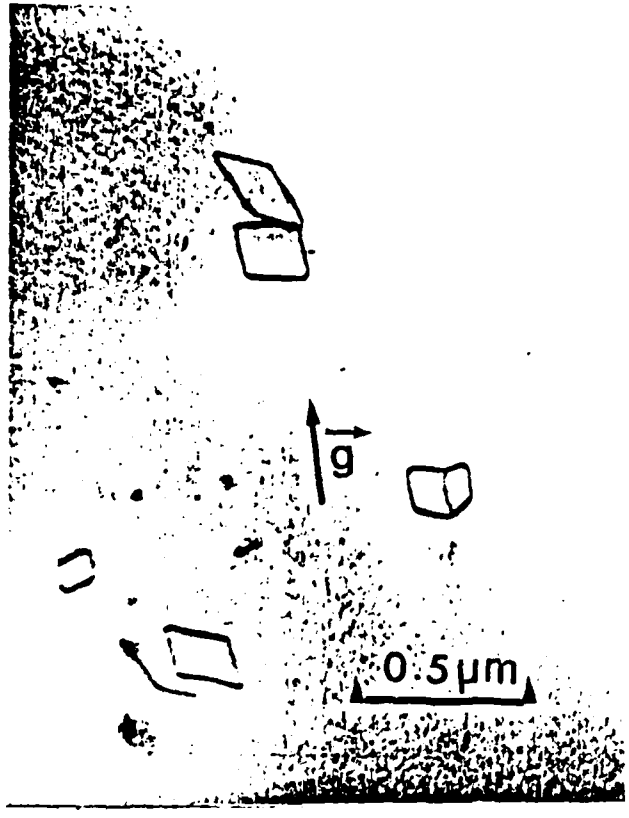

(g)

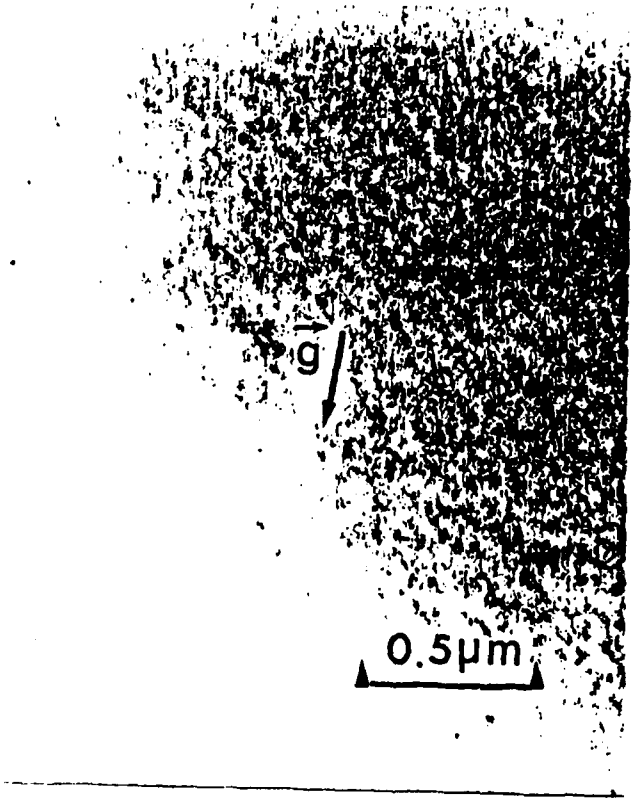

(h)

II-83-61

Fig 14 (g) & (h)

Fig. 15

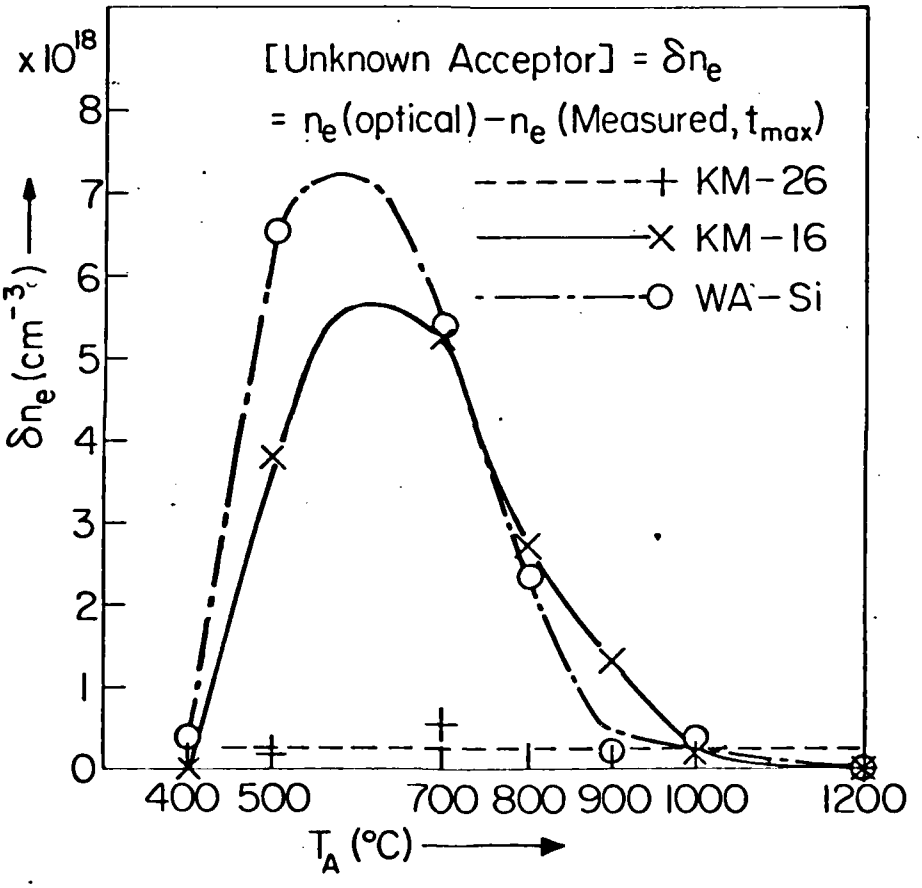
x 10^18
[Unknown Acceptor] = δn_e
= n_e(optical) − n_e (Measured, t_max)
KM-26
KM-16
WA-Si
δn_e (cm^-3)
8
7
6
5
4
3
2
1
0
400 500 700 800 900 1000 1200
T_A (°C)

Fig. 16

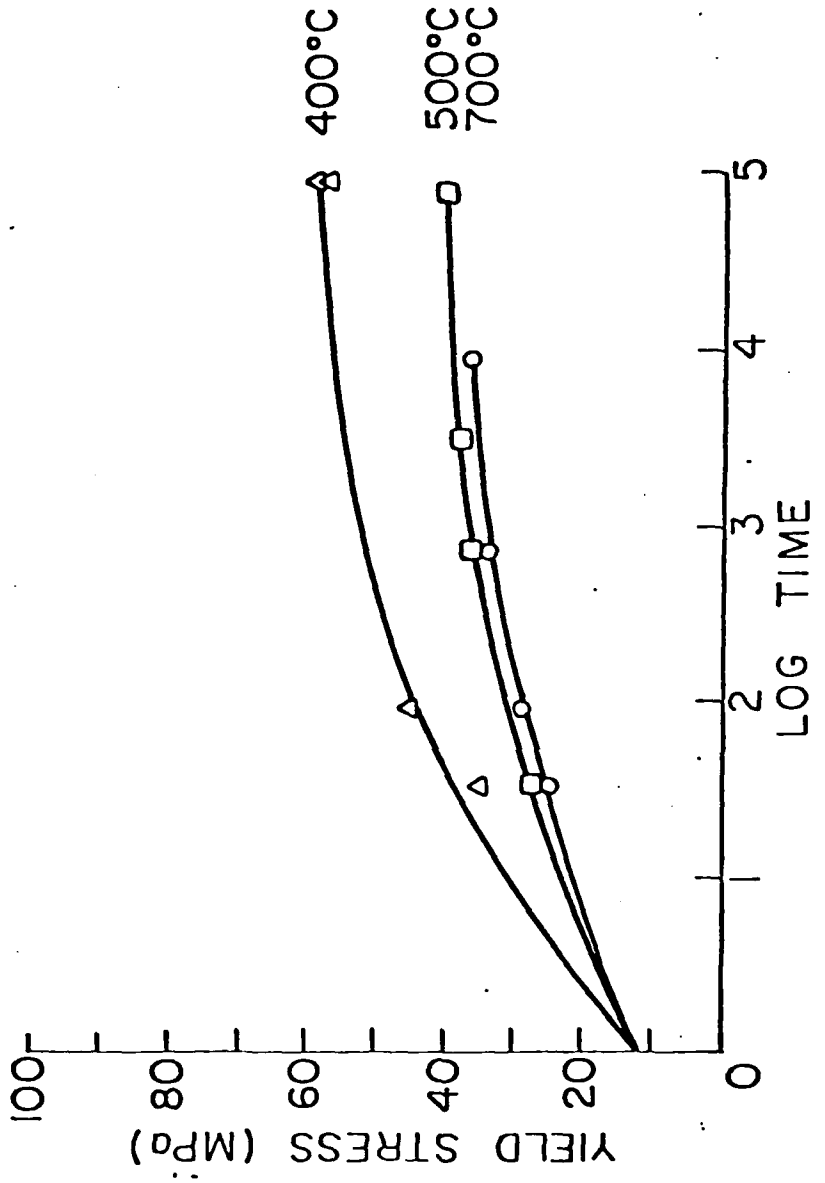
400°C
500°C
700°C
YIELD STRESS (MPa)
0
20
40
60
80
100
1
2
3
4
5
LOG TIME

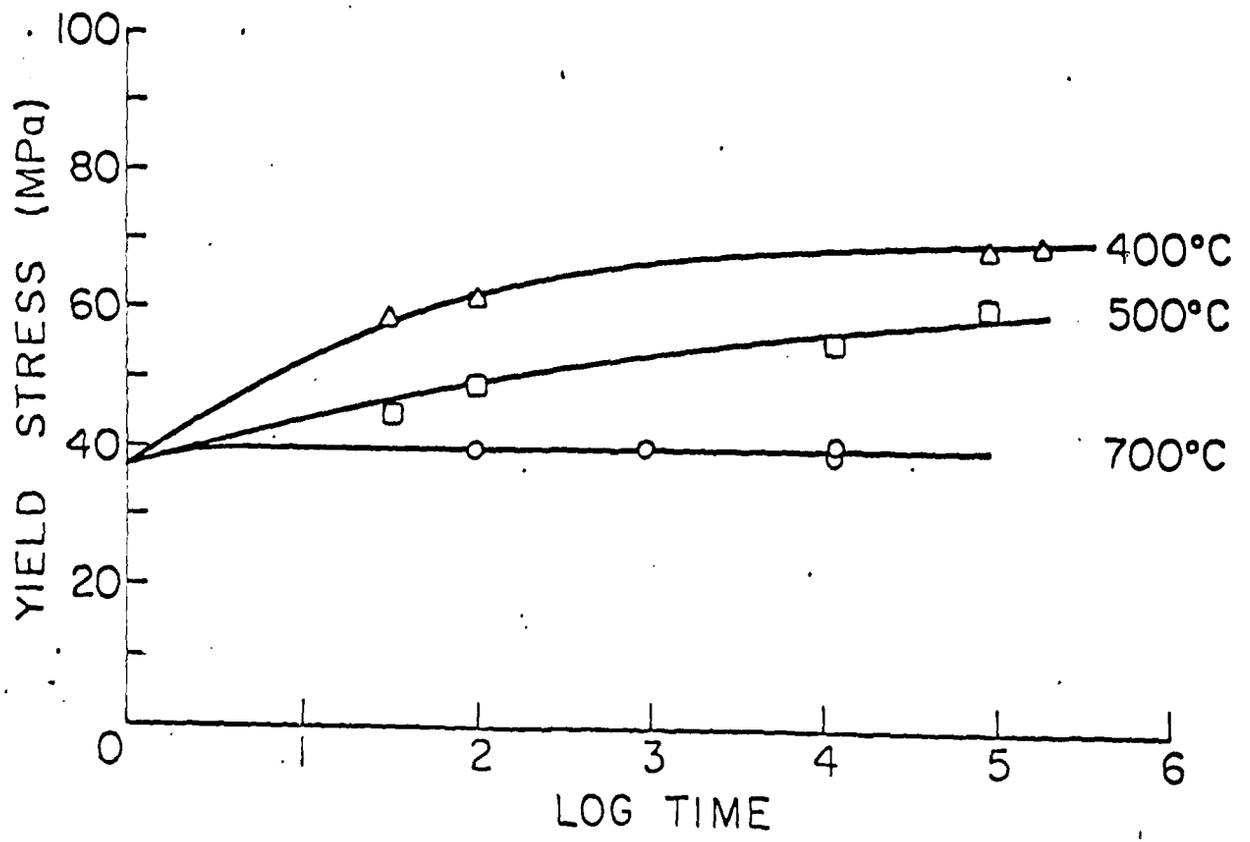
YIELD STRESS (MPa)
100
80
60
40
20
0
1
2
3
4
5
6
LOG TIME
400°C
500°C
700°C

Fig. 17

AD-A107 598 UNIVERSITY OF SOUTHERN CALIFORNIA LOS ANGELES ELECTR--ETC F/G 20/12
THE EFFECT OF SOLUTE-VACANCY PAIRS ON THE PHYSICAL PROPERTIES O--ETC(U)
MAY 81 W G SPITZER, J M WHELAN, S M COPLEY AFOSR-76-2990

UNCLASSIFIED AFOSR-TR-81-0746 NL

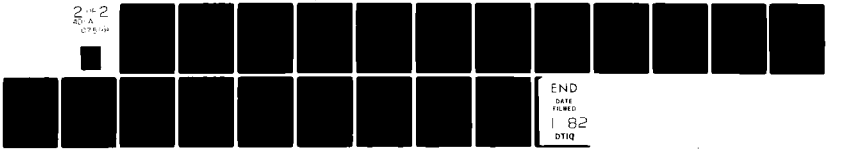

END
DATE FILMED
1 82
DTIC

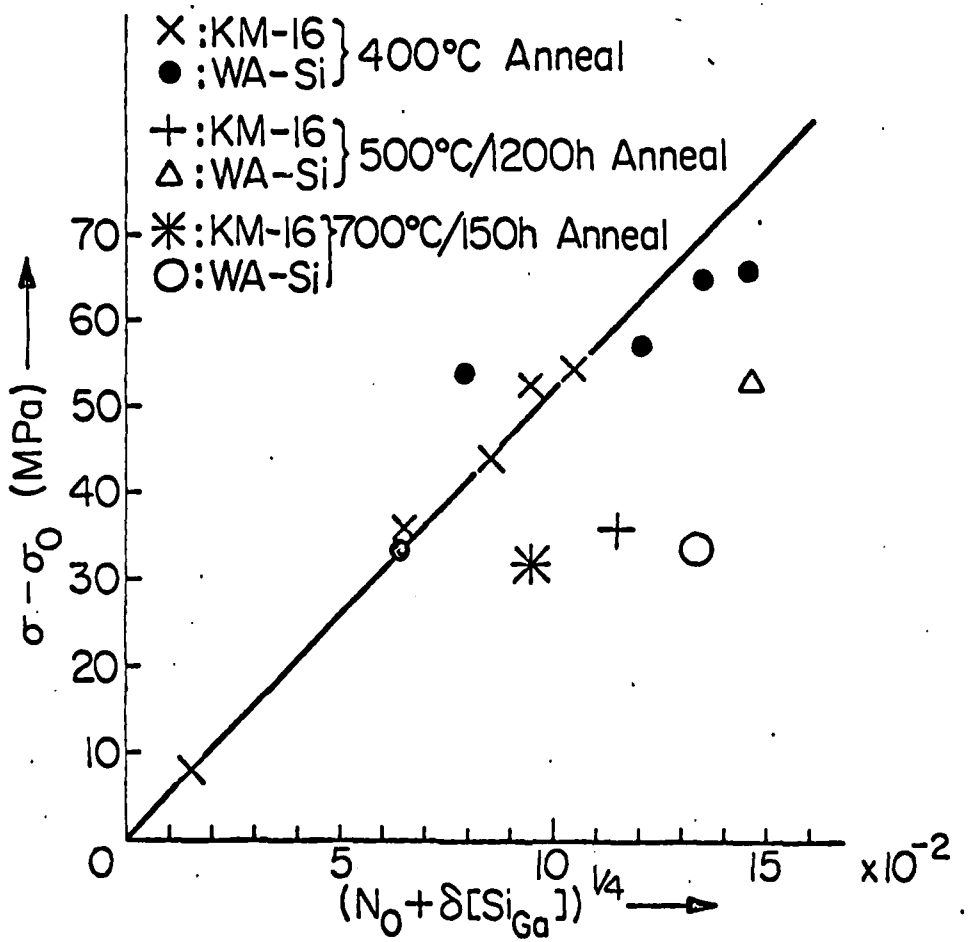

II-83-65

Fig 18

4. Strengthening of GaAs Single Crystals by Formation of Silicon-Vacancy Pairs

V. Ganeson and S. M. Copley*

Department of Materials Science
University of Southern California
Los Angeles, CA 90007

Several investigations have shown that annealing can produce dramatic changes in the properties and microstructure of heavily Si-doped GaAs. These investigations include: measurements of free carrier density,[1] photoluminescence[2,3] and localized vibrational maode (LVM) infrared absorption;[3,4] characterization of dislocation substructure by transmission electron microscopy;[5,6] and measurement of critical resolved shear stress.[6,7] The results of these investigations strongly suggest that the annealing-induced changes are related to specific changes in point defect structure. Indeed, a qualitative correlation has been found between changes in these properties and changes in the concentration of $(Si^{\bullet}_{Ga}-V'_{Ga})^{x}$ pairs. (The various defect species are indicated as follows: F_M denotes F atom sitting on M site and V_M denotes a vacancy on an M site. Superscripts denote the charge state of the species. A dot represents a positive charge, a dash repre-

*Member American Ceramic Society

sents a negative charge and an x represents a neutral species. Square brackets indicate site fraction.)

The difficulty in attaining a quantitative correlation of results from previous investigations arises because the results were obtained employing different ingots or different sections of the same ingot. Thus the specimens had different Si concentrations and the concentrations were not reliably determined. This research was undertaken with the goal of establishing a quantitative correlation between certain physical properties and the point defect structure and microstructure of Si-doped GaAs.

In this note, we report the results of stress-strain measurements and correlate these with preliminary results of free-carrier density and LVM infrared absorption. All measurements were made on the same material.

Two Si-doped crystal ingots grown by the horizontal Bridgeman method were investigated. These ingots are referred to as KM-16 and WA-Si. Various methods were employed for the determination of Si concentrations in the ingots. Initially, the atomic absorption method was tried and comparisons were made with commercially available Si standard solutions. However, lack of reproducibility due to solution aging effects and lack of a dedicated piece of equipment made this technique impractical and unreliable. Methods of spectrochemical analysis and

electron probe microanalysis were then employed. The electron probe analysis was found to be convenient and reliable. The data obtained by spectrochemical analysis agreed with the electron probe microanalysis measurements. The electron probe microanalysis measurements indicated that Si concentration varied from 3 to 6 x 10^{19} cm^{-3} from the bottom to the top of the WA-Si ingot. The KM-16 ingot showed much better uniformity with a Si variation of less than 10 pct. The average Si concentration of the samples obtained for mechanical testing from the KM-16 ingot was 2.5 x 10^{19} cm^{-3}. The average concentration of samples obtained from a specific location in the WA-Si ingot was 4.7 x 10^{19} cm^{-3}.

Single crystal compression specimens with square cross-section (5.1 mm x 5.1 mm x 10.2 mm) and with long axis perpendicular to the crystal growth direction were cut from each ingot using a two-circle goniometer and a precision cut-off wheel. The crystallographic orientations of the long axes (stress axes) of specimens cut from the KM-16 and WA-Si ingots are shown in Fig. 1. The Schmid factor ($\cos \phi \cos \theta$, where θ is the angle between the stress axis and the slip plane normal and ϕ is the angle between the stress axis and the slip direction) for specimens from the two ingots is clearly the same even though their orientations are different.

The compression specimens were annealed at 1200°C in quartz ampoules and then quenched in oil. The specimens were aged at 400, 500 and 700°C for 30, 90, 900, 7.2×10^4 and 1.2×10^5 minutes (the 1.2×10^5 minute aging treatment was omitted at 700°C). Details of the annealing and aging treatments were previously described.[6]

Stress-strain curves for all specimens were obtained at 400°C by loading in compression at a constant force rate. The stress rate during yielding was 14.1 MPa s^{-1}. The yield stress values reported were for a 0.2 pct offset strain. Details of the stress-strain testing procedure are reported elsewhere.[7,8]

Figures 2 and 3 show yield stress versus aging time curves for specimens from the KM-16 and WA-Si ingots, respectively. The yield stress plotted at t = 0 is the value corresponding to the sample annealed at 1200°C for one hour and then quenched without subsequent aging. With the exception of the Wa-Si specimens aged at 700°C, the yield stress increases monotonically with increasing aging time in agreement with previous results by Swaminathan and Copley.[6] They attributed this increase in yield stress to an increase in the concentration of $(Si^{\bullet}_{Ga}-V'_{Ga})^{x}$ pairs, which impede the motion of dislocations. A large difference in yield stress also can be noted between the annealed and aged specimens from the KM-16 and WA-Si ingots. The yield stress values for specimens from KM-16 are lower

than those for specimens from WA-Si at all temperatures and for all periods of aging. Because the Schmid factors for specimens from the two ingots are equal, we conclude that the difference results from a difference in critical resolved shear stress. This suggests that the $(Si^{\bullet}_{Ga}-V'_{Ga})^{x}$ pairs were present in all specimens and that their concentration was greatest in specimens from the WA-Si ingot, which had the greatest Si concentration.

Recently, Chen and Spitzer obtained values of free carrier density and concentrations of various point defects in specimens taken from one of the ingots (KM-16) used for the present study.[9] The free carrier density for each specimen was measured by determining the frequency of the free carrier plasma minimum observed in the infrared reflectivity. The concentrations of various point defects were determined from known LVM absorption bands by multiplying the peak LVM absorption less background, the band width at half maximum and the absorption cross-section.

Figure 4 shows the results for specimens annealed one hour at 1100°C, quenched and then aged various times at 400°C. As was previously observed by Kung and Spitzer, the decrease in free carrier density with increasing aging time can be accounted for entirely by the decrease in $Si^{\bullet}_{Ga}$ donors. Also, the other Si defect concentrations, $[Si'_{As}]$, $[(Si^{\bullet}_{Ga} - S'_{As})^{*}]$, [367 cm^{-1} defect] and [369 cm^{-1} defect] remain nearly constant during annealing. Chen and Spitzer

determined by transmission electron microscopy that no precipitates or dislocation loops were present in the 400°C aged specimens. Based on these observations Chen and Spitzer concluded that the decrease in $[Si^{\bullet}_{Ga}]$ during the 400°C aging results from the formation of electrically neutral $(Si^{\bullet}_{Ga} - V'_{Ga})^{x}$ pairs.

If it is assumed that the decrease in $[Si^{\bullet}_{Ga}]$ results completely from the formation of $(Si^{\bullet}_{Ga} - V'_{Ga})^{x}$ pairs, then it is possible to relate the pair concentration to the yield stress, employing the equation

$$\sigma - \sigma_o = A(N_o - \delta[Si^{\bullet}_{Ga}])^{m} \qquad (1)$$

where σ is the yield stress, σ_o is the yield stress for the annealed and quenched specimens, N_o is the number of $(Si^{\bullet}_{Ga} - V'_{Ga})^{x}$ pairs for the quenched specimens and A and m are constants. Figure 5 shows that a good correlation is attained with $N_o = 1 \times 10^{15}$ cm^{-3} and $m = 1/4$.

Chen and Spitzer have pointed out that the one fourth power dependence is consistent with previous results of Chin et al[10] for crystals of NaCl, NaBr, KCl and KBr doped with divalent impurity ions such as Ca^{2+}, Sr^{2+} and Ba^{2+}, where it was found that the critical resolved shear stress varied with the one half power of the divalent ion concentration. If, in the case of NaCl doped with Ca^{2+}, we assume that the defect responsible for hardening was $(Ca^{\bullet}_{Na} - V'_{Na})^{x}$, then the concentration of the defect is

determined by the reaction

$$Ca^{\bullet}_{Na} + V'_{Na} = (Ca^{\bullet}_{Na} - V'_{Na})^{x} \qquad (2)$$

Apply in the law of mass action gives

$$[(Ca^{\bullet}_{Na} - V'_{Na})^{x}] = K_p [Ca^{\bullet}_{Na}] [V'_{Na}] \qquad (3)$$

If $[Ca^{\bullet}_{Na}]$ is large compared to the number thermal vacancies, then $[V'_{Na}] \tilde{=} [Ca^{\bullet}_{Na}]$ to maintain charge neutrality. Thus

$$[(Ca^{\bullet}_{Na} - V'_{Na})^{x}] = K_p [Ca^{\bullet}_{Na}]^2 \qquad (4)$$

so $(\sigma - \sigma_o) \propto [Ca^{\bullet}_{Na}]^{\frac{1}{2}} \propto [(Ca^{\bullet}_{Na} - V'_{Na})^{x}]^{\frac{1}{4}}$ as we have found in the case of the $(Si^{\bullet}_{Ga} - V'_{Ga})^{x}$ pairs.

Acknowledgements

This work was supported by the Air Force Office of Scientific Research (AFSC) under Contract 76-2990. The authors are grateful to Drs. R. T. Chen and W. G. Spitzer for allowing use of their unpublished data.

References

1. J. K. Kung and W. G. Spitzer, "Effects of Annealing on the Carrier Concentration of Heavily Si-Doped GaAs.", J. Appl. Phys. 44 [2] 912-16 (1973).
2. C. J. Hwang, "Optical Properties of n-Type GaAs. III. Relative Band-edge Recombination Efficiency of Si- and Te-Doped Crystals before and after Heat Treatment", J. Appl. Phys. 40 [11] 4591-97 (1969).
3. J. K. Kung and W. G. Spitzer, "Si-Defect Concentrations in Heavily Si-Doped GaAs: Changes Induced by Annealing", J. Appl. Phys. 45 [10] 4477-86 (1974).
4. L. H. Skolnik, W. G. Spitzer, A. Kahan, H. Euler and R. G. Hunsperger, "Localized Vibrational Mode Absorption of Ion-Implanted Silicon in GaAs", J. Appl. Phys. 43 [5] 2146-50 (1972).
5. G. H. Narayanan and A. H. Kachare, "An Electron Microscopy Study of the Effects of Annealing on the Defect Structure of Heavily Silicon-Doped Gallium Arsenide", Phys. Stat. Sol. 26A [2] 657-69 (1974).
6. V. Swaminathan and S. M. Copley, "Hardening of GaAs by Solute-Vacancy Pairs", J. Appl. Phys. 47 [10] 4405-13 (1976).
7. V. Swaminathan and S. M. Copley, "Temperature and Orientation Dependence of Plastic Deformation in GaAs Single Crystals Doped with Si, Cr or Zn", J. Am. Ceram. Soc. 58 [11-12] 482-85 (1975).

8. V. Ganeson, "Concentration Dependence of Plastic Deformation in GaAs Single Crystals Doped with Si", Masters Thesis, University of Southern California, January 1979.

9. R. T. Chen and W. G. Spitzer, private communication (1981).

10. G. Y. Chin, L. G. Van Uitert, M. L. Green, G. J. Zydjik and T. K. Kometani, "Strengthening of Alkali Halides by Divalent-Ion Additions", J. Am. Ceram. Soc. 56 [7] 369-72 (1973).

Figures

Figure 1: Stress axis orientation of samples cut from the KM-16 and WA-Si ingots determined by the Laue back reflection method.

Figure 2: Yield stress versus annealing time for samples from ingot KM-16 for various annealing temperatures.

Figure 3: Yield stress versus annealing time for samples from ingot WA-Si for various annealing temperatures.

Figure 4: Isothermal annealing curves at 400°C giving defect or measured carrier concentrations for GaAs:Si samples (after Chen and Spitzer).

Figure 5: A plot of $\sigma - \sigma_o$ versus $(N_o - \delta[Si_{Ga}])^{\frac{1}{4}}$ for samples annealed at 400°C.

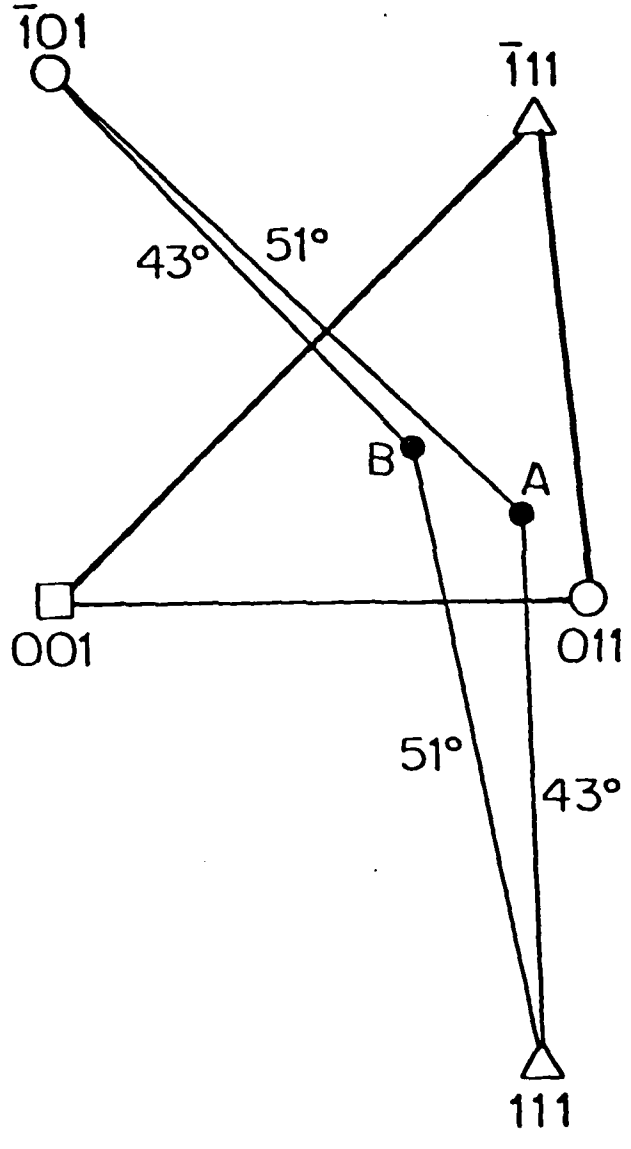

Figure 1: Stress axis orientation of samples cut from the KM-16 and WA-Si ingots determined by the Laue back reflection method.

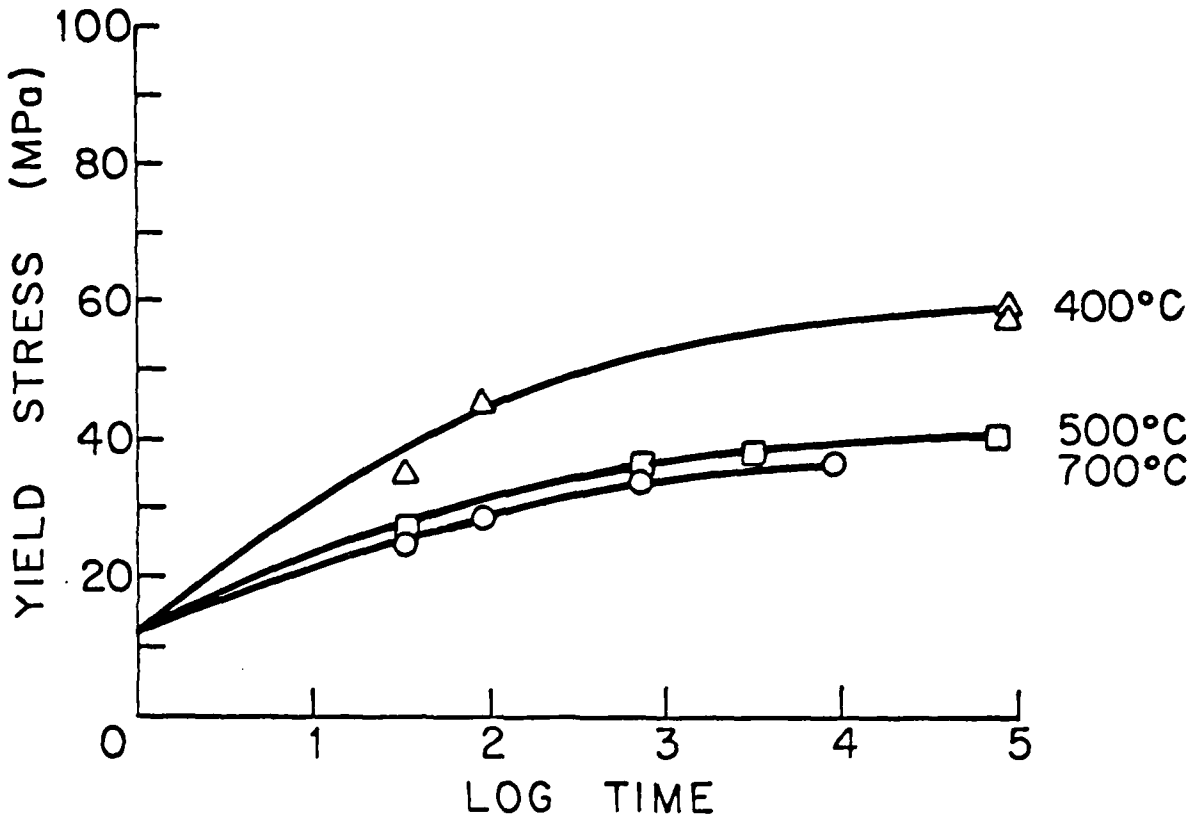

II-B4-12

Figure 2: Yield stress versus annealing time for samples from ingot KM-16 for various annealing temperatures.

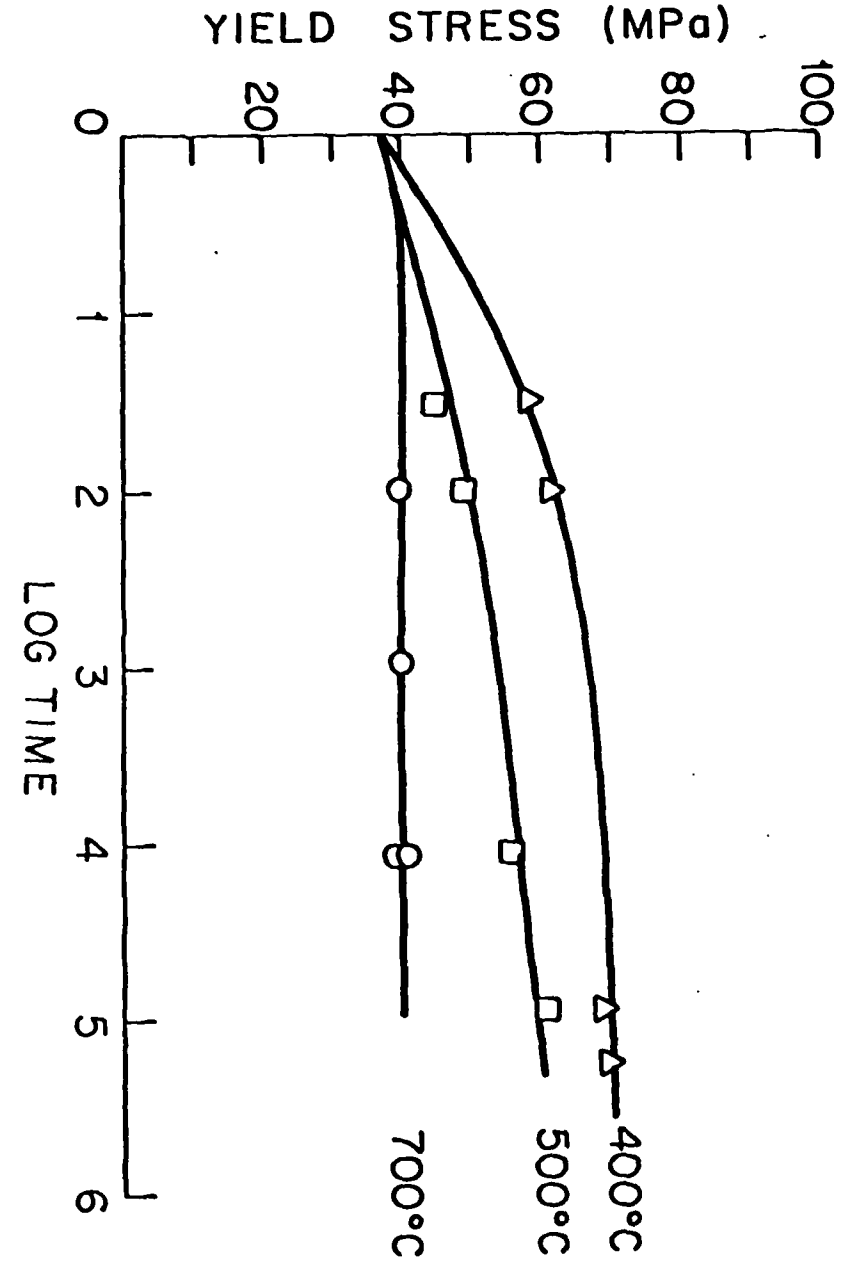

Figure 3: Yield stress versus annealing time for samples from ingot WA-Si for various annealing temperatures.

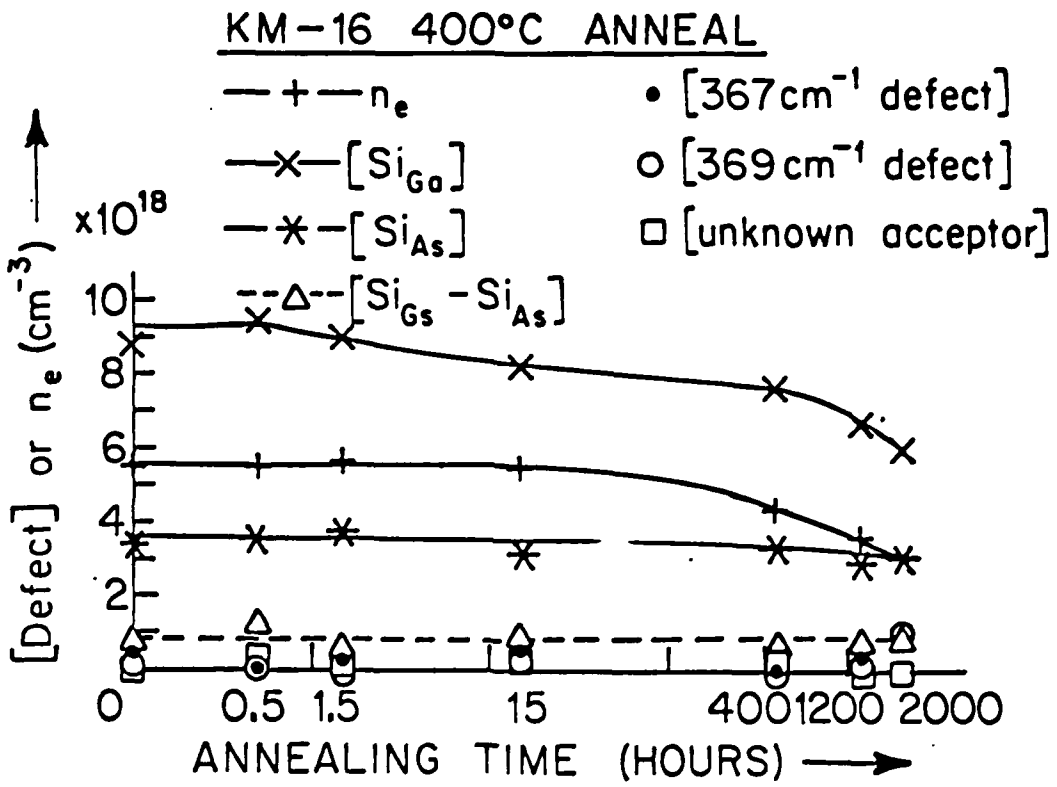

Figure 4: Isothermal annealing curves at 400°C giving defect or measured carrier concentrations for GaAs:Si samples (after Chen and Spitzer).

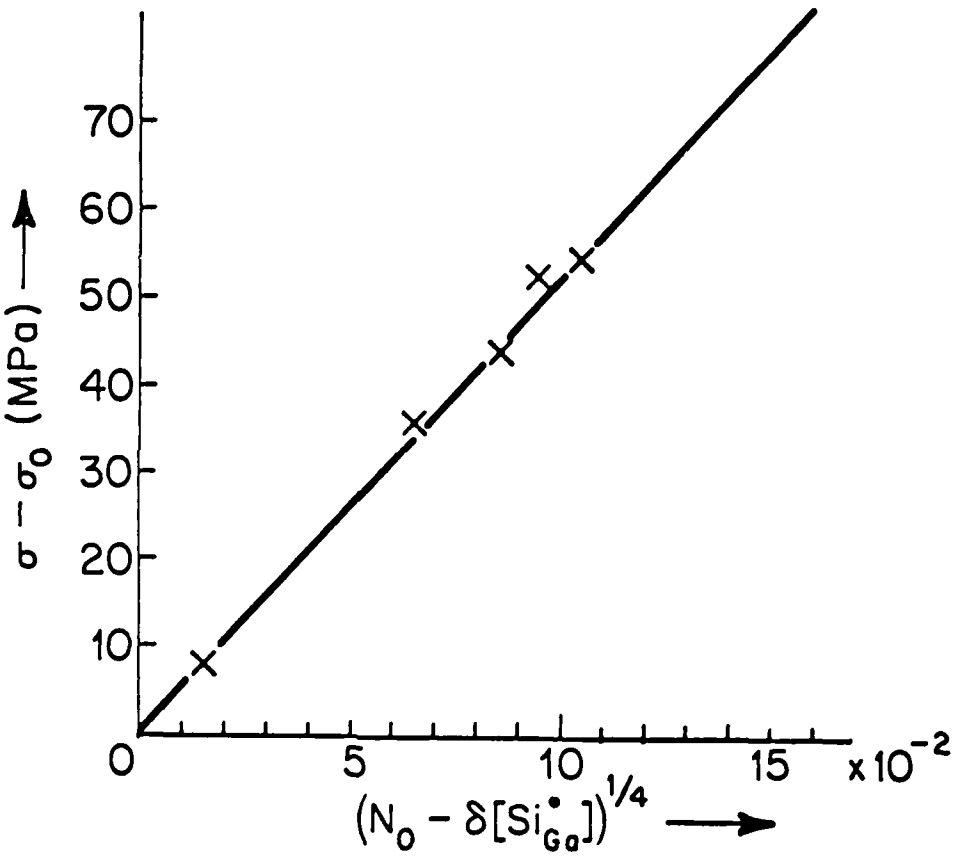

Figure 5: A plot of $\sigma - \sigma_o$ versus $(N_o - \delta[Si_{Ga}])^{\frac{1}{4}}$ for samples annealed at 400°C.

5. Measurements of [Si]

Knowledge of the absolute Si concentrations coupled with Hall effect and optical data would be helpful in assigning absolute concentrations of Si-Si pairs and possibly the more complex Si defects in heavily Si doped GaAs. To be useful the Si concentrations should be precise to within 10%. This is presently beyond the capability of secondary ion mass spectroscopy (SIMS) even when used with ion implanted standards. Atomic absorption spectroscopy may be feasible for concentrations in the mid $10^{18}cm^{-3}$ range and higher - ones which contain more than simple Si_{Ga} and Si_{As} defects. Ideally one would like an analytical method capable of the 10% precision for GaAs samples containing $5x10^{17}$ Si atoms cm^{-3} in which the primary defect is Si_{Ga}. This would allow the establishment of the correspondence between electrical, optical and the independent analytical methods for establishing the total Si.

We proposed to develop such a procedure which offered a 10% precision at Si concentration of $10^{17}cm^{-3}$. It has not been successfully demonstrated but has shown enough encouragement to cause us to continue its study on a no cost basis. The approach was to dissolve the GaAs:Si samples in a Sn solution containing a known concentration of O at 600°C. Upon dissolution the Si reacts with the dissolved O to form $S_iO_2(s)$. The amount of Si is estimated from the charges in the O concentration in the Sn solvent. Thermodynamically the approach is sound. Oxygen concentrations were to be determined by measuring the O fugacities by making the Sn solvent one electrode of a calcie stabilized zirconia which also serves as the solution container. A pt reference electrode in a controlled atmosphere completed the cell. The emf of the cell is proportional to the log of the ratio of the oxygen fugacities at each electrode. The O concentrations is then calculated using Henry's law. Thus

the Henry law constant was to have been measured.

An apparatus was built for allowing the insertion of the GaAs samples into the Sn electrode after removing surface oxides. A major complication developed in that the emf's of the cells were not as stable as those in which Ga was the solvent and upon which the approach was originally based. A simplified cell has been constructed with provision for controlling the O fugicity in the gas phase above the Sn. The object is to establish the stability limits of the cell. This phase should be completed by the end of this summer. An extra incentive is that the above method should be applicable to precisely measuring the oxygen concentrations in GaAs. Lack of such information has lead to much speculation about the role of O in semi insulating GaAs substrates.

III. PERSONNEL ASSOCIATED WITH RESEARCH EFFORT

Over the 5 year research effort there have been a number of people associated with this project. The following alphabetical list indicates the nature and time of the association.

1. R. T. Chen, graduate student; worked on the optical, electrical, and TEM studies from 1976 to 1980. This work formed the basis of his Ph.D. dissertation. He received his Ph.D. in 1980 and is now employed at the Rockwell International Science Center as a Member of the Technical Staff.
2. S. M. Copley, Professor of Materials Science; from 1976 to 1979 he directed the work done on the metallurgical studies including the critical resolved shear stress measurements of the GaAs:Si.
3. V.Ganeson, graduate student; he measured mechanical properties of GaAs:Si from 1976 to 1978. He received his M. S. degree and is now employed at Science Industries Inc. (Harbor City, CA).
4. J. Graham, graduate student; he is working on the technique to measure the total [Si]. He started in 1980 and is continuing this work at the present time.
5. O. K. Kim, graduate student; he spent 1976-77 working on the crystal growth system and then shifted to another project. He received a Ph.D. and is now a Member of the Technical Staff at Bell Telephone Laboratories.
6. G. H. Narayanan, Assistant Professor of Materials Science; an electron microscopist, he supervised the TEM work done on this project during its first 3 years. He then left USC to work in the Metallurgical Division of Boeing Aircraft Company.
7. V. Rana, Post Doctoral Fellow; he worked for almost 6 months during the period when the samples were being electron irriadiated. He is now a Member of the Technical Staff at Bell Telephone Laboratories.

8. W. G. Spitzer, Professor of Materials Science and Physics; Principal Investigator.
9. P. S. Vijayakumar, Post Doc; he spent 2 years at the beginning of the project working on crystal growth and materials characterization. He is now employed at Arco Solar Energy Corporation.
10. J. M. Whelan, Professor of Materials Science; he has supervised the work directed towards accurate [Si] determinations started in 1980.

IV. PUBLICATIONS

The following papers have or will acknowledge the support of this grant:

1) R. T. Chen and W. G. Spitzer, Silicon Site Transfer in GaAs Induced by Lithium Saturation Diffusion, Electromechanical Society Meeting, Los Angeles, October 14-19, 1979.

2) R. T. Chen and W. G. Spitzer, Infrared Absorption and Microstructure of Li-Saturated Si-Doped GaAs, J. Electrochem. Soc. 127, 1607 (1980).

3) R. T. Chen and W. G. Spitzer, Infrared Absorption Bands Induced by Si-Related Defects in GaAs: Absorption Cross Sections, J. Appl. Phys. 51, 1532 (1980).

4) R. T. Chen and W. G. Spitzer, Si-Defect Concentrations in Heavily Si-Doped GaAs: Annealing Induced Changes-II, submitted to J. Electronic Materials and has been accepted for publication.

5) V. Ganeson and S. M. Copley, Strengthening of GaAs Single Crystals by Formation of Silicon-Vacancy Pairs, to be submitted to J. Amer. Ceramic Soc.

6) J. Graham and J. M. Whelan, An Electrochemical Technique for Measurement of Si Concentrations in GaAs, to be submitted for publication upon completion of work at the end of the summer, 1981. Journal uncertain.

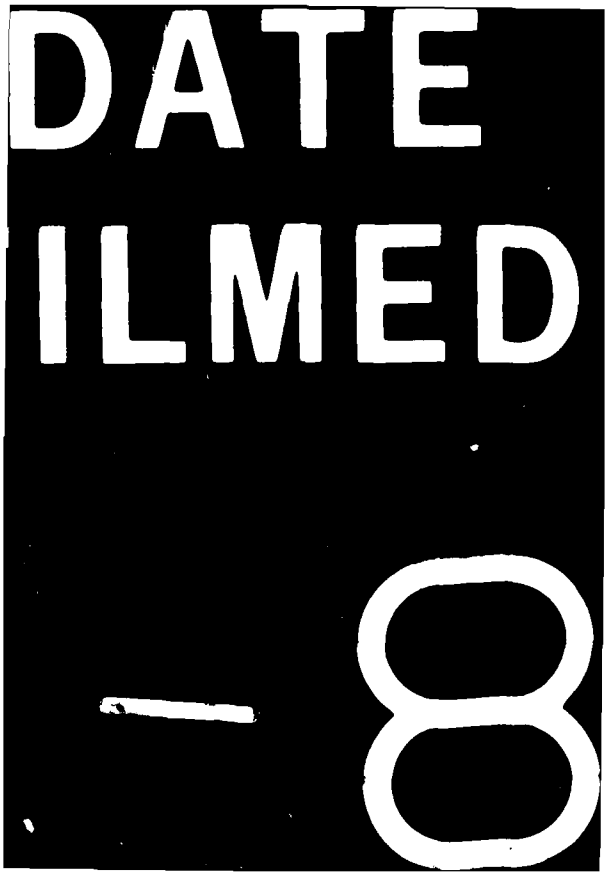
DATE
ILMED
8